

Nucleation and growth of lattice crystals

Andrea Braides, Giovanni Scilla and Antonio Tribuzio

Abstract

A variational lattice model is proposed to define an evolution of sets from a single point (nucleation) following a criterion of “maximization” of the perimeter. At a discrete level, the evolution has a “checkerboard” structure and its shape is affected by the choice of the norm defining the dissipation term. For every choice of the scales, the convergence of the discrete scheme to a family of expanding sets with constant velocity is proved.

Keywords: discrete systems, nucleation, minimizing movements, geometric evolution, pinning, microstructure

MSC(2010): 35B27, 74Q10, 53C44, 49M25, 49J45.

1 Introduction

In this paper we propose a variational model for nucleation and growth of a set by *maximization* of its perimeter through an energy-dissipation balance at fixed time step. We follow an implicit Euler scheme used by Almgren, Taylor and Wang to prove existence of sets moving by mean curvature by *minimization* of the perimeter (see [4]). In that case, fixed a time step $\tau > 0$, one can define iteratively the discrete orbits E_k^τ at fixed τ from an initial set E_0 as $E_0^\tau = E_0$ and E_k^τ as a solution of

$$\min\left\{P(E) + \frac{1}{\tau}D^p(E, E_{k-1}^\tau)\right\}, \quad D^p(E, F) = \int_{E\Delta F} \text{dist}_p(x, \partial F) dx, \quad (1.1)$$

where $\text{dist}_p(x, \partial E) = \min\{\|x - y\|_p : y \in \partial E\}$, $p \in [1, \infty]$. The term D^p is interpreted as a *dissipation*, and (1.1) can be seen as a minimization of P subject to a constraint due to the dissipation, which forces E_k^τ to be close to E_{k-1}^τ for τ small. In [4] it is proved (in the case $p = 2$) that the piecewise-constant interpolations $E^\tau(t) = E_{\lfloor t/\tau \rfloor}^\tau$ converge to a decreasing family of sets $E(t)$ which move by mean curvature.

Such a scheme cannot be directly followed taking maximization of the perimeter as a driving mechanism, which would correspond to replacing P with $-P$. Indeed, we may have sets E such that $E\Delta E_0$ has small measure (and hence with small dissipation) but with arbitrarily large perimeter, so that the minimum value for $k = 1$ in (1.1) is $-\infty$ and the scheme arrests at the first step. In order to overcome this issue, we discretize our problem by introducing a spatial length scale ε . For technical reasons explained below, we will examine only a two-dimensional setting, and for simplicity parameterize our problem on the lattices $\varepsilon\mathbb{Z}^2$. We then restrict to sets that can be written as the union of squares of side length ε and centers in $\varepsilon\mathbb{Z}^2$. Within this class we shall consider the problem of *nucleation*; i.e., of motion from a minimal set, a single ε -square E_0^ε (which we may suppose to be centered in 0). With fixed ε and τ , the discrete orbits are defined as $E_0^{\varepsilon, \tau} = E_0^\varepsilon$ and $E_k^{\varepsilon, \tau}$ as a solution of

$$\min\left\{-P_\varepsilon(E) + \frac{1}{\tau}D_\varepsilon^p(E, E_{k-1}^{\varepsilon, \tau}) : E_{k-1}^{\varepsilon, \tau} \subseteq E\right\}, \quad (1.2)$$

where P_ε is the restriction of the perimeter functional to unions of ε -squares, and D_ε^p is a discretization of the dissipation D^p which, for every $E \supseteq F$, reduces to

$$D_\varepsilon^p(E, F) = \varepsilon^2 \sum_{i \in E \cap \varepsilon \mathbb{Z}^2} \text{dist}_p(i, (\varepsilon \mathbb{Z}^2 \setminus F)).$$

Note that we consider a *growing* family of sets with respect to inclusion. With fixed $\tau = \tau_\varepsilon$ we will characterize the cluster points $E(t)$ as $\varepsilon \rightarrow 0$ of the interpolated functions $E^\varepsilon(t) = E_{\lfloor \varepsilon t / \tau \rfloor}^{\varepsilon, \tau}$, which are the generalization to varying energies of the Almgren-Taylor-Wang scheme scaled in the time variable. Note the different scaling of the time variable, which is the one that better describes the evolution. The form of E will depend on the interplay between ε and τ ; more precisely, on the limit ratio α of ε^2/τ as $\varepsilon \rightarrow 0$. We remark that the chosen time scaling can be directly interpreted as giving the *minimizing movements along the sequence* $-\varepsilon P_\varepsilon$ at scale τ , which are defined in [7]. This scaling is also justified by the fact that the energies $-\varepsilon P_\varepsilon$ have a non-trivial Γ -limit.

We describe the case $0 < \alpha < +\infty$, which is the most relevant. It is not restrictive to suppose that $\alpha\tau = \varepsilon^2$. By the homogeneity properties of the perimeter and the dissipation, we note that $E_k^{\varepsilon, \tau} = \varepsilon A_k^\alpha$, where $A_0^\alpha = q$ (the unit square centered in 0), and we solve iteratively

$$\min \left\{ -P_1(A) + \alpha D_1^p(A, A_{k-1}^\alpha) : A_{k-1}^\alpha \subseteq A \right\}. \quad (1.3)$$

The first step is particularly meaningful, and consists in solving the minimum problem

$$\min \left\{ -P_1(A) + \alpha D_1^p(A, q) : q \subseteq A \right\}. \quad (1.4)$$

We have

- the first set A_1^α is a part of the checkerboard of unit squares in \mathbb{R}^2 containing 0 (which we call the *even checkerboard*). While this fact is clear ‘locally’, the proof that the whole set is a single checkerboard requires a non-trivial covering argument, in which \mathbb{R}^2 is covered by sets in which the minimal set A is (part of) the correct checkerboard. This argument can be avoided in the case $p = \infty$, which has been treated directly in [12];

- since every square of the (even) checkerboard gives an independent contribution of energy and dissipation, a point $i \in \mathbb{Z}^2$ may belong to A_1^α if and only if ($i_1 + i_2 \in 2\mathbb{Z}$ and) the corresponding contribution is non positive; i.e.,

$$-4 + \alpha \|i\|_p \leq 0; \quad (1.5)$$

- if $\alpha \notin \{4/\|i\|_p : i \in \mathbb{Z}^2, i_1 + i_2 \in 2\mathbb{Z}\}$ then A_1^α is uniquely determined by (1.5), and it is the union of all squares in the even checkerboard with centers in the set

$$\mathcal{N}_\alpha^p = \{i \in \mathbb{Z}^2 \cap B_{4/\alpha}^p : i_1 + i_2 \in 2\mathbb{Z}\},$$

where $B_r^p = \{x \in \mathbb{R}^2 : \|x\|_p < r\}$. Note that $\mathcal{N}_\alpha^p = \{0\}$ if $\alpha > 4$;

We consider only α with such a unique minimizer. The subset \mathcal{N}_α^p of \mathbb{Z}^2 will be called the *nucleus* of the process. Correspondingly, we have the continuum set P_α^p obtained as the convexification of \mathcal{N}_α^p . Note that P_α^1 and P_α^∞ are always squares, but for the other p the form of P_α^p does depend on α .

The most delicate argument in the study of the discrete scheme is the characterization of the sets A_k^α for $k > 1$. Similarly to the case $k = 1$ this is done by covering \mathbb{R}^2 with a family of small sets, mainly squares and rectangles, in each of which we prove that the minimal set is again the even checkerboard. In order to construct this covering we have to define the ‘edges’ of

the nucleus \mathcal{N}_α^p , and consider separately the regions of \mathbb{R}^2 that project on those edges according to the p -distance. At this point we have a technical hypothesis to add; namely, that all such regions are infinite (which is satisfied if these edges enclose a convex shape but may not be the case for some exceptional values of α). The complex construction of this covering is the reason why we limit our analysis to a two-dimensional setting.

With this characterization, using (1.5) we immediately have that the centers of the squares in A_k^α are exactly the points $i \in \mathbb{Z}^2$ with $i_1 + i_2 \in 2\mathbb{Z}$ and distance not greater than $4/\alpha$ from A_{k-1}^α , so that

$$A_k^\alpha \cap \mathbb{Z}^2 = (A_{k-1}^\alpha \cap \mathbb{Z}^2) + (A_1^\alpha \cap \mathbb{Z}^2).$$

In a sense, every square in A_{k-1}^α acts as the ‘center’ of a nucleus. Note in this step that if A_1^α were not unique, then we would have an ‘increasing non-uniqueness’ of A_k^α , which in particular may even not be the intersection of the square checkerboard with a convex region.

Since the centers of the squares in A_k^α are obtained as sums of k elements in \mathcal{N}_α^p , a result on *Minkowsky sums* of sets shows then that the convex envelope of $A_k^\alpha \cap \mathbb{Z}^2$ is the convex envelope of $k\mathcal{N}_\alpha^p$, which is an interesting and not a trivial fact. At this point we can go back to the original problem and describe the discrete orbits.

$$E_k^{\varepsilon, \tau} = \varepsilon A_k^\alpha = \varepsilon k P_\alpha^p, \quad E^\varepsilon(t) = E_{\lfloor \varepsilon t / \tau \rfloor}^{\varepsilon, \tau} = \varepsilon \left\lfloor \frac{\alpha}{\varepsilon} \right\rfloor P_\alpha^p.$$

Letting $\varepsilon \rightarrow 0$ we then conclude that the desired evolution is a linear evolution of sets

$$E(t) = \alpha t P_\alpha^p.$$

Note that $P_\alpha^p = \{0\}$ and hence the evolution is *pinned* if $\alpha > 4$. Moreover, remarking that $\alpha P_\alpha^p \sim B_4^p$ for α small, we also recover the case $\alpha = 0$, corresponding to the regime $\varepsilon^2 \ll \tau$, for which $E(t) = 4tB_1^p$.

We note that in [10] the same discretization approach had been followed for the (positive) perimeter and non-trivial initial data. The resulting evolution therein is a discretized motion by square-crystalline curvature (see [3]), which highlights the anisotropy of the lattice intervening in the perimeter part, while the effect of the dissipation is confined in the form of the mobility. In the present analysis the effect of the dissipation and of the perimeter parts are combined in the determination of the shape of the nucleus, but the perimeter term actually acts as an approximation of an area and is less relevant for small values of α . Note that our discretization approach can be regarded as a ‘backward’ version of [10] if the index k is considered as parameterizing negative time (see [7, Section 10.2]). Other analyses of minimizing movements on lattices related to the perimeter can be found in [11, 27, 26, 28]. We note that checkerboard, stripes and other structures arise in antiferromagnetic systems related to maximization of the perimeter (see [8] for a variational analysis in terms of Γ -convergence, and the wide literature in Statistical Mechanics, e.g. [19, 16]). Some cases in which microstructures on lattices are involved and produce interesting variants of motion by crystalline curvature are studied in [9, 13]. For an overview on geometric motion on planar lattices see the recent lecture notes [14].

Even though our interest is mainly in the analytical issues of this nucleation process, it is suggestive and interesting to connect this work with the process of biomineralization, where nucleation occurs via the formation of a small nucleus of a new phase inside the large volume of the old phase (see, e.g., [17]). At very small size, adding even one more molecule increases the free energy of the system and this produces, on average, the dissolution of the nucleus. Above a threshold, when the contribution of the surface free energy becomes negligible, every addition of a molecule to the lattice lowers the free energy and allows for the growth of the nucleus. In this direction, lattice systems have been widely used as a simple model in simulations of complex

phenomena, as the vapor-liquid nucleation (see, e.g., [20, Section 8.9]). From a completely different point of view, our structure results can be related to the investigation of the influences of environmental heterogeneities on the spatial self-organization of microbial communities (see, e.g., [15, 23]); in particular, how interactions of different type (mutualism/commensalism) between competing neighboring genotypes and their mutual distance can produce spatial patterns of varying complexity and intermixing, as a random distribution, a spatial segregation or even a checkerboard, and how they may affect the collective behaviour and the rate of growth of the colony.

Outline of the paper. In Section 2 we fix some notation and recall some preliminaries in Discrete Geometry. We introduce the class of admissible sets that we will consider throughout the paper, and the notions of *effective boundary* and *discrete edge* of a set. In Section 3 we define perimeter energies P_ε and, for a general norm φ , dissipations D_ε^φ we will deal with, together with the main functional $\mathcal{F}_{\varepsilon,\tau}^\varphi$. Correspondingly, we introduce the time-discrete minimization scheme for a suitably scaled version of the energies $\mathcal{F}_{\varepsilon,\tau}^\varphi$ (Section 3.1).

The convergence analysis of this scheme at the regime $\varepsilon \ll \tau$ is carried out in Section 4. In Section 5 we address the problem of determining the solutions of scheme (1.4) at the critical regime $\varepsilon = \alpha\tau$, under a monotonicity constraint on the discrete trajectories. We introduce here also a first restriction on the dissipations D_ε^φ , by requiring that φ be an *absolute norm*; i.e., $\varphi(\mathbf{x}) = \varphi(|x_1|, |x_2|)$. The explicit characterization of the first step A_α^1 of the discrete evolution, provided with Proposition 27, is based on a local analysis by means of the 2×2 -square tilings introduced in Section 5.1 and the key submodularity-type norm-inequality (5.8). In order to prove that an analogous structure result can be obtained for each step A_α^k , $k \geq 2$; i.e., for minimizers of the energy $\mathcal{F}_\alpha^\varphi(\cdot, A_\alpha^{k-1})$, we will assume that φ is a *symmetric absolute normalized norm* (see Section 5.2), complying with a technical assumption (H3), and that the competitors fulfill suitable geometric assumptions (see (5.13)). The proof of this stability result, given with Proposition 30, is the content of Section 5.5 and relies on a localization argument only reminiscent of that used in the proof of Proposition 27, as we are forced to define a new covering outside every discrete edge contained in the effective discrete boundary of the current step A_α^{k-1} . In Section 5.6, with Theorem 38 we characterize the time-discrete flow $\{A_\alpha^k\}_{k \geq 0}$ as a geometric iterative process, based on properties of Minkowski sums.

In Section 6 we describe the resulting limit evolutions and we prove the existence of a pinning threshold (see Definition 40). We conclude our analysis by exhibiting, in Section 6.1, some examples where both the microscopic and the limit evolutions can be explicitly characterized. The closing Section 6.2 contains some conjectures on evolutions *without the monotonicity constraint*.

2 Notation and preliminaries

The generic point of \mathbb{R}^2 will be denoted by $\mathbf{x} = (x_1, x_2)$, the Euclidean norm by $|\cdot|$ in any dimension. The space of subsets of \mathbb{R}^2 with finite perimeter endowed with the Hausdorff distance $d_{\mathcal{H}}$ is denoted by \mathcal{X} , and the 1-dimensional Hausdorff measure by \mathcal{H}^1 (see for instance [2]).

The function $\varphi : \mathbb{R}^2 \rightarrow [0, +\infty)$ denotes any norm in the plane. We use the standard notation for the ℓ^p -norm, for every $1 \leq p \leq \infty$; that is,

$$\|\mathbf{x}\|_p = (|x_1|^p + |x_2|^p)^{\frac{1}{p}} \text{ if } 1 \leq p < \infty, \quad \|\mathbf{x}\|_\infty = \max\{|x_1|, |x_2|\} \text{ if } p = \infty,$$

for every $\mathbf{x} \in \mathbb{R}^2$. For every $r > 0$, $B_r^\varphi(\mathbf{x}) = \{\mathbf{y} \in \mathbb{R}^2 : \varphi(\mathbf{x} - \mathbf{y}) < r\}$ is the open ball of radius r and center \mathbf{x} corresponding to the norm φ , while $q_r(\mathbf{x}) = \mathbf{x} + [-r/2, r/2]^2$ is the r -square of side-length r centered at \mathbf{x} ; when $\mathbf{x} = (0, 0)$, we will use the shorthand B_r^φ and q_r in place of $B_r^\varphi(\mathbf{x})$ and

$q_r(\mathbf{x})$, respectively. For every $\mathbf{x} \in \mathbb{R}^2$, $E \subseteq \mathbb{R}^2$ we set $d^\varphi(\mathbf{x}, E) = \inf_{\mathbf{y} \in E} \varphi(\mathbf{x} - \mathbf{y})$. The segment connecting $\mathbf{x}_1, \mathbf{x}_2 \in \mathbb{R}^2$ is denoted by $[\mathbf{x}_1, \mathbf{x}_2] := \{\mathbf{y} \in \mathbb{R}^2 : \mathbf{y} = s\mathbf{x}_1 + (1-s)\mathbf{x}_2, s \in [0, 1]\}$.

Definition 1. Given two unit vectors $\mathbf{v}_1, \mathbf{v}_2 \in \mathbb{S}^1$, $\theta(\mathbf{v}_2, \mathbf{v}_1) \in [-\pi, \pi]$ denotes the *signed angle between \mathbf{v}_1 and \mathbf{v}_2* , defined as

$$\theta(\mathbf{v}_2, \mathbf{v}_1) = (\theta_2 - \theta_1 + \pi \pmod{2\pi}) - \pi,$$

where θ_1 and θ_2 are the angles corresponding to the exponential representations of \mathbf{v}_1 and \mathbf{v}_2 , respectively.

Let \mathbb{Z}^2 be the standard square lattice. We consider the partition of \mathbb{Z}^2 given by $\mathbb{Z}^2 = \mathbb{Z}_e^2 \cup \mathbb{Z}_o^2$, where $\mathbb{Z}_e^2 = \{\mathbf{i} \in \mathbb{Z}^2 : i_1 + i_2 \in 2\mathbb{Z}\}$ and $\mathbb{Z}_o^2 = (1, 0) + \mathbb{Z}_e^2$.

We will call a *lattice set* any subset $J \subseteq \mathbb{Z}^2$, and $\#J$ denotes its cardinality. We also recall that the *boundary* of a lattice set J is the set

$$\partial J = \{\mathbf{i} \in J \mid \text{there exists } \mathbf{j} \in \mathbb{Z}^2 \setminus J : |\mathbf{i} - \mathbf{j}| = 1\}.$$

Given a lattice set J , the *convex hull* of J is the smallest convex subset of \mathbb{R}^2 containing J , which is denoted by $\text{conv}(J)$. A polygon whose vertices are points of the lattice is said a *lattice polygon*. The set $\text{conv}(J)$ is an example of a (convex) lattice polygon, for every $J \subset \mathbb{Z}^2$.

Let $\varepsilon > 0$ be a fixed parameter and consider the lattice $\varepsilon\mathbb{Z}^2$. All the notation given above for subsets of \mathbb{Z}^2 extends also to subsets of $\varepsilon\mathbb{Z}^2$. We identify any lattice set $J \subset \varepsilon\mathbb{Z}^2$ with the subset $E(J)$ of \mathbb{R}^2 given by the union of ε -squares centered at points of J ; namely,

$$E(J) := \bigcup_{\mathbf{i} \in J} q_\varepsilon(\mathbf{i}).$$

Accordingly, we define the class of *admissible sets* as

$$\mathcal{D}_\varepsilon := \{E \subset \mathbb{R}^2 : E = E(J) \text{ for some lattice set } J \subseteq \varepsilon\mathbb{Z}^2\}, \quad (2.1)$$

and to each set $E \in \mathcal{D}_\varepsilon$ we associate the lattice set $Z_\varepsilon(E) := E \cap \varepsilon\mathbb{Z}^2$, the *set of centers* of E . When $\varepsilon = 1$ we will simply write \mathcal{D} and $Z(E)$ in place of \mathcal{D}_1 and $Z_1(E)$, respectively.

Definition 2 (the classes of *checkerboard sets*). We introduce the classes of *even* and *odd ε -checkerboard sets*

$$\mathcal{A}_\varepsilon^e = \{E \in \mathcal{D}_\varepsilon : Z_\varepsilon(E) \subseteq \varepsilon\mathbb{Z}_e^2\}, \quad (2.2)$$

and analogously the class $\mathcal{A}_\varepsilon^o$ by requiring that $J \subseteq \varepsilon\mathbb{Z}_o^2$. We refer to $E(\varepsilon\mathbb{Z}_e^2)$ and $E(\varepsilon\mathbb{Z}_o^2)$ as the *even* and *odd ε -checkerboard*, respectively. In the following we will write \mathcal{D} , \mathcal{A}^e , \mathcal{A}^o in place of \mathcal{D}_1 , \mathcal{A}_1^e , \mathcal{A}_1^o , and we will use the shorthand *checkerboard set* (in place of “1-checkerboard set”) to denote any set in \mathcal{A}^e and \mathcal{A}^o .

2.1 Preliminaries on lattice geometry

For our purposes we fix some notation and introduce some basic definitions in lattice geometry that will be useful for the analysis performed in Subsection 5.4.

Definition 3. A lattice set $J \subseteq \mathbb{Z}_e^2$ is said to be *\mathbb{Z}_e^2 -convex* if $\text{conv}(J) \cap \mathbb{Z}_e^2 = J$. Analogously, $J \subseteq \mathbb{Z}_o^2$ is *\mathbb{Z}_o^2 -convex* if $\text{conv}(J) \cap \mathbb{Z}_o^2 = J$. Accordingly, we define the subclass $\mathcal{A}_{\text{conv}}^e \subset \mathcal{D}$ as

$$\mathcal{A}_{\text{conv}}^e = \{E \in \mathcal{D} : Z(E) \text{ is } \mathbb{Z}_e^2\text{-convex}\},$$

and, analogously, the subclass $\mathcal{A}_{\text{conv}}^o$ by requiring $Z(E)$ to be \mathbb{Z}_o^2 -convex. We also set the class $\mathcal{A}_{\text{conv}} := \mathcal{A}_{\text{conv}}^e \cup \mathcal{A}_{\text{conv}}^o$.

The notion of *convex lattice set* has already been given for $\mathcal{J} \subset \mathbb{Z}^2$ (see for instance [18]). Note that \mathcal{J} is \mathbb{Z}_e^2 -convex if and only if there exists a convex set $K \subset \mathbb{R}^2$ such that $\mathcal{J} = K \cap \mathbb{Z}_e^2$, and the same holds for \mathbb{Z}_o^2 -convex sets.

For every lattice set $\mathcal{J} \subseteq \mathbb{Z}_e^2$ (or \mathbb{Z}_o^2) there holds $\partial\mathcal{J} = \mathcal{J}$, since \mathcal{J} consists of isolated points of \mathbb{Z}^2 . Since in the following we will deal with checkerboard sets we need a finer definition of boundary for such lattice sets.

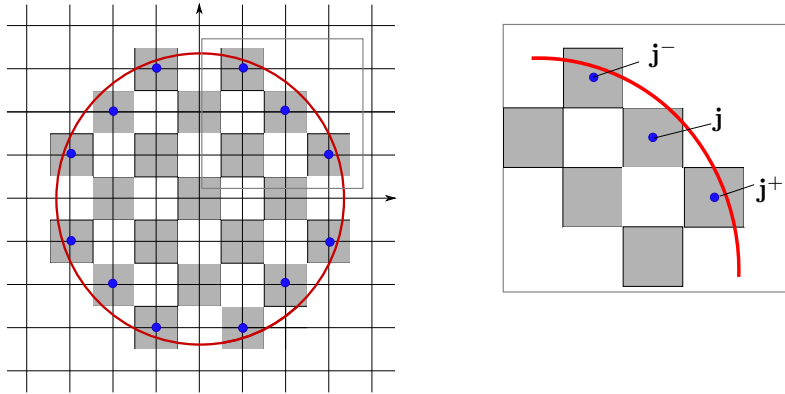


Figure 1: The (discrete) effective boundary of E (in blue).

Definition 4. Let $\mathcal{J} \subset \mathbb{Z}_e^2$ be a lattice set. We define the *effective (discrete) boundary* of \mathcal{J} as

$$\partial^{\text{eff}}\mathcal{J} = \{\mathbf{j} \in \mathcal{J} : \text{there exists } \mathbf{j}_0 \in \mathbb{Z}_e^2 \setminus \mathcal{J} \text{ such that } \|\mathbf{j} - \mathbf{j}_0\| = \sqrt{2}\}.$$

The same definition is given for lattice sets $\mathcal{J} \subset \mathbb{Z}_o^2$. Let $E \in \mathcal{A}^e \cup \mathcal{A}^o$, we will write $\partial^{\text{eff}}E = \partial^{\text{eff}}Z(E)$, see Figure 1.

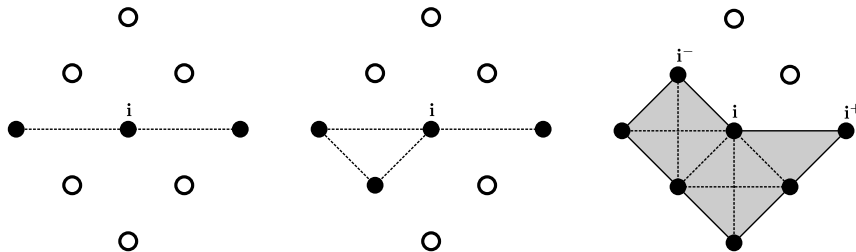


Figure 2: The black dots are lattice points of \mathcal{J} . The first two figures are different examples of “degenerate” \mathbf{i} . On the right an example of a non-degenerate \mathbf{i} and corresponding \mathbf{i}^- and \mathbf{i}^+ ; in gray polygon \mathcal{P} .

Given $E \in \mathcal{A}^e \cup \mathcal{A}^o$, and consider $\mathbf{i} \in \partial^{\text{eff}}E$. We set $\mathcal{J} = \{\mathbf{j} \in Z(E) : \|\mathbf{j} - \mathbf{i}\|_1 \leq 2\}$. Then \mathbf{i} is said to be *non-degenerate* if the set

$$\bigcup_{\substack{\mathbf{j}_1, \mathbf{j}_2 \in \mathcal{J} \\ \|\mathbf{j}_1 - \mathbf{j}_2\| \leq 2}} [\mathbf{j}_1, \mathbf{j}_2]$$

is the boundary of a triangulation of a simple polygon \mathcal{P} . Then, we can define two boundary points $\mathbf{i}^-, \mathbf{i}^+ \in \partial^{\text{eff}}E$ as the vertices of \mathcal{P} , respectively, preceding and following \mathbf{i} in the clockwise orientation of $\partial\mathcal{P}$, as depicted in Figure 2. We will say that \mathbf{i}^- *precedes* \mathbf{i} and that \mathbf{i}^+ *follows* \mathbf{i} .

In the sequel, we will often consider the following non-degeneracy condition on sets $E \in \mathcal{A}_{\text{conv}}$:

$$\text{every } \mathbf{i} \in \partial^{\text{eff}} E \text{ is non-degenerate.} \quad (2.3)$$

Condition (2.3) allows to define an orientation of $\partial^{\text{eff}} E$, since for every $\mathbf{i} \in \partial^{\text{eff}} E$ we can define \mathbf{i}^- and \mathbf{i}^+ as above. The following definitions are therefore well-posed.

Definition 5 (Discrete convex vertices). Let $E \in \mathcal{A}_{\text{conv}}$ satisfy (2.3). Given $\mathbf{j} \in \partial^{\text{eff}} E$, let \mathbf{j}^+ (resp., \mathbf{j}^-) follow (resp., precede) \mathbf{j} in $\partial^{\text{eff}} E$ in the clockwise orientation. We define the *right* and *left outward unit normal vector* at \mathbf{j} as

$$\boldsymbol{\nu}^+(\mathbf{j}) := \frac{(j_2 - j_2^+, j_1^+ - j_1)}{\sqrt{(j_2^+ - j_2)^2 + (j_1^+ - j_1)^2}}, \quad \boldsymbol{\nu}^-(\mathbf{j}) := \frac{(j_2^- - j_2, j_1 - j_1^-)}{\sqrt{(j_2 - j_2^-)^2 + (j_1 - j_1^-)^2}},$$

respectively. Then we say that \mathbf{j} is a *discrete convex vertex* (or *discrete vertex*) if

$$\theta(\boldsymbol{\nu}^+(\mathbf{j}), \boldsymbol{\nu}^-(\mathbf{j})) < 0$$

where θ is introduced in Definition 1.

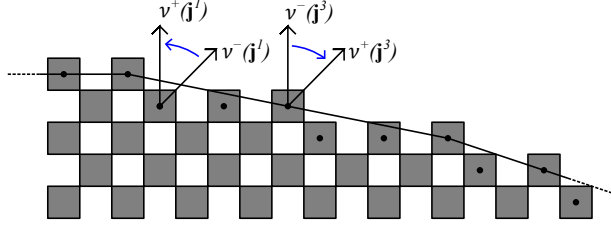


Figure 3: A discrete vertex of E may be a boundary point (not a vertex) of $\text{conv}(Z(E))$.

Remark 6 (Vertices and discrete vertices). The definition of discrete vertex given above is motivated by the fact that the vertices of $\text{conv}(Z(E))$ are discrete (convex) vertices of E . Whereas, points $\mathbf{j} \in \partial^{\text{eff}} E$ such that

$$\theta(\boldsymbol{\nu}^+(\mathbf{j}), \boldsymbol{\nu}^-(\mathbf{j})) > 0$$

are always contained in the interior of $\text{conv}(Z(E))$ (Figure 3). This choice will also facilitate the definition of *discrete edge* (see Definition 7 below).

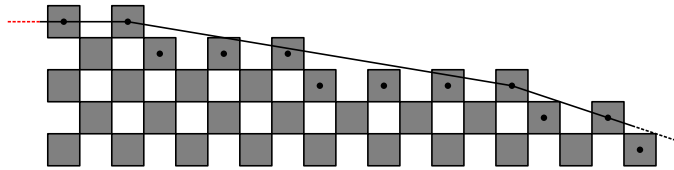


Figure 4: An example of a discrete vertex of E contained in the interior of $\text{conv}(Z(E))$.

Note that we may have discrete vertices of E lying on the boundary of $\text{conv}(Z(E))$ which are not vertices of $\text{conv}(Z(E))$ (see Fig. 3), and discrete vertices of E in the interior of $\text{conv}(Z(E))$, as well (see Fig. 4).

Definition 7 (Discrete edges). Let $E \in \mathcal{A}_{\text{conv}}$ satisfy (2.3). We define a *discrete edge* as a set of consecutive points of $\partial^{\text{eff}} E$, say $\ell = \{\mathbf{j}^l\}_{l=0}^L$ where $L \geq 2$ and \mathbf{j}^0 and \mathbf{j}^L are discrete vertices. We define the *outward unit normal vector* of the discrete edge ℓ as

$$\boldsymbol{\nu}(\ell) := \frac{(j_2^0 - j_2^L, j_1^L - j_1^0)}{\sqrt{(j_2^L - j_2^0)^2 + (j_1^L - j_1^0)^2}}.$$

We denote by $\mathcal{E}(E)$ the set of all discrete edges $\ell \subset \partial^{\text{eff}} E$.

Let $E \in \mathcal{A}_{\text{conv}}$ satisfy (2.3). For every $\ell \in \partial^{\text{eff}} E$ we define the *slope* of ℓ as

$$s(\ell) := \frac{\nu(\ell)_1}{\nu(\ell)_2} \in [-\infty, +\infty], \quad (2.4)$$

where $\nu(\ell)_k$, $k = 1, 2$ indicate the components of $\boldsymbol{\nu}(\ell)$, with the convention that $\frac{\pm 1}{0} = \pm\infty$.

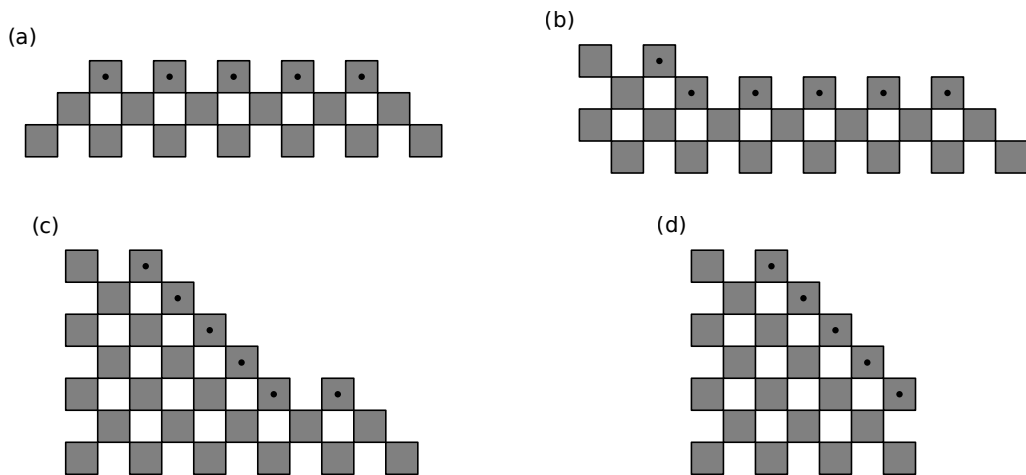


Figure 5: Some examples of discrete edges.

Remark 8. We list all the possible cases of discrete edges of sets $E \in \mathcal{A}_{\text{conv}}$ satisfying (2.3) that are symmetric with respect to the axes and the bisectors $x_2 = \pm x_1$. Such symmetric sets will play a central role in the sequel of the paper. Up to rotations of angle $k\pi$ and reflections we can restrict this characterization to discrete edges $\ell \in \mathcal{E}(E)$ such that $\ell = \{\mathbf{j}^l\}_{l=0}^L \subset \{\mathbf{x} \in \mathbb{R}^2 : x_2 > 0\}$ having $s(\ell) \in [0, 1]$. We have the following characterization:

- (i) if $s(\ell) = 0$ then $\mathbf{j}^l = \mathbf{j}^{l-1} + (2, 0)$ for every $1 \leq l \leq L$;
- (ii) if $s(\ell) \in (0, \frac{1}{3}]$ then $\mathbf{j}^l = \mathbf{j}^{l-1} + (2, 0)$ for every $1 < l \leq L$ and $\mathbf{j}^1 = \mathbf{j}^0 + (1, -1)$;
- (iii) if $s(\ell) \in (\frac{1}{3}, 1)$ then $\mathbf{j}^l = \mathbf{j}^{l-1} + (1, -1)$ for every $1 \leq l < L$ and $\mathbf{j}^L = \mathbf{j}^{L-1} + (2, 0)$;
- (iv) if $s(\ell) = 1$ then $\mathbf{j}^l = \mathbf{j}^{l-1} + (1, -1)$ for every $1 \leq l \leq L$.

These four types of discrete edge are pictured in Fig. 5(a), (b), (c) and (d), respectively.

Definition 9. For every norm φ and every $E \in \mathcal{D}$, we introduce the *projection map of integer points on E* ; that is, the set-valued map $\pi_E^\varphi : \mathbb{Z}^2 \rightarrow \mathcal{P}(\mathbb{Z}^2)$ defined as

$$\pi_E^\varphi(\mathbf{j}) := \operatorname{argmin}_{\mathbf{j}' \in Z(E)} \varphi(\mathbf{j} - \mathbf{j}'). \quad (2.5)$$

2.2 Minkowski sum of sets

We recall that the Minkowski sum of sets A and B is defined as $A + B = \{a + b \mid a \in A, b \in B\}$, and $A + \emptyset = \emptyset$. If $m \in \mathbb{N}$, we denote by mA the set $\{ma \mid a \in A\}$ and, if A is non-empty, we will often write $A[m]$ to indicate the sum $A + A + \cdots + A$ m -times. Among the many properties of Minkowski sum, we recall the commutability of Minkowski sum and the compatibility to the operation of taking the convex hull; that is,

$$\text{conv}(A + B) = \text{conv}(A) + \text{conv}(B). \quad (2.6)$$

We recall without proof a result about the Minkowski sum of two convex polygons (see, e.g., [5]).

Proposition 10. *Let A and B be convex polygons in \mathbb{R}^2 . Let $L_A := \{l_{i,A}\}_{i=1,\dots,n}$ and $L_B := \{l_{j,B}\}_{j=1,\dots,m}$ be the sets of the edges of A and B , respectively. Let $\mathcal{V}_A := \{\nu_{i,A}\}_{i=1,\dots,n}$ and $\mathcal{V}_B := \{\nu_{j,B}\}_{j=1,\dots,m}$ be the sets of the outer normal vectors of A and B , respectively. Then,*

- (i) *if $\mathcal{V}_A \cap \mathcal{V}_B = \emptyset$, then $L_{A+B} = L_A \cup L_B$ and $\mathcal{V}_{A+B} = \mathcal{V}_A \cup \mathcal{V}_B$;*
- (ii) *if $|\mathcal{V}_A \cap \mathcal{V}_B| = p$, $1 \leq p \leq \min\{n, m\}$, then $|L_{A+B}| = n + m - p$. More precisely, if $\nu_{i,A} = \nu_{j,B}$ for some $i \in \{1, \dots, n\}$ and $j \in \{1, \dots, m\}$, then $l_{i,A} + l_{j,B} \in L_{A+B}$, $l_{i,A} \notin L_{A+B}$, $l_{j,B} \notin L_{A+B}$ and $\nu_{i,A} = \nu_{j,B} \in \mathcal{V}_{A+B}$. If, instead, $\nu_{i,A} \neq \nu_{j,B}$, then $l_{i,A} \in L_{A+B}$, $l_{j,B} \in L_{A+B}$, $\nu_{i,A} \in \mathcal{V}_{A+B}$ and $\nu_{j,B} \in \mathcal{V}_{A+B}$.*

In particular, if $A = B$, then $L_{A+A} = \{l_{i,A} + l_{i,A}\}_{i=1,\dots,n}$ and $\mathcal{V}_{A+A} = \mathcal{V}_A$.

2.3 The lattice point-counting problem: m -fold Minkowski sums

Let $B = \{\mathbf{w}_1, \mathbf{w}_2\}$ be a basis of \mathbb{R}^2 . The set

$$\Lambda = \Lambda(B) := \{z_1 \mathbf{w}_1 + z_2 \mathbf{w}_2 : z_1, z_2 \in \mathbb{Z}\}$$

is called a *lattice* of \mathbb{R}^2 with basis B . The corresponding *fundamental cell* is defined as

$$\{\mu_1 \mathbf{w}_1 + \mu_2 \mathbf{w}_2 : \mu_1, \mu_2 \in [0, 1)\}$$

whose area is $|\det(B)|$. It can be checked that the area of the fundamental cell is independent of the choice of the basis and is referred to as the *determinant* of Λ , $\det(\Lambda)$. Lattices are additive subgroups of \mathbb{R}^2 and they are discrete sets. Examples of lattices are the standard lattice \mathbb{Z}^2 , with basis $\{(1, 0), (0, 1)\}$ and $|\det(\mathbb{Z}^2)| = 1$, and the ‘‘checkerboard lattice’’ \mathbb{Z}_e^2 , with basis $\{(-1, 1), (1, 1)\}$ and $|\det(\mathbb{Z}_e^2)| = 2$. \mathbb{Z}_o^2 is not a lattice, since $(1, 0) + (0, 1) = (1, 1) \notin \mathbb{Z}_o^2$.

It will be useful in the sequel to obtain an estimate on the number of the lattice points contained in $m\Omega$, $m \in \mathbb{N}$ for Ω lattice convex polygon. For this, we first recall a fundamental result for counting the lattice points in Ω .

Theorem 11 (Pick’s Theorem, [25]). *Let Λ be any lattice in \mathbb{R}^2 , let $\mathcal{J} \subset \Lambda$ be a finite set and $\Omega = \text{conv}(\mathcal{J})$. Then*

$$\#(\Omega \cap \Lambda) = \frac{1}{|\det(\Lambda)|} |\Omega| + \frac{1}{2} \#(\partial\Omega \cap \Lambda) + 1, \quad (2.7)$$

where $|\Omega|$ is the area of Ω and $\partial\Omega$ its topological boundary.

A non-trivial problem in discrete geometry is the comparison between the set of the lattice points contained in the homothetic copy $m\Omega$ of a convex lattice polyhedron Ω with the m -fold Minkowski sum $(\Omega \cap \mathbb{Z}^n)[m]$, $n \geq 2$ (see, e.g., [21]). It will be sufficient for our purposes here to mention that in the two dimensional setting the two lattice sets coincide (see [21, Corollary 2.4]). Moreover, an inspection of the proof reveals that the result still holds if we replace \mathbb{Z}^2 with any two-dimensional lattice Λ .

Proposition 12. *Let Λ be any lattice in \mathbb{R}^2 , let $\mathcal{J} \subset \Lambda$ be a finite set and $\mathcal{Q} = \text{conv}(\mathcal{J})$ be two-dimensional. Then the equality*

$$(\mathcal{Q} \cap \Lambda)[m] = (m\mathcal{Q}) \cap \Lambda \quad (2.8)$$

holds for every $m \in \mathbb{N}$.

Now, in view of Proposition 12 and by iterating formula (2.7), Pick's Theorem generalizes to $m\mathcal{Q}$, $m \geq 1$, as

$$\#((m\mathcal{Q}) \cap \Lambda) = \frac{1}{|\det(\Lambda)|} |\mathcal{Q}| m^2 + \frac{1}{2} \#(\partial\mathcal{Q} \cap \Lambda) m + 1. \quad (2.9)$$

2.4 Submodularity and absolute norms

We briefly recall the concept of submodularity which is well known in discrete convex analysis (see, e.g., [24, Ch. 2, eq. (2.17)]). Setting $\mathbb{R}_+^2 := \{\mathbf{x} = (x_1, x_2) \in \mathbb{R}^2 \mid x_1, x_2 \geq 0\}$, for every $\mathbf{x}, \mathbf{y} \in \mathbb{R}^2$ we define

$$\mathbf{x} \vee \mathbf{y} := (\max\{x_1, y_1\}, \max\{x_2, y_2\}) \quad \text{and} \quad \mathbf{x} \wedge \mathbf{y} := (\min\{x_1, y_1\}, \min\{x_2, y_2\}).$$

A function $f : \mathbb{R}_+^2 \rightarrow \mathbb{R}$ is said to be *submodular* if it satisfies the following inequality

$$f(\mathbf{x} \vee \mathbf{y}) + f(\mathbf{x} \wedge \mathbf{y}) \leq f(\mathbf{x}) + f(\mathbf{y}), \quad \text{for every } \mathbf{x}, \mathbf{y} \in \mathbb{R}_+^2. \quad (2.10)$$

It is known (see [22, Proposition 5]) that every positively homogeneous function defined in the cone \mathbb{R}_+^2 is subadditive if and only if it is submodular. In particular, this yields that every *absolute norm* φ (i.e., $\varphi(\mathbf{x})$ depends only on $|x_1|$ and $|x_2|$) complies with (2.10). We recall that an absolute norm is *monotonic*:

$$|x_1| \leq |y_1| \quad \text{and} \quad |x_2| \leq |y_2| \quad \text{imply} \quad \varphi(\mathbf{x}) \leq \varphi(\mathbf{y}). \quad (2.11)$$

3 Setting of the problem

We will deal with *negative discrete perimeters*; that is, the Euclidean perimeter functional (with negative sign) restricted to \mathcal{D}_ε relaxed to the space \mathcal{X} . Namely, we define the functionals $F_\varepsilon : \mathcal{X} \rightarrow (-\infty, +\infty]$ as

$$F_\varepsilon(E) = \begin{cases} -\mathcal{H}^1(\partial E) & E \in \mathcal{D}_\varepsilon \\ +\infty & \text{otherwise.} \end{cases} \quad (3.1)$$

Note that these energies are related to the corresponding interaction energies defined on lattice sets

$$F_\varepsilon^{\text{lat}}(\mathcal{J}) = -\varepsilon \#\{(\mathbf{i}, \mathbf{j}) \in \varepsilon\mathbb{Z}^2 \times \varepsilon\mathbb{Z}^2 \mid \mathbf{i} \in \mathcal{J}, \mathbf{j} \notin \mathcal{J}, |\mathbf{i} - \mathbf{j}| = \varepsilon\},$$

where $\mathcal{J} \subset \varepsilon\mathbb{Z}^2$, and $F_\varepsilon^{\text{lat}}(Z_\varepsilon(E)) = F_\varepsilon(E)$. The functionals F_ε , in turn, may be seen as *nearest-neighbor* (NN) antiferromagnetic interaction energies associated to a lattice spin-system; i.e., given $u : \varepsilon\mathbb{Z}^2 \rightarrow \{-1, 1\}$ one defines

$$E_\varepsilon(u) = -\frac{\varepsilon}{4} \sum_{\substack{\mathbf{i}, \mathbf{j} \in \varepsilon\mathbb{Z}^2 \\ |\mathbf{i} - \mathbf{j}| = \varepsilon}} (u(\mathbf{i}) - u(\mathbf{j}))^2,$$

whence $F_\varepsilon(E(\{u = 1\})) = E_\varepsilon(u)$. The asymptotic behavior as $\varepsilon \rightarrow 0$ of energies like F_ε has been studied, e.g., in [1].

Let $\varphi : \mathbb{R}^2 \rightarrow [0, +\infty)$ be a norm. For every pair of lattice sets $E, E' \in \mathcal{D}_\varepsilon$, we define the dissipations

$$D_\varepsilon^\varphi(E, E') = \varepsilon^2 \sum_{\mathbf{i} \in Z_\varepsilon(E) \Delta Z_\varepsilon(E')} d_\varepsilon^\varphi(\mathbf{i}, \partial Z_\varepsilon(E')), \quad (3.2)$$

where, given $\mathcal{J} \subset \varepsilon\mathbb{Z}^2$, d_ε^φ denotes the *discrete distance* of any lattice point $\mathbf{i} \in \varepsilon\mathbb{Z}^2$ to $\partial\mathcal{J}$ defined as

$$d_\varepsilon^\varphi(\mathbf{i}, \partial\mathcal{J}) = \begin{cases} \inf\{\varphi(\mathbf{i} - \mathbf{j}) \mid \mathbf{j} \in \mathcal{J}\} & \text{if } \mathbf{i} \notin \mathcal{J} \\ \inf\{\varphi(\mathbf{i} - \mathbf{j}) \mid \mathbf{j} \in \varepsilon\mathbb{Z}^2 \setminus \mathcal{J}\} & \text{if } \mathbf{i} \in \mathcal{J}. \end{cases}$$

Remark 13. In the sequel, the following integral formulation of the dissipation (3.2) will be useful. Indeed, for every $E' \in \mathcal{X}$ we set $d_\varepsilon^\varphi(\mathbf{i}, \partial E') = d_\varepsilon^\varphi(\mathbf{i}, \partial(E' \cap \varepsilon\mathbb{Z}^2))$. Furthermore, we can extend $d_\varepsilon^\varphi(\cdot, \partial E')$ to \mathbb{R}^2 by setting $d_\varepsilon^\varphi(\mathbf{x}, \partial E') := d_\varepsilon^\varphi(\mathbf{i}, \partial E')$ for $\mathbf{x} \in q_\varepsilon(\mathbf{i})$. Thus, for every $E, E' \in \mathcal{X}$, let $E_\varepsilon, E'_\varepsilon \in \mathcal{D}_\varepsilon$ be the corresponding discretizations; *i.e.*, $Z_\varepsilon(E_\varepsilon) = E \cap \varepsilon\mathbb{Z}^2$ and the same for E'_ε , we may write

$$\int_{E \Delta E'} d_\varepsilon^\varphi(\mathbf{x}, \partial E') \, d\mathbf{x} = \varepsilon^2 \sum_{\mathbf{i} \in Z_\varepsilon(E_\varepsilon) \Delta Z_\varepsilon(E'_\varepsilon)} d_\varepsilon^\varphi(\mathbf{i}, \partial E'_\varepsilon) = D_\varepsilon^\varphi(E_\varepsilon, E'_\varepsilon).$$

We will consider the dissipation in (3.2) as defined on every pair of sets of finite perimeter; *i.e.*, $D_\varepsilon^\varphi : \mathcal{X} \times \mathcal{X} \rightarrow [0 + \infty]$.

3.1 The time-discrete minimization scheme with a monotonicity constraint

For any $\varepsilon > 0$ and $\tau > 0$, let F_ε and D_ε^φ be defined as in (3.1) and (3.2), respectively. We introduce a discrete motion with underlying time step τ obtained by successive minimization. At each time step we will minimize an energy $\mathcal{F}_{\varepsilon, \tau}^\varphi : \mathcal{X} \times \mathcal{X} \rightarrow (-\infty, +\infty]$ defined as

$$\mathcal{F}_{\varepsilon, \tau}^\varphi(E, F) = \varepsilon F_\varepsilon(E) + \frac{1}{\tau} D_\varepsilon^\varphi(E, F), \quad (3.3)$$

with a *monotonicity constraint* on the discrete trajectories. Namely, we recursively define an increasing (with respect to inclusion) sequence $E_{\varepsilon, \tau}^k$ in \mathcal{D}_ε by requiring the following:

$$\begin{cases} E_{\varepsilon, \tau}^0 = q_\varepsilon, \\ E_{\varepsilon, \tau}^{k+1} \in \operatorname{argmin}_{E \in \mathcal{D}_\varepsilon, E \supset E_{\varepsilon, \tau}^k} \mathcal{F}_{\varepsilon, \tau}^\varphi(E, E_{\varepsilon, \tau}^k), \quad k \geq 0. \end{cases} \quad (3.4)$$

In some cases we will also analyze solutions of the corresponding *unconstrained* scheme; that is,

$$\begin{cases} E_{\varepsilon, \tau}^0 = q_\varepsilon, \\ E_{\varepsilon, \tau}^{k+1} \in \operatorname{argmin}_{E \in \mathcal{D}_\varepsilon} \mathcal{F}_{\varepsilon, \tau}^\varphi(E, E_{\varepsilon, \tau}^k), \quad k \geq 0, \end{cases} \quad (3.5)$$

in which the minimization problems are performed over the whole class \mathcal{D}_ε . The discrete orbits associated to functionals $\mathcal{F}_{\varepsilon, \tau}^\varphi$ are thus defined by

$$E_{\varepsilon, \tau}(t) := E_{\varepsilon, \tau}^{\lfloor t/\tau \rfloor}, \quad t > 0. \quad (3.6)$$

We say that a curve $E : [0, +\infty) \rightarrow \mathcal{X}$ is a *minimizing movement* for the problem (3.4) or (3.5) at *regime* τ - ε if it is pointwise limit (in the Hausdorff topology) of discrete orbits $E_{\varepsilon, \tau}$, as $\varepsilon, \tau \rightarrow 0$ up to subsequences.

Remark 14 (choice of scaling). The scale ε in the energies $\varepsilon F_\varepsilon$ above is suggested by energetic considerations (see [12, (6)-(7)]) and leads to a non-trivial limit of the discrete solutions defined in (3.6). This choice is motivated by the fact that $\varepsilon F_\varepsilon$ has a nontrivial Γ -limit, as we will show in Section 4.1. The energy scaling may also be seen as a time scaling of the discrete flow generated by taking the relaxation on \mathcal{D}_ε of the energy functional $-\mathcal{H}^1$ (see [7, Section 10.2]).

4 Fast convergences and the emergence of a critical regime

As remarked in [7, Ch. 8], minimizing movements along families of functionals will depend in general on the *regime* τ - ε ; in our case, on the ratio between the two parameters τ and ε that characterizes the motion. We first provide the following result that ensures a compactness property of the minimizers of the energies $\mathcal{F}_{\varepsilon,\tau}^\varphi$. In this section φ denotes a general norm, without any restriction.

Lemma 15. *Let F_ε and D_ε^φ be defined as in (3.1) and (3.2), respectively, and $\mathcal{F}_{\varepsilon,\tau}^\varphi$ be as in (3.3). Let $E' \in \mathcal{D}_\varepsilon$ be an admissible set. For every fixed $\tau > 0$ consider*

$$E_{\varepsilon,\tau} \in \underset{E \in \mathcal{X}}{\operatorname{argmin}} \mathcal{F}_{\varepsilon,\tau}^\varphi(E, E').$$

Then, $Z_\varepsilon(E_{\varepsilon,\tau}) \subset E' + B_{4\tau}^\varphi$ and $d_{\mathcal{H}}(E_{\varepsilon,\tau}, E' + B_{4\tau}^\varphi) < 3\sqrt{2}\varepsilon$ for ε small enough.

Proof. For any $E \in \mathcal{D}_\varepsilon$, the variation of the energy $\mathcal{F}_{\varepsilon,\tau}^\varphi$ when removing a square of center $\mathbf{i} \in \varepsilon\mathbb{Z}^2$ is

$$\mathcal{F}_{\varepsilon,\tau}^\varphi(E, E') - \mathcal{F}_{\varepsilon,\tau}^\varphi(E \setminus q_\varepsilon(\mathbf{i}), E') \leq 4\varepsilon^2 - \frac{\varepsilon^2}{\tau} d_\varepsilon^\varphi(\mathbf{i}, \partial E')$$

which is strictly negative when $d_\varepsilon^\varphi(\mathbf{i}, \partial E') > 4\tau$, thus implying that $Z_\varepsilon(E_{\varepsilon,\tau}) \subset E' + B_{4\tau}^\varphi$. Furthermore, since it is always convenient to add an isolated square $q_\varepsilon(\mathbf{j})$ if $\mathbf{j} \in Z_\varepsilon(E' + B_{4\tau}^\varphi)$ then, for every $\mathbf{j} \in 3\varepsilon\mathbb{Z}^2 \cap E' + B_{4\tau}^\varphi$ we must have $E_{\varepsilon,\tau} \cap q_{3\varepsilon}(\mathbf{j}) \neq \emptyset$. Since otherwise $\mathcal{F}_{\varepsilon,\tau}^\varphi(E_{\varepsilon,\tau} \cup q_\varepsilon(\mathbf{j}), E') < \mathcal{F}_{\varepsilon,\tau}^\varphi(E_{\varepsilon,\tau}, E')$. \square

Remark 16. The regime $\tau/\varepsilon \rightarrow 0$ is completely characterized by the previous lemma. Indeed, in this case, when τ and ε are small enough, $B_{4\tau} \cap \varepsilon\mathbb{Z}^2 = \{(0,0)\}$ and the minimizing movement is trivially $E(t) \equiv \{(0,0)\}$. This degenerate evolution is called a *pinned motion*. We will focus on such motions in Section 6, where we will also introduce a “pinning threshold”.

4.1 Γ -convergence of interaction energies

This section is devoted to the study of the asymptotic behavior of energies $\varepsilon F_\varepsilon$. To this end, we associate to any admissible set $E \in \mathcal{D}_\varepsilon$ the corresponding characteristic function $\chi_E \in L^\infty(\mathbb{R}^2)$ and compute the Γ -limit with respect to the local weak*-topology. We then generalize energies in (3.1) by considering $F_\varepsilon : L^\infty(\mathbb{R}^2) \rightarrow (-\infty, +\infty]$ as

$$F_\varepsilon(u) = \begin{cases} F_\varepsilon(E) & u = \chi_E, E \in \mathcal{D}_\varepsilon \\ +\infty & \text{otherwise,} \end{cases} \quad (4.1)$$

with a slight abuse of notation.

Theorem 17. *Let F_ε be defined as in (4.1), and set $G_\varepsilon := \varepsilon F_\varepsilon$. Then G_ε Γ -converge as $\varepsilon \rightarrow 0$ to the energy*

$$G(u) = \begin{cases} 4 \int_{\mathbb{R}^2} \left(\left| u(\mathbf{x}) - \frac{1}{2} \right| - \frac{1}{2} \right) d\mathbf{x} & u \in L^\infty(\mathbb{R}^2; [0, 1]) \\ +\infty & \text{otherwise,} \end{cases}$$

with respect to the local weak*-topology.

Proof. It will suffice to prove the result for $u \in L^\infty(\mathbb{R}^2; [0, 1])$, otherwise the assertion is trivial. We can assume, without loss of generality, that u has compact support, and let $E_\varepsilon \in \mathcal{D}_\varepsilon$ be a sequence of sets such that χ_{E_ε} locally weakly-* converge to u .

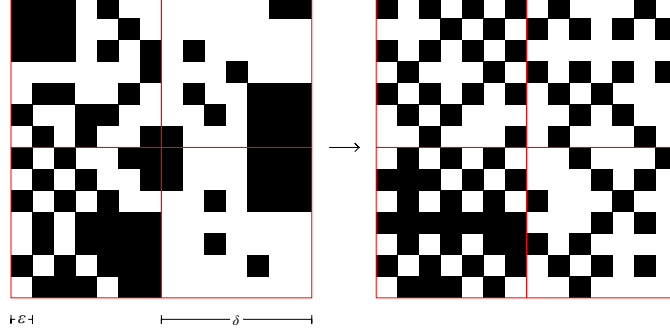


Figure 6: On the left the set E_ε , on the right we exhibit a set E_ε^δ satisfying (i) and (ii).

We now provide a rearrangement of the centers of E_ε which is energy decreasing. Let $\delta > 0$ be fixed. We consider the lattice $\delta\mathbb{Z}^2$ and sets $E_\varepsilon^\delta \in \mathcal{D}_\varepsilon$ satisfying $\#(Z_\varepsilon(E_\varepsilon^\delta) \cap q_\delta(\mathbf{i})) = \#(Z_\varepsilon(E_\varepsilon) \cap q_\delta(\mathbf{i}))$ and with the following properties:

- (i) if $\varepsilon^2 \#(Z_\varepsilon(E_\varepsilon) \cap q_\delta(\mathbf{i})) \leq \delta^2/2$ then $Z_\varepsilon(E_\varepsilon^\delta \cap q_\delta(\mathbf{i})) \subset \varepsilon\mathbb{Z}_\varepsilon^2$,
 - (ii) if $\varepsilon^2 \#(Z_\varepsilon(E_\varepsilon) \cap q_\delta(\mathbf{i})) > \delta^2/2$ then $Z_\varepsilon(E_\varepsilon^\delta \cap q_\delta(\mathbf{i})) \supset \varepsilon\mathbb{Z}_\varepsilon^2 \cap q_\delta(\mathbf{i})$,
- for every $\mathbf{i} \in \delta\mathbb{Z}^2$ (see Figure 6).

Now, for every $E \in \mathcal{D}_\varepsilon$ and $F \in \mathcal{X}$ we define

$$F_\varepsilon(E; F) = F_\varepsilon(E \cap E(\varepsilon\mathbb{Z}^2 \cap F)),$$

and analogously $G_\varepsilon(E; F)$. In both cases (i) and (ii) we have $F_\varepsilon(E_\varepsilon; q_\delta(\mathbf{i})) \geq F_\varepsilon(E_\varepsilon^\delta; q_\delta(\mathbf{i}))$. Since the contribution of the interaction between two adjacent δ -squares $q_\delta(\mathbf{i})$ and $q_\delta(\mathbf{j})$ is less than $2\delta\varepsilon$ and the number of δ -squares whose intersection with $\text{supp}(u) \neq \emptyset$ is proportional to $1/\delta^2$, we get

$$G_\varepsilon(E_\varepsilon) \geq G_\varepsilon(E_\varepsilon^\delta) - C \frac{\varepsilon}{\delta}$$

for some positive constant C . Now, from the convergence of χ_{E_ε} to u , for every $\mathbf{i} \in \delta\mathbb{Z}^2$ we get

$$G_\varepsilon(E_\varepsilon^\delta; q_\delta(\mathbf{i})) + O(\varepsilon) = -4|E_\varepsilon \cap q_\delta(\mathbf{i})| + O(\varepsilon) = -4 \int_{q_\delta(\mathbf{i})} u(\mathbf{x}) \, d\mathbf{x} := u_\delta(\mathbf{i}), \quad (4.2)$$

$$G_\varepsilon(E_\varepsilon; q_\delta(\mathbf{i})) + O(\varepsilon) = -4|q_\delta(\mathbf{i}) \setminus E_\varepsilon| + O(\varepsilon) = -4 \int_{q_\delta(\mathbf{i})} (1 - u(\mathbf{x})) \, d\mathbf{x} := u_\delta(\mathbf{i}) \quad (4.3)$$

in cases (i) and (ii), respectively. After identifying u_δ with its piecewise-constant interpolation, taking the limit as $\varepsilon \rightarrow 0$ first, we get

$$\liminf_{\varepsilon \rightarrow 0} G_\varepsilon(E_\varepsilon) \geq \int_{\mathbb{R}^2} u_\delta(\mathbf{x}) \, d\mathbf{x},$$

and then taking the limit as $\delta \rightarrow 0$ we obtain the liminf inequality.

The construction of a recovery sequence follows an analogous argument. Let $u \in L^\infty(\mathbb{R}^2; [0, 1])$ have a compact support. Consider the lattice $\sqrt{\varepsilon}\mathbb{Z}^2$ and define

$$u_\varepsilon(\mathbf{i}) = \frac{1}{\varepsilon} \int_{q_{\sqrt{\varepsilon}}(\mathbf{i})} u(\mathbf{x}) \, d\mathbf{x}, \quad \text{for every } \mathbf{i} \in \sqrt{\varepsilon}\mathbb{Z}^2.$$

As a recovery sequence we will choose E_ε having the same mean (unless a small error) of u in every $\sqrt{\varepsilon}$ -square with maximal perimeter term. Indeed, we can take a set $E_\varepsilon \in \mathcal{D}_\varepsilon$ satisfying $\#(Z_\varepsilon(E_\varepsilon) \cap q_{\sqrt{\varepsilon}}(\mathbf{i})) = \lceil u_\varepsilon(\mathbf{i})/\varepsilon \rceil$ and such that:

- (i) if $u_\varepsilon(\mathbf{i}) \leq 1/2$, then $Z_\varepsilon(E_\varepsilon) \cap q_{\sqrt{\varepsilon}}(\mathbf{i}) \subset \varepsilon\mathbb{Z}_e^2$;
- (ii) if $u_\varepsilon(\mathbf{i}) > 1/2$, then $Z_\varepsilon(E_\varepsilon) \cap q_{\sqrt{\varepsilon}}(\mathbf{i}) \supset \varepsilon\mathbb{Z}_e^2 \cap q_{\sqrt{\varepsilon}}(\mathbf{i})$.

Then, χ_{E_ε} weakly-* converge to u and

$$G_\varepsilon(E_\varepsilon; q_{\sqrt{\varepsilon}}(\mathbf{i})) + O(\varepsilon) = \begin{cases} -4 \int_{q_{\sqrt{\varepsilon}}(\mathbf{i})} u(\mathbf{x}) \, d\mathbf{x} & \text{if } u_\varepsilon(\mathbf{i}) \leq \frac{1}{2} \\ -4 \int_{q_{\sqrt{\varepsilon}}(\mathbf{i})} (1 - u(\mathbf{x})) \, d\mathbf{x} & \text{if } u_\varepsilon(\mathbf{i}) > \frac{1}{2} \end{cases}$$

for every $\mathbf{i} \in \sqrt{\varepsilon}\mathbb{Z}^2$, which proves that χ_{E_ε} is a recovery sequence and concludes the proof. \square

Remark 18. Note that, in the proof of Theorem 17 we have exhibited a recovery sequence whose supports E_ε also converges to $E = \text{supp}(u)$ in the Hausdorff sense. This remark allows us to reduce the computation of the Γ -limit of G_ε to functions weakly-* converging to u having supports in \mathcal{D}_ε converging to E with respect to the Hausdorff distance.

Remark 19 (Γ -limit on characteristic functions). An immediate consequence of Theorem 17 is that, among all the functions having the same support E , the ground state of the energy G is achieved by the simple function $1/2 \chi_E$. In particular, since any family of sets $\{E_\varepsilon\}$ converging in the Hausdorff sense to E are such that χ_{E_ε} is weakly-* compact, from Theorem 17 we infer that

$$\Gamma(d_{\mathcal{H}})\text{-}\lim_{\varepsilon \rightarrow 0} G_\varepsilon(E) = -2|E|,$$

once noted that the recovery sequences are ε -checkerboard sets.

4.2 Convergence of the minimizing-movement scheme

We prove that when $\varepsilon/\tau \rightarrow 0$ every minimizing movement of scheme (3.5) may be seen as the solution of a continuum problem having a gradient-flow structure with respect to the limit energy. In this regime the monotonicity constraint is not needed to obtain a completely characterized limit motion. A straightforward consequence is that the solution of the unconstrained problem corresponds to that of the monotone scheme (3.4).

Theorem 20. *Let $F_\varepsilon, D_\varepsilon^\varphi$ and $\mathcal{F}_{\varepsilon, \tau}^\varphi$ be as in (3.1), (3.2) and (3.3), respectively. Then there exists a unique minimizing movement of the unconstrained scheme (3.5) at regime $\varepsilon/\tau \rightarrow 0$ and it satisfies*

$$E(t) = B_{4t}^\varphi, \quad t \geq 0.$$

Moreover, for every discrete solution $E_{\varepsilon, \tau}$ of (3.5) we have $\chi_{E_{\varepsilon, \tau}(t)} \xrightarrow{*} \frac{1}{2} \chi_{B_{4t}^\varphi}$ for all $t \geq 0$ as $\varepsilon \rightarrow 0$.

Proof. The first claim is a direct consequence of Lemma 15. Indeed, $d_{\mathcal{H}}(E_{\varepsilon,\tau}(t), B_{4\lfloor t/\tau \rfloor}) < C\lfloor t/\tau \rfloor\varepsilon$, which goes to zero locally uniformly at regimes $\varepsilon/\tau \rightarrow 0$. In an analogous way as for (4.1), we further generalize the dissipations in Remark 13 as functionals $D_\varepsilon^\varphi : L^\infty(\mathbb{R}^2) \times \mathcal{X} \rightarrow [0, +\infty]$ defined by

$$D_\varepsilon^\varphi(u, E') = \begin{cases} D_\varepsilon^\varphi(E, E') & u = \chi_E, E \in \mathcal{D}_\varepsilon \\ +\infty & \text{otherwise.} \end{cases}$$

Accordingly, we write $\mathcal{F}_{\varepsilon,\tau}^\varphi(u, E') = \varepsilon F_\varepsilon(u) + \frac{1}{\tau} D_\varepsilon^\varphi(u, E')$ for every $u \in L^\infty(\mathbb{R}^2)$ with F_ε as in (4.1). Since for every sequence $\{E_\varepsilon\} \subset \mathcal{D}_\varepsilon$ such that χ_{E_ε} weakly-* converge to u we have

$$D_\varepsilon^\varphi(E_\varepsilon, q_\varepsilon) \rightarrow \int_{\mathbb{R}^2} u(\mathbf{x})\varphi(\mathbf{x}) \, d\mathbf{x},$$

then Theorem 17 yields that $\mathcal{F}_{\varepsilon,\tau}^\varphi$ Γ -converge, as $\varepsilon \rightarrow 0$, to the functional \mathcal{F}_τ^φ given by

$$\mathcal{F}_\tau^\varphi(u) := \int_{\mathbb{R}^2} \left(|4u(\mathbf{x}) - 2| - 2 + \frac{1}{\tau} u(\mathbf{x})\varphi(\mathbf{x}) \right) d\mathbf{x}, \quad (4.4)$$

with respect to the weak-* topology. Energy \mathcal{F}^φ has a unique minimizer in $L^\infty(\mathbb{R}^2; [0, 1])$, given by $u = 1/2 \chi_{B_{4\tau}^\varphi}$. Indeed

$$\begin{aligned} \int_{\mathbb{R}^2} \left(|4u(\mathbf{x}) - 2| - 2 + \frac{1}{\tau} u(\mathbf{x})\varphi(\mathbf{x}) \right) d\mathbf{x} &= \int_{\{u \leq 1/2\}} \left(\frac{\varphi(\mathbf{x})}{\tau} - 4 \right) u(\mathbf{x}) \, d\mathbf{x} \\ &\quad + \int_{\{u > 1/2\}} \left(4u(\mathbf{x}) - 4 + \frac{\varphi(\mathbf{x})}{\tau} u(\mathbf{x}) \right) d\mathbf{x}. \end{aligned}$$

Both integrands are positive for almost every $\varphi(\mathbf{x}) > 4\tau$ and are minimized when $u \equiv 1/2$. Then, since Γ -convergence implies the convergence of minimum problems (see for instance [6, Theorem 1.21]) and the minimum is unique, we get that $\chi_{E_{\varepsilon,\tau}^1}$ weakly-* converges to $u_\tau^1 = 1/2 \chi_{B_{4\tau}^\varphi}$ as $\varepsilon \rightarrow 0$. Note also that, by virtue of Lemma 15, $E_{\varepsilon,\tau}^1 \rightarrow B_{4\tau}^\varphi$ in the Hausdorff sense and moreover by the minimality of $E_{\varepsilon,\tau}^1$ and Remark 13 follows that

$$\begin{aligned} \varepsilon F_\varepsilon(E_{\varepsilon,\tau}^1) &\leq \varepsilon F_\varepsilon(E_\varepsilon) + \frac{1}{\tau} (D_\varepsilon^\varphi(E_\varepsilon, q_\varepsilon) - D_\varepsilon^\varphi(E_{\varepsilon,\tau}^1, q_\varepsilon)) \\ &\leq \varepsilon F_\varepsilon(E_\varepsilon) + \frac{1}{\tau} \int_{\mathbb{R}^2} (\chi_{E_\varepsilon}(x) - \chi_{E_{\varepsilon,\tau}^1}(\mathbf{x})) (\varphi(\mathbf{x}) + \varepsilon) d\mathbf{x} \leq \varepsilon F_\varepsilon(E_\varepsilon) + o(1), \end{aligned} \quad (4.5)$$

for every χ_{E_ε} weakly* converging to u_τ^1 .

Now we show the Γ -convergence of $\mathcal{F}_{\varepsilon,\tau}^\varphi(\cdot, E_{\varepsilon,\tau}^1)$, which will allow us to deduce the convergence of the whole scheme by an inductive procedure. Consider $E_\varepsilon \in \mathcal{D}_\varepsilon$ such that χ_{E_ε} are converging weakly-* to some $u \in L^\infty(\mathbb{R}^2)$. Mimicking the arguments of the proof of Theorem 17, we consider $E'_\varepsilon \in \mathcal{D}_\varepsilon$ satisfying $\#(Z_\varepsilon(E'_\varepsilon) \cap q_{\sqrt{\varepsilon}}(\mathbf{i})) = \#(Z_\varepsilon(E_\varepsilon) \cap q_{\sqrt{\varepsilon}}(\mathbf{i}))$ and such that:

(i) if $\#(Z_\varepsilon(E_\varepsilon) \cap q_{\sqrt{\varepsilon}}(\mathbf{i})) \leq \#(Z_\varepsilon(E_{\varepsilon,\tau}^1) \cap q_{\sqrt{\varepsilon}}(\mathbf{i}))$ then $Z_\varepsilon(E'_\varepsilon \cap q_{\sqrt{\varepsilon}}(\mathbf{i})) \subset Z_\varepsilon(E_{\varepsilon,\tau}^1)$,

(ii) if $\#(Z_\varepsilon(E_\varepsilon) \cap q_{\sqrt{\varepsilon}}(\mathbf{i})) > \#(Z_\varepsilon(E_{\varepsilon,\tau}^1) \cap q_{\sqrt{\varepsilon}}(\mathbf{i}))$ then $Z_\varepsilon(E'_\varepsilon \cap q_{\sqrt{\varepsilon}}(\mathbf{i})) \supset Z_\varepsilon(E_{\varepsilon,\tau}^1) \cap q_{\sqrt{\varepsilon}}(\mathbf{i})$,

for every $\mathbf{i} \in \sqrt{\varepsilon}\mathbb{Z}^2 \cap B_{4\tau}^\varphi$, and $Z_\varepsilon(E'_\varepsilon) \setminus B_{4\tau}^\varphi = Z_\varepsilon(E_\varepsilon) \setminus B_{4\tau}^\varphi$. Reasoning as in the proof of Theorem 17 and from (4.5), $\chi_{E'_\varepsilon}$ still weakly-* converges to u and $\varepsilon F_\varepsilon(E_\varepsilon) + o(1) \geq \varepsilon F_\varepsilon(E'_\varepsilon)$. Then we get

$$\begin{aligned} \mathcal{F}_{\varepsilon,\tau}^\varphi(E_\varepsilon, E_{\varepsilon,\tau}^1) + o(1) &\geq \mathcal{F}_{\varepsilon,\tau}^\varphi(E'_\varepsilon, E_{\varepsilon,\tau}^1) \\ &= \varepsilon F_\varepsilon(E'_\varepsilon) + \frac{1}{\tau} D_\varepsilon^\varphi(E_\varepsilon \setminus B_{4\tau}^\varphi, E_{\varepsilon,\tau}^1) + \frac{1}{\tau} \sum_{\mathbf{i} \in \sqrt{\varepsilon}\mathbb{Z}^2 \cap B_{4\tau}^\varphi} D_\varepsilon^\varphi(E'_\varepsilon \cap q_{\sqrt{\varepsilon}}(\mathbf{i}), E_{\varepsilon,\tau}^1). \end{aligned}$$

Since $D_\varepsilon^\varphi(E'_\varepsilon \cap q_{\sqrt{\varepsilon}}(\mathbf{i}), E_{\varepsilon, \tau}^1) = C\varepsilon^3 |\#Z_\varepsilon(E_\varepsilon) - \#Z_\varepsilon(E_{\varepsilon, \tau}^1)| + O(\varepsilon^2)$ and $d_\varepsilon^\varphi(\mathbf{x}, \partial E_{\varepsilon, \tau}^1)$ converge uniformly to $d^\varphi(\mathbf{x}, B_{4\tau}^\varphi)$ for every $\mathbf{x} \notin E_\tau^1$, we get that

$$\Gamma\text{-}\lim_{\varepsilon \rightarrow 0} \mathcal{F}_{\varepsilon, \tau}^\varphi(u, E_{\varepsilon, \tau}^1) = \int_{\mathbb{R}^2} \left(|4u(\mathbf{x}) - 2| - 2 + \frac{1}{\tau} u(\mathbf{x}) d^\varphi(\mathbf{x}, B_{4\tau}^\varphi) \right) d\mathbf{x}, \quad (4.6)$$

since the same argument applies to every recovery sequence E_ε . By arguing as above, we get $\chi_{E_{\varepsilon, \tau}^2}$ converge to $1/2 \chi_{B_{8\tau}^\varphi}$ and by induction the result follows. \square

Arguing as in the proof of Theorem 20 we obtain the following result.

Corollary 21. *Let $F_\varepsilon, D_\varepsilon^\varphi$ and $\mathcal{F}_{\varepsilon, \tau}^\varphi$ be defined as in (3.1)–(3.3). Then there exists a unique minimizing movement of scheme (3.4) at regime $\varepsilon/\tau \rightarrow 0$ and it satisfies $E(t) = B_{4t}^\varphi$ for $t \geq 0$. Moreover, for every discrete solution $E_{\varepsilon, \tau}$ of (3.4) we have $\chi_{E_{\varepsilon, \tau}(t)} \xrightarrow{*} \frac{1}{2} \chi_{B_{4t}^\varphi}$ for $t \geq 0$ as $\varepsilon \rightarrow 0$.*

Remark 22. Arguing as in Remark 19, for any $E' \in \mathcal{X}$ and every E'_ε converging to E' in $d_{\mathcal{H}}$ such that $\varepsilon F(E'_\varepsilon) \rightarrow -2|E'|$ we get, from (4.6), that

$$\Gamma(d_{\mathcal{H}})\text{-}\lim_{\varepsilon \rightarrow 0} \mathcal{F}_{\varepsilon, \tau}^\varphi(E, E'_\varepsilon) = \mathcal{F}_\tau^\varphi(E, E') := -2|E| + \frac{1}{2\tau} \int_{E \Delta E'} d^\varphi(x, E') dx.$$

Note that the minima of $\mathcal{F}_\tau^\varphi(\cdot, E')$ are solutions of

$$\left(-2 + \frac{1}{2\tau} d^\varphi(x, E') \right) \nu_E(x) \mathcal{H}^1 \llcorner \partial E = 0;$$

that is, $E \in \mathcal{X}$ such that $d^\varphi(x, E') \equiv 4\tau$ for \mathcal{H}^1 -almost every $x \in \partial E$. This gives that the limit scheme

$$\begin{cases} E_\tau^0 = \{(0, 0)\}, \\ E_\tau^{k+1} \in \operatorname{argmin}_{E \in \mathcal{X}} \mathcal{F}_\tau^\varphi(E, E_\tau^k). \end{cases} \quad (4.7)$$

is solved by $E_\tau^k = B_{4k\tau}^\varphi$. Hence, by Theorem 20 and Corollary 21 the minimizing movements of schemes (3.4) and (3.5) at regimes $\varepsilon/\tau \rightarrow 0$ are solutions of limit scheme (4.7).

5 The critical regime: a microscopic checkerboard structure

So far, we have shown that scheme (3.4) is completely characterized in the regimes $\tau/\varepsilon \rightarrow 0$ (Remark 16) and $\varepsilon/\tau \rightarrow 0$ (Remark 22). Throughout this section we will study the regimes where ε/τ has a non-zero finite limit, which turn out to be richer of features than the others.

Without loss of generality we consider only the case $\varepsilon = \alpha\tau$, where $\alpha > 0$ is a positive constant. The main goal is to determine any solution to the iterative variational scheme (3.4). Within this regime, instead of solving a family of schemes depending on ε , by a rescaling argument we can solve one minimization scheme in the unique environment \mathbb{Z}^2 . Indeed, for every $E, F \in \mathcal{D}_\varepsilon$, the energies defined in (3.3) can be rewritten as

$$\begin{aligned} \mathcal{F}_{\varepsilon, \tau}^\varphi(E, F) &= -\varepsilon \mathcal{H}^1(\partial E) + \frac{1}{\tau} D_\varepsilon^\varphi(E, F) = -\varepsilon \mathcal{H}^1(E) + \frac{\varepsilon^2}{\tau} \sum_{\mathbf{i} \in Z_\varepsilon(E) \Delta Z_\varepsilon(F)} d_\varepsilon^\varphi(\mathbf{i}, \partial F) \\ &= \varepsilon \left(-\mathcal{H}^1(\partial E) + \alpha \sum_{\mathbf{i} \in Z_\varepsilon(E) \Delta Z_\varepsilon(F)} d_\varepsilon^\varphi(\mathbf{i}, \partial F) \right) = \varepsilon^2 \mathcal{F}_\alpha^\varphi\left(\frac{1}{\varepsilon} E, \frac{1}{\varepsilon} F\right), \end{aligned}$$

where we have defined $\mathcal{F}_\alpha^\varphi : \mathcal{D} \times \mathcal{D} \rightarrow \mathbb{R}$ as

$$\mathcal{F}_\alpha^\varphi(E', F') = -\mathcal{H}^1(\partial E') + \alpha \sum_{\mathbf{i} \in Z(E') \Delta Z(F')} d^\varphi(\mathbf{i}, \partial F'). \quad (5.1)$$

Thus, the solutions of (3.4) are $E_{\varepsilon, \tau}^k = \varepsilon E_\alpha^k$ for every $\varepsilon > 0$, $k \in \mathbb{N}$, where $\{E_\alpha^k\}$ solves the scaled scheme

$$\begin{cases} E_\alpha^0 = q, \\ E_\alpha^{k+1} \in \operatorname{argmin}_{E \in \mathcal{D}, E \supset E_\alpha^k} \mathcal{F}_\alpha(E, E_\alpha^k), \quad k \geq 0. \end{cases} \quad (5.2)$$

We will prove that scheme (5.2) has a unique solution $\{E_\alpha^k\}$ whenever α is outside a countable set (see Remark 24 below). If α is greater than a threshold value $\tilde{\alpha} > 0$, the corresponding solution is trivially $E_\alpha^k \equiv q$, and we will say that the motion is *pinned*. If instead α is below the *pinning threshold* (see Definition 40) the solutions $\{E_\alpha^k\}$ have a checkerboard structure; that is, $E_\alpha^k \in \mathcal{A}^e$ for every $k \in \mathbb{N}$, and they are obtained by the iterative formula

$$Z(E_\alpha^{k+1}) = Z(E_\alpha^k) + Z(E_\alpha^1), \quad \text{for every } k \in \mathbb{N}, k \geq 1.$$

We call this process *nucleation from the origin*, and the lattice set $Z(E_\alpha^1)$, which we call the *nucleus* of the process, completely characterizes the motion. The limit evolution will be a motion of expanding polygons with constant velocity; both the velocity and the shape of the limit sets will be a discretization (depending on α) of those of the minimizing movement of (3.4) at regime $\varepsilon/\tau \rightarrow 0$ studied in Section 4. This result will be proven under a technical assumption on the ‘‘convexity’’ of the nucleus $Z(E_\alpha^1)$ (cf. (5.13)) which will allow us to use a localization method to solve any minimization problem of the scheme (5.2).

The following result is a rereading of Lemma 15 in the scaled setting. We note that, as for Lemma 15, the following result holds for every norm.

Lemma 23. *Let $\mathcal{F}_\alpha^\varphi : \mathcal{D} \times \mathcal{D} \rightarrow \mathbb{R}$ be as in (5.1), where \mathcal{D} is defined as in (2.1) with $\varepsilon = 1$. Then, for any given $E' \in \mathcal{D}$ it holds that*

$$\mathcal{F}_\alpha^\varphi(E(\mathcal{J}), E') \leq \mathcal{F}_\alpha^\varphi(E, E'), \quad \text{where } \mathcal{J} = \left\{ \mathbf{i} \in Z(E) : d^\varphi(\mathbf{i}, \partial E') \leq \frac{4}{\alpha} \right\}$$

for every $E \in \mathcal{D}$. In particular, for every $\{E_\alpha^k\}$ discrete solution of the scheme (5.2), there holds

$$Z(E_\alpha^{k+1}) \subset \left\{ \mathbf{i} \in \mathbb{Z}^2 : d^\varphi(\mathbf{i}, \partial E_\alpha^k) \leq \frac{4}{\alpha} \right\}, \quad \text{for every } k \in \mathbb{N}. \quad (5.3)$$

Proof. The result immediately follows from the fact that for every $E' \in \mathcal{D}$ the variation of adding an isolated square to any $E \in \mathcal{D}$ is $\mathcal{F}_\alpha^\varphi(E \cup q(\mathbf{i}), E') - \mathcal{F}_\alpha^\varphi(E, E') = -4 + \alpha d^\varphi(\mathbf{i}, \partial E')$. \square

Remark 24 (non-uniqueness). Note that for every $\mathbf{i} \in \mathbb{Z}^2$ such that $d^\varphi(\mathbf{i}, \partial E_\alpha^k) = \frac{4}{\alpha}$ (if any), the energy contribution of the square $q(\mathbf{i})$ is zero; that is,

$$\mathcal{F}_\alpha^\varphi(E_\alpha^{k+1} \cup q(\mathbf{i}), E_\alpha^k) = \mathcal{F}_\alpha^\varphi(E_\alpha^{k+1} \setminus q(\mathbf{i}), E_\alpha^k).$$

Therefore, in this case, there is non-uniqueness of solutions for the problem (5.2). Note that, if $\varphi(\mathbf{x}) = \frac{4}{\alpha}$ has no integer solutions then, by the periodicity of \mathbb{Z}^2 , the same holds true for equation $d^\varphi(\mathbf{x}, \partial E) = \frac{4}{\alpha}$ for every $E \in \mathcal{D}$. This in particular implies that the k -th minimization problem of the scheme (5.2) has non-unique solution if and only if the first minimization problem has non-unique solution.

With the previous remark in mind, we define the *singular set* Λ^φ as

$$\Lambda^\varphi := \left\{ \frac{4}{\varphi(\mathbf{i})} : \mathbf{i} \in \mathbb{Z}_e^2 \setminus \{(0,0)\} \right\}. \quad (5.4)$$

Note that the set Λ^φ is countable and has a unique accumulation point in 0.

Example 25. We take φ as the ℓ^∞ -norm and choose $\alpha = 4$, so that $\alpha \in \Lambda^\varphi$ as defined in (5.4). In this case, the set of lattice points having zero energy is $\{\mathbf{i} \in \mathbb{Z}^2 : \|\mathbf{i}\|_\infty = 1\}$. This yields that $\mathcal{F}_\alpha^\varphi(q, q) = \mathcal{F}_\alpha^\varphi(E, q) = -4$ for every admissible set $E \subset q \cup \{q(\mathbf{i}) : |i_1| = |i_2| = 1\}$ which implies that the minimum of the first step of (5.2) is not unique. As already noted in Remark 24, the same situation arises at each minimization step of the scheme (5.2).

Without entering into the details, we may check that every parametrized family $E : [0, +\infty) \rightarrow \mathcal{X}$ of connected sets satisfying

$$E(0) = \{(0,0)\}, \quad E(t) \subset E(s) \text{ for every } t < s, \quad \|v_\perp(t)\|_\infty \leq 4 \text{ for every } t \geq 0, \quad (5.5)$$

is a minimizing movement, where v_\perp denotes the normal velocity of $\partial E(t)$. Indeed, for every fixed $t > 0$, from (5.5) we have $E(t) \subseteq [-4t, 4t]^2$, since $E(t)$ is connected. Then, for any $\tau > 0$ define

$$E_{\varepsilon, \tau}^k := E(E(k\tau) \cap \varepsilon \mathbb{Z}_e^2).$$

Since $E(k\tau) \subseteq [-4k\tau, 4k\tau]^2 = [-k\varepsilon, k\varepsilon]^2$, $E_{\varepsilon, \tau}^k$ can be obtained by solving the first k steps of (3.4). The corresponding discrete solutions $E_{\varepsilon, \tau}(t)$ converge to $E(t)$ as $\varepsilon, \tau \rightarrow 0$ in the Hausdorff sense for every $t > 0$, whence $E(t)$ is a minimizing movement.

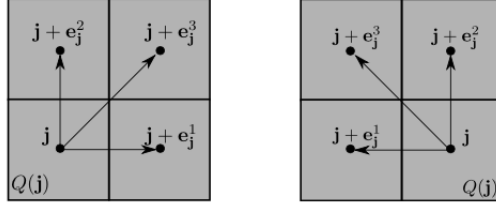


Figure 7: Examples of 2×2 squares of the covering. On the left the case $j_1, j_2 > 0$, on the right $j_1 > 0, j_2 < 0$.

5.1 A localization argument: the 2×2 -square tiling

In order to determine the optimal structure of a minimizer, we will argue locally by defining the following covering of admissible sets.

Definition 26 (2×2 -square coverings). For every $\mathbf{j} = (j_1, j_2) \in \mathbb{Z}^2$, we define the vectors $\mathbf{e}_j^1 = (\text{sgn}(j_1), 0)$, $\mathbf{e}_j^2 = (0, \text{sgn}(j_2))$, $\mathbf{e}_j^3 = \mathbf{e}_j^1 + \mathbf{e}_j^2$ and, correspondingly, the 2×2 square (see Fig. 7)

$$Q(\mathbf{j}) := q(\mathbf{j}) \cup \bigcup_{k=1}^3 q(\mathbf{j} + \mathbf{e}_j^k). \quad (5.6)$$

Let $E \in \mathcal{D}$ be an admissible set. Then, we define the family of sets

$$\mathcal{S}_e(E) := \{Q(\mathbf{j}) : \mathbf{j} \in \mathbb{Z}_e^2 \text{ with } j_1, j_2 \text{ odd, } Q(\mathbf{j}) \cap E \neq \emptyset\}, \quad (5.7)$$

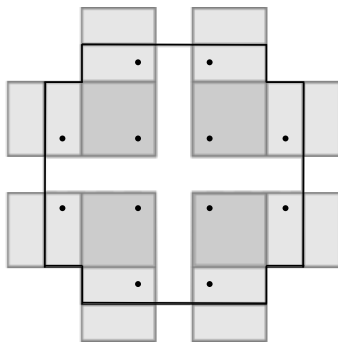


Figure 8: The picture clarifies the 2×2 -square covering for a set E , whose boundary is marked by a bold black line. The darker 2×2 squares are in $\mathcal{S}_e^c(E)$, the lighter ones in $\mathcal{S}_e^b(E)$. The areas in white are those left uncovered.

which is a covering of non-overlapping squares of $E \setminus \mathcal{C}_0$, where $\mathcal{C}_0 := \bigcup\{q(\mathbf{i}) \mid i_1 i_2 = 0\}$ (see Fig. 8). We can subdivide the squares of $\mathcal{S}_e(E)$ in those contained in E and those that are not, defining the partition $\mathcal{S}_e(E) = \mathcal{S}_e^b(E) \cup \mathcal{S}_e^c(E)$ where $\mathcal{S}_e^c(E) = \{Q(\mathbf{j}) \in \mathcal{S}_e(E) \mid Q(\mathbf{j}) \subseteq E\}$ and $\mathcal{S}_e^b(E) = \{Q(\mathbf{j}) \in \mathcal{S}_e(E) \mid Q(\mathbf{j}) \cap E^c \neq \emptyset\}$.

5.2 Choice of the dissipation term

We restrict our analysis to dissipations (3.2) induced by an absolute norm φ ; *i.e.*, $\varphi(\mathbf{x})$ depends only on $|x_1|$ and $|x_2|$, with the additional assumptions

(H1) φ is symmetric (or permutation invariant); that is, $\varphi(x_1, x_2) = \varphi(x_2, x_1)$ for every $\mathbf{x} \in \mathbb{R}^2$;

(H2) φ complies with the normalization condition $\varphi(1, 0) = \varphi(0, 1) = 1$.

We refer to an absolute norm with these properties as a *symmetric absolute normalized norm*. The ℓ^p -norms, $1 \leq p \leq \infty$, are examples of such norms. This choice is of course motivated by the symmetry properties of the corresponding unit balls, which simplify the computations and the arguments of the proofs. Moreover, as remarked in Section 2.4 an absolute norm is a submodular function on \mathbb{R}^2 , a property that will be crucial in the sequel as it will allow to reduce the main minimization problem to a finite number of local minimization problems, taking into account four-point interactions. Indeed, we can infer from (2.10) a submodularity-type inequality involving only the norms of the four lattice points contained in any of the 2×2 squares of the coverings defined above. Namely,

$$\varphi(\mathbf{i}) + \varphi(\mathbf{i} + \mathbf{e}_i^3) \leq \varphi(\mathbf{i} + \mathbf{e}_i^1) + \varphi(\mathbf{i} + \mathbf{e}_i^2), \quad (5.8)$$

for every $\mathbf{i} \in \mathbb{Z}^2$.

5.3 The first step of the evolution: checkerboards nucleating from a point

With the covering argument of Section 5.1 and the key norm inequality (5.8) at hand, we are now in position to give the explicit characterization of the first step E_α^1 of the discrete evolution, showing that it is an even checkerboard. A local analysis by means of the 2×2 -square tilings will allow us to prove, with the following Proposition 27, that the set of centers of E_α^1 coincides with

the discretization of the ball $B_{\frac{4}{\alpha}}$ on the even lattice \mathbb{Z}_e^2 . We stress the generality of the following result, which only requires φ to be an absolute norm without any additional assumption, in particular we do not assume (H1) and (H2).

Proposition 27. *Let φ be an absolute norm, let $\alpha > 0$ be such that $\alpha \notin \Lambda^\varphi$ and let $\mathcal{F}_\alpha^\varphi$ be as in (5.1). Then the first minimization problem of scheme (5.2) has a unique solution*

$$E_\alpha^1 = \operatorname{argmin}_{E \in \mathcal{D}, E \supset q} \mathcal{F}_\alpha^\varphi(E, q)$$

and it satisfies

$$E_\alpha^1 = E(\mathbb{Z}_e^2 \cap B_{\frac{4}{\alpha}}). \quad (5.9)$$

In particular, $E_\alpha^1 \in \mathcal{A}_{\text{conv}}^e$.

Proof. The argument does not require the normalization assumption (H2); we then set

$$\varphi_{\max} := \max\{\varphi(1, 0), \varphi(0, 1)\}, \quad \varphi_{\min} := \min\{\varphi(1, 0), \varphi(0, 1)\},$$

and we assume, without loss of generality, that $\varphi_{\max} = \varphi(1, 0)$. Note that $\frac{4}{\varphi_{\min}}, \frac{4}{\varphi_{\max}} \in \Lambda^\varphi$.

If $\alpha > \frac{4}{\varphi_{\min}}$ we get $E_\alpha^1 = q$ since $\mathcal{F}_\alpha^\varphi(q(\mathbf{i}), q) > 0$ for every $\mathbf{i} \in \mathbb{Z}^2 \setminus \{(0, 0)\}$ and (5.9) trivially holds. If $\frac{4}{\varphi_{\max}} < \alpha < \frac{4}{\varphi_{\min}}$, we get that for any $\mathbf{i} = (i_1, i_2)$ with $i_1 \neq 0$ there holds $\mathcal{F}_\alpha^\varphi(q(\mathbf{i}), q) > 0$, thus $Z(E_\alpha^1) \subset \{0\} \times \mathbb{Z}$.



Figure 9: Clusters of two or three lattice points are “locally” not energetically convenient.

Let $E \in \mathcal{D}$ be a competitor such that $Z(E) \subset \{0\} \times \mathbb{Z}$. If $\mathbf{i} \in Z(E) \setminus \{(0, 0)\}$ has two nearest-neighbors, removing $q(\mathbf{i})$ leaves the total perimeter unchanged but decreases the dissipation (see Figure 9). If instead \mathbf{i} has only one nearest-neighbor $\mathbf{i}' \neq (0, 0)$, if $|i_2| < |i'_2|$ then shifting $q(\mathbf{i})$ towards the origin does not decrease the perimeter but reduces the dissipation; if instead $|i_2| > |i'_2|$ the same holds shifting $q(\mathbf{i}')$ (see Figure 9). Hence, we may restrict our analysis to the two configurations $E(\mathbb{Z}_e^2 \cap B_{\frac{4}{\alpha}})$ and $E(\mathbb{Z}_o^2 \cap B_{\frac{4}{\alpha}}) \cup q$. A comparison between the two energy contributions yields that the variation from the odd checkerboard to the even one is less than 0, thus $E_\alpha^1 = E(\mathbb{Z}_e^2 \cap B_{\frac{4}{\alpha}})$.

Now let $\alpha < \frac{4}{\varphi_{\max}}$. We consider the covering described in Definition 26. First, we note that the energy of every admissible set E complies with the estimate

$$\mathcal{F}_\alpha^\varphi(E, q) \geq \sum_{Q(\mathbf{j}) \in \mathcal{S}_e(\mathbb{R}^2)} \mathcal{F}_\alpha^\varphi(E \cap Q(\mathbf{j}), q) + \mathcal{F}_\alpha^\varphi(E \cap \mathcal{C}_0, q), \quad (5.10)$$

the equality holding if and only if $\{E \cap Q(\mathbf{j})\}$ and $E \cap \mathcal{C}_0$ are non-overlapping; this is the case of sets E having a checkerboard structure. Inequality (5.10) corresponds to localizing the energy, neglecting interactions between neighboring squares.

From Lemma 23, we can reduce our analysis to admissible sets contained in $E_{\alpha, \varphi} := \mathbb{Z}^2 \cap B_{\frac{4}{\alpha}}^\varphi$ and inequality (5.10) holds restricting the sum to every $Q(\mathbf{j}) \in \mathcal{S}_e(E_{\alpha, \varphi})$ since $\mathcal{F}_\alpha^\varphi(q(\mathbf{j}), q) > 0$ for every $\varphi(\mathbf{j}) > \frac{4}{\alpha}$. We will prove that

$$\begin{aligned} \min_{E \in \mathcal{D}, E \supset q} \mathcal{F}_\alpha^\varphi(E \cap Q(\mathbf{j}), q) &= \mathcal{F}_\alpha^\varphi(E(\mathbb{Z}_e^2 \cap B_{\frac{4}{\alpha}}^\varphi) \cap Q(\mathbf{j}), q) \\ \min_{E \in \mathcal{D}, E \supset q} \mathcal{F}_\alpha^\varphi(E \cap \mathcal{C}_0, q) &= \mathcal{F}_\alpha^\varphi(E(\mathbb{Z}_e^2 \cap B_{\frac{4}{\alpha}}^\varphi) \cap \mathcal{C}_0, q) \end{aligned} \quad (5.11)$$

for every $Q(\mathbf{j}) \in \mathcal{S}_e(E_{\alpha,\varphi})$; that is, the optimal structure is an even checkerboard set in each of the following cases: (a) inside $Q(\mathbf{j}) \in \mathcal{S}_e^c(E_{\alpha,\varphi})$; (b) inside $Q(\mathbf{j}) \in \mathcal{S}_e^b(E_{\alpha,\varphi})$; (c) on $E_{\alpha,\varphi} \cap \mathcal{C}_0$. In the sequel, E will denote a general competitor $E \in \mathcal{D}$, $E \subset E_{\alpha,\varphi}$.

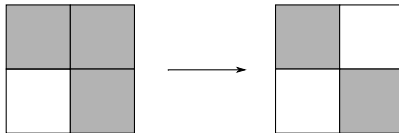


Figure 10: It is convenient to remove $q(\mathbf{i})$ if \mathbf{i} has two nearest-neighbors.

(a) Consider $Q(\mathbf{j}) \in \mathcal{S}_e^c(E_{\alpha,\varphi})$ and let $q(\mathbf{i}) \subset Q(\mathbf{j}) \cap E$. Note that the class $\mathcal{S}_e^c(E)$ is not empty if and only if $\alpha < \frac{\varphi_{\max}}{2}$. Moreover, since adding an isolated square in $Q(\mathbf{j})$ is always energetically convenient, we can restrict to configurations of $Q(\mathbf{j}) \cap E$ consisting of exactly two squares $q(\mathbf{i}')$ and $q(\mathbf{i}'')$ (see Fig. 10). Now, if $q(\mathbf{i}') \cup q(\mathbf{i}'')$ has no checkerboard structure; that is, \mathbf{i}' and \mathbf{i}'' are nearest-neighbors, both the checkerboard configurations E' and E'' , containing $q(\mathbf{i}')$ and $q(\mathbf{i}'')$ respectively, decrease the energy. Indeed, the corresponding variation of the energy is given by

$$\mathcal{F}_\alpha^\varphi(E', q) - \mathcal{F}_\alpha^\varphi(q(\mathbf{i}') \cup q(\mathbf{i}''), q) \leq -2 + \alpha\varphi_{\max}, \quad \mathcal{F}_\alpha^\varphi(E'', q) - \mathcal{F}_\alpha^\varphi(q(\mathbf{i}') \cup q(\mathbf{i}''), q) \leq -2 + \alpha\varphi_{\max}.$$

This variation is never positive, since when $\alpha > \frac{2}{\varphi_{\max}}$ the class $\mathcal{S}_e(E_{\alpha,\varphi})$ is empty. Thus, any

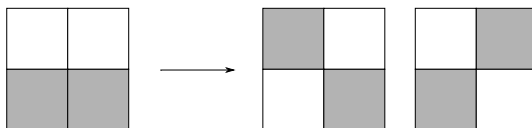


Figure 11: Any checkerboard configuration inside $Q(\mathbf{j})$ is a competitor with less energy.

checkerboard configuration inside $Q(\mathbf{j})$ is a competitor with less energy than E (see Fig. 11). Now we should compare the energies of the two possible checkerboard configurations inside $Q(\mathbf{j})$. For this, we note that the variation of the energy in order to pass from the odd checkerboard configuration $q(\mathbf{j} + \mathbf{e}_j^1) \cup q(\mathbf{j} + \mathbf{e}_j^2)$ to the even one $q(\mathbf{j}) \cup q(\mathbf{j} + \mathbf{e}_j^3)$ is

$$\begin{aligned} \mathcal{F}_\alpha^\varphi(q(\mathbf{j}) \cup q(\mathbf{j} + \mathbf{e}_j^3), q) - \mathcal{F}_\alpha^\varphi(q(\mathbf{j} + \mathbf{e}_j^1) \cup q(\mathbf{j} + \mathbf{e}_j^2), q) \\ = \alpha(\varphi(\mathbf{j}) + \varphi(\mathbf{j} + \mathbf{e}_j^3) - \varphi(\mathbf{j} + \mathbf{e}_j^1) - \varphi(\mathbf{j} + \mathbf{e}_j^2)), \end{aligned}$$

which is non-positive by (5.8).

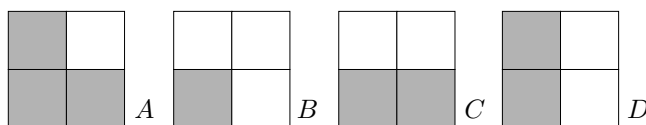


Figure 12: The possible cases of $Q(\mathbf{j}) \cap E_{\alpha,\varphi}$.

(b) Now, let $Q(\mathbf{j}) \in \mathcal{S}_e^b(E_{\alpha,\varphi})$. Without loss of generality, we may assume that $j_1, j_2 > 0$, the situation being completely symmetric in the other cases. Inside such a 2×2 square, we have four possible cases for $Q(\mathbf{j}) \cap E_{\alpha,\varphi}$, as pictured in Fig. 12. We claim that the configuration with minimal energy inside $Q(\mathbf{j})$ is a checkerboard set. Consider first $\alpha > \frac{2}{\varphi_{\max}}$, then $\mathbf{i} \in B_{\frac{1}{\alpha}}^\varphi$ if and

only if $|i_1| \leq 1$, thus the only possible cases for $Q(\mathbf{j}) \cap E_{\alpha, \varphi}$ are those labeled by B and D in Fig. 12. Since

$$\mathcal{F}_\alpha^\varphi(q(\mathbf{j}), q) < \mathcal{F}_\alpha^\varphi(\mathbf{e}_j^2, q), \quad \mathcal{F}_\alpha^\varphi(q(\mathbf{j}), q) - \mathcal{F}_\alpha^\varphi(q(\mathbf{j}) \cup q(\mathbf{j} + \mathbf{e}_j^2), q) = 2 - \alpha\varphi_{\max} < 0$$

in both cases the optimal configuration is $q(\mathbf{j})$. Consider now $\alpha < \frac{2}{\varphi_{\max}}$. Reasoning as before we can assume $Q(\mathbf{j}) \cap E = q(\mathbf{i}') \cup q(\mathbf{i}'')$. In cases B , C and D , if \mathbf{i}' and \mathbf{i}'' were nearest neighbors, with, *e.g.*, $\varphi(\mathbf{i}') > \varphi(\mathbf{i}'')$, then removing $q(\mathbf{i}')$ would produce a negative variation; that is,

$$\mathcal{F}_\alpha^\varphi(q(\mathbf{i}''), q) - \mathcal{F}_\alpha^\varphi(q(\mathbf{i}') \cup q(\mathbf{i}''), q) \leq 2 - \alpha\varphi(\mathbf{i}') < 2 - \alpha\left(\frac{4}{\alpha} - \varphi_{\max}\right) \leq -2 + \alpha\varphi_{\max}.$$

Thus the minimal configuration is the even checkerboard. For what concerns the case A , since $\varphi(\mathbf{j} + \mathbf{e}_j^3) > \frac{4}{\alpha}$ and by (5.8) we have that

$$\mathcal{F}_\alpha^\varphi(q(\mathbf{j}), q) < \mathcal{F}_\alpha^\varphi(q(\mathbf{j}) \cup q(\mathbf{j} + \mathbf{e}_j^3), q) \leq \mathcal{F}_\alpha^\varphi(q(\mathbf{j} + \mathbf{e}_j^1) \cup q(\mathbf{j} + \mathbf{e}_j^2), q)$$

which again leads to the result.

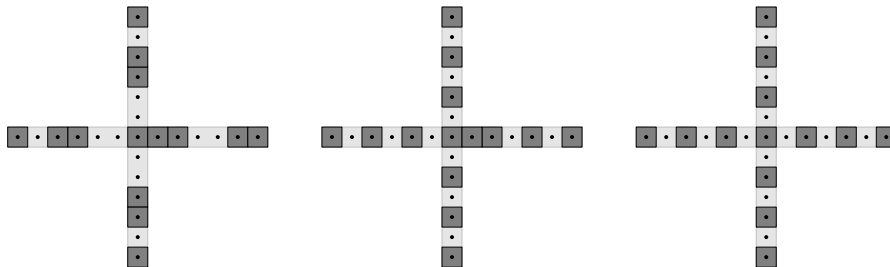


Figure 13: Optimal configuration for $E_{\alpha, \varphi} \cap \mathcal{C}_0$.

(c) Finally, we consider $E_{\alpha, \varphi} \cap \mathcal{C}_0$. Reasoning as in the case $\frac{4}{\varphi_{\max}} < \alpha < \frac{4}{\varphi_{\min}}$, we can restrict our analysis to competitors having a checkerboard structure union q on the coordinate axes. A comparison between the two energy contributions on each axis yields that the variation from the odd checkerboard to the even one is less than 0, and equals 0 if and only if $\alpha \in \Lambda$. Thus, the minimal configuration is the even checkerboard (see Figure 13). With (5.10) and the finite superadditivity of the infimum, this implies that

$$\begin{aligned} \min_{E \in \mathcal{D}, E \supset q} \mathcal{F}_\alpha^\varphi(E, q) &\geq \min_{E \in \mathcal{D}, E \supset q} \left(\sum_{Q(\mathbf{j}) \in \mathcal{S}_e(E_{\alpha, \varphi})} \mathcal{F}_\alpha^\varphi(E \cap Q(\mathbf{j}), q) + \mathcal{F}_\alpha^\varphi(E \cap \mathcal{C}_0, q) \right) \\ &\geq \sum_{Q(\mathbf{j}) \in \mathcal{S}_e(E_{\alpha, \varphi})} \min_{E \in \mathcal{D}, E \supset q} \mathcal{F}_\alpha^\varphi(E \cap Q(\mathbf{j}), q) + \min_{E \in \mathcal{D}, E \supset q} \mathcal{F}_\alpha^\varphi(E \cap \mathcal{C}_0, q) \\ &= \sum_{Q(\mathbf{j}) \in \mathcal{S}_e(E_{\alpha, \varphi})} \mathcal{F}_\alpha^\varphi(E(\mathbb{Z}_e^2 \cap B_{\frac{1}{\alpha}}^\varphi) \cap Q(\mathbf{j}), q) + \mathcal{F}_\alpha^\varphi(E(\mathbb{Z}_e^2 \cap B_{\frac{1}{\alpha}}^\varphi) \cap \mathcal{C}_0, q) \\ &= \mathcal{F}_\alpha^\varphi(E(\mathbb{Z}_e^2 \cap B_{\frac{1}{\alpha}}^\varphi), q), \end{aligned} \tag{5.12}$$

whence the equality follows, thus concluding the proof. Uniqueness comes from step (c). \square

Note that the local minimum problems studied in points (a) and (b) in the proof above might be satisfied also by the odd checkerboard if (5.8) reduces to an equality (*e.g.* when $\varphi = \|\cdot\|_1$). Nevertheless, for odd checkerboards the equality in (5.12) no longer holds and this implies that $E_{\alpha, \varphi}$ is the unique minimum.

Definition 28. For every $\alpha > 0$, $\alpha \notin \Lambda^\varphi$, we define the *nucleus* of the motion given by the scheme (5.2) as the lattice set

$$\mathcal{N}_\alpha^\varphi := Z(E_\alpha^1)$$

where $E_\alpha^1 = \operatorname{argmin}_{E \in \mathcal{D}, E \supset q} \mathcal{F}_\alpha^\varphi(E, q)$, which is well defined by Proposition 27.

We stress that the assumption on φ to be an absolute norm is crucial in order to obtain the previous structure result of Proposition 27. Indeed, if not fulfilled, the set E_α^1 may not be a checkerboard as shown by the following simple example.

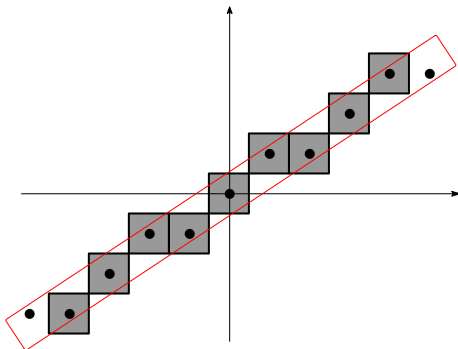


Figure 14: The black dots represent the lattice set $\mathbb{Z}^2 \cap B_{\frac{\alpha}{4}}^\varphi$, while the set E_α^1 is pictured in gray.

Example 29 (non-checkerboard minimizers). We consider the norm

$$\varphi(\mathbf{x}) = \max \left\{ \frac{|3x_1 + 2x_2|}{10}, |3x_2 - 2x_1| \right\},$$

and we assume that $\alpha \in (\frac{20}{13}, \frac{40}{21})$. In this case, for every such α , the set $B_{\frac{\alpha}{4}}^\varphi$ is a rectangle and

$$\mathcal{J}^{\varphi, \alpha} := B_{\frac{\alpha}{4}}^\varphi \cap \mathbb{Z}^2 = \{(0, 0), \pm(1, 1), \pm(2, 1), \pm(3, 2), \pm(4, 3), \pm(5, 3)\}$$

(see Fig. 14). We show that the first step of (5.2) E_α^1 is not a checkerboard set. First note that the points $(0, 0)$ and $\pm(3, 2)$ are isolated in $\mathcal{J}^{\varphi, \alpha}$ so their contribution is $-4 + \alpha\varphi(\mathbf{i})$ which is always negative, thus $Z(E_\alpha^1)$ contains these points. Hence, we are reduced to study the minimal configurations of the pairs of nearest-neighbours $\{(1, 1), (2, 1)\}$ and $\{(4, 3), (5, 3)\}$:

$$\mathcal{F}_\alpha^\varphi(q(1, 1) \cup q(2, 1), q) = -6 + 2\alpha < -4 + \alpha = \mathcal{F}_\alpha^\varphi(q(1, 1), q) = \mathcal{F}_\alpha^\varphi(q(2, 1), q)$$

and

$$\begin{aligned} \mathcal{F}_\alpha^\varphi(q(4, 3), q) &= -4 + \frac{9}{5}\alpha < -6 + \alpha \left(\frac{9}{5} + \frac{21}{10} \right) = \mathcal{F}_\alpha^\varphi(q(4, 3) \cup q(5, 3), q) \\ &< -4 + \alpha \frac{21}{10} = \mathcal{F}_\alpha^\varphi(q(5, 3), q). \end{aligned}$$

The same holds for $\{(-1, -1), (-2, -1)\}$ and $\{(-4, -3), (-5, -3)\}$, and this gives that

$$E_\alpha^1 = E(\mathcal{J}^{\varphi, \alpha} \setminus \{\pm(5, 3)\})$$

which is not a checkerboard (see Fig. 14).

We conclude noting that, if we renounce to the monotonicity constraint $E \supset q$, the minimization problem above may admit, for suitable values of α , also a checkerboard solution E_α^1 of odd parity. In order not to distract the reader's attention from the monotone case, we prefer to postpone this generalization of Proposition 27 to Subsection 6.2 (see Proposition 48).

5.4 The structure result for non-trivial initial datum

Proposition 27 shows that the first step E_α^1 of discrete scheme (5.2) is a checkerboard set and that $Z(E_\alpha^1)$ is a \mathbb{Z}_e^2 -convex set (see Definition 3). Our aim now is to prove that an analogous structure result can be obtained for minimizers of the energy $\mathcal{F}_\alpha^\varphi(\cdot, E)$, where φ is a symmetric absolute normalized norm (see Section 5.2), also for a general $E \in \mathcal{A}_{\text{conv}}$ fulfilling suitable assumptions (see (5.13) below), and then to iteratively apply it to $E = E_\alpha^{k-1}$ for $k \geq 1$. The proof of this stability result will rely on a localization argument only reminiscent of that used in the proof of Proposition 27. Indeed, we have to face a technical issue: since the dissipation term $D^\varphi(\cdot, E)$ does not satisfy a submodularity inequality analogous to (5.8), the 2×2 -square covering no longer works. We will then define suitable coverings “outside” every discrete edge (see Definition 7) of E which mimic the 2×2 -square covering, and then match them altogether. For this, we need the following “convexity” conditions:

(i) on the norm, we assume that

$$(H3) \quad \varphi(h, h+1) - \varphi(h, h) \geq \frac{1}{2}, \quad \text{for every } h \in \mathbb{N};$$

(ii) on the structure of $\partial^{\text{eff}} E$, we require that

$$\theta(\boldsymbol{\nu}(\ell'), \boldsymbol{\nu}(\ell)) < 0 \quad \text{for every } \ell, \ell' \in \mathcal{E}(E) \text{ such that } \ell \text{ precedes (clockwise) } \ell', \quad (5.13)$$

where θ is introduced in Definition 1.

The ℓ^p -norms, $1 \leq p \leq \infty$, are a class of norms complying with (H1)–(H3). We also note that assumption (H3) will play a role only in Step 5 of the proof of Proposition 30.

In order to avoid some (interesting) pathological phenomena (as a one-dimensional motion, see Example 37), we assume non-degeneracy conditions on the sets E and on the minimizer of $\mathcal{F}_\alpha^\varphi(\cdot, E)$; namely, (H2) and (2.3). Finally, to simplify the exposition, we assume that

$$E \text{ is symmetric with respect to the axes and the lines } x_2 = \pm x_1. \quad (5.14)$$

We now state the main result of this section.

Proposition 30. *Let φ be a symmetric absolute normalized norm complying with (H3) and let $\alpha > 0$ be such that $\alpha \notin \Lambda^\varphi$. Let $E \in \mathcal{A}_{\text{conv}}^e$ be a set satisfying (2.3), (5.13) and (5.14). Then there exists a unique solution of the minimization problem*

$$E_\alpha = \operatorname{argmin}_{E' \supset E, E' \in \mathcal{D}} \mathcal{F}_\alpha^\varphi(E', E) \quad (5.15)$$

and it satisfies

$$Z(E_\alpha) = \left\{ \mathbf{i} \in \mathbb{Z}_e^2 : d^\varphi(\mathbf{i}, E) < \frac{4}{\alpha} \right\}. \quad (5.16)$$

In particular, $E_\alpha \in \mathcal{A}_{\text{conv}}^e$.

Before entering in the details of the proof, we premise some remarks.

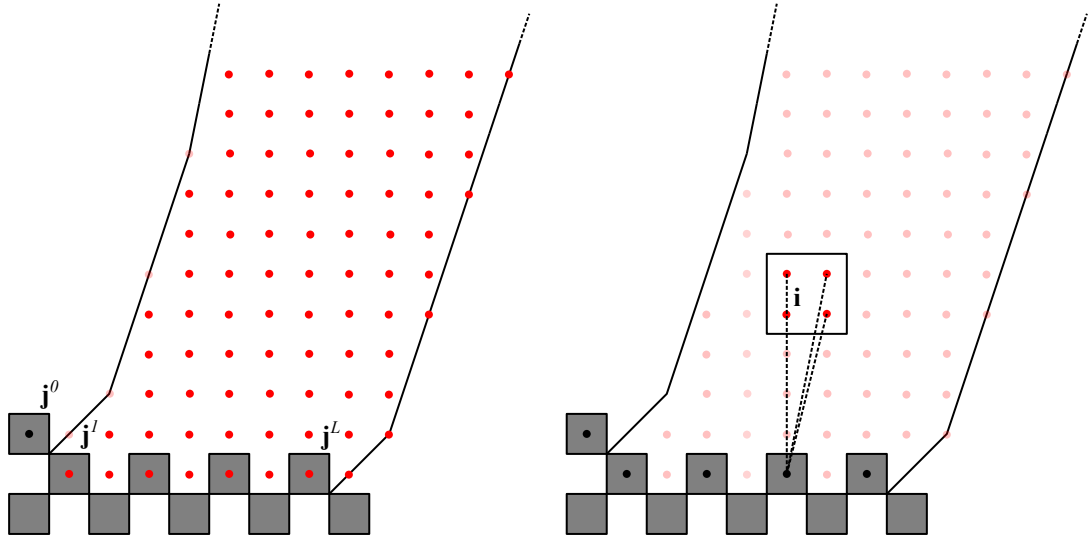


Figure 15: In red an example of $A(\ell)$ for ℓ as in (ii) of Remark 8. On the left, lighter dots are outside $A(\ell)$. On the right, the projection of the centers of a 2×2 -square on a common point of ℓ .

Remark 31 (Projection of a 2×2 square). Let E be given as in the statement of Proposition 30. We partition the lattice points of the region of the plane “outside” E into sets $A(\ell)$ according to the discrete edge $\ell \in \mathcal{E}(E)$ they project onto. We follow the classification of discrete edges given in Remark 8, and we start with case (ii); that is, $\ell \subset \{\mathbf{x} \in \mathbb{R}^2 : x_2 > 0\}$ and $s(\ell) \in (0, \frac{1}{3}]$. For such edges we define the set

$$A(\ell) := \{\mathbf{i} \in \mathbb{Z}^2 : i_1 \geq j_1^1, i_2 \geq j_2^1, \pi_E^\varphi(\mathbf{i}) \subset \{\mathbf{j}^l\}_{l=1}^L \text{ or } \pi_E^\varphi(\mathbf{i}) \ni \mathbf{j}^L\}, \quad (5.17)$$

consisting of all the lattice points that project on $\ell \setminus \{\mathbf{j}^0\}$ (Fig. 15). The choice of excluding the points projecting also on \mathbf{j}^0 , although arbitrary, will simplify the definition of the covering in the proof of Proposition 30; moreover, thanks to this choice, if ℓ and ℓ' are two consecutive edges then $A(\ell)$ and $A(\ell')$ are disjoint.

We can assume, up to translations and for the sake of simplicity, that $\ell := \{\mathbf{j}^l\}_{l=0}^L = \{(1, 1)\} \cup \{(2l, 0)\}_{l=1}^L$. From the fact that φ is monotonic, for every $\mathbf{i} \in A(\ell)$ it holds that

$$\pi_E^\varphi(\mathbf{i}) \ni \begin{cases} \mathbf{j}^l & 2l - 1 \leq i_1 \leq 2l + 1 \text{ with } 0 < l < L \\ \mathbf{j}^L & i_1 \geq 2L - 1. \end{cases}$$

This yields that for every $\mathbf{i} \in A(\ell)$ such that $Z(Q(\mathbf{i})) \subset A(\ell)$ there holds

$$\left(\bigcap_{\mathbf{j} \in Z(Q(\mathbf{i}))} \pi_E^\varphi(\mathbf{j}) \right) \cap (\ell \setminus \{\mathbf{j}^0\}) \neq \emptyset. \quad (5.18)$$

This means that the four lattice points inside $Q(\mathbf{i})$ project onto a common point of ℓ , see Fig. 15. An analogous result holds in case (i) of Remark 8, when $s(\ell) = 0$.

Now consider $\ell \in \mathcal{E}(E)$ complying with case (iii) of Remark 8; that is, $\ell \subset \{\mathbf{x} \in \mathbb{R}^2 : x_2 > 0\}$ and $s(\ell) \in (\frac{1}{3}, 1)$. In this case the sets of lattice points that project on $\ell \setminus \{\mathbf{j}^L\}$ is defined as

$$A(\ell) := \{\mathbf{i} \in \mathbb{Z}^2 : \|\mathbf{i} - (j_1^0, j_2^{L-1})\|_1 \geq |j_2^0 - j_2^{L-1}|, i_2 \geq j_2^{L-1}, \pi_E^\varphi(\mathbf{i}) \subset \{\mathbf{j}^l\}_{l=0}^{L-1} \text{ or } \pi_E^\varphi(\mathbf{i}) \ni \mathbf{j}^{L-1}\}, \quad (5.19)$$

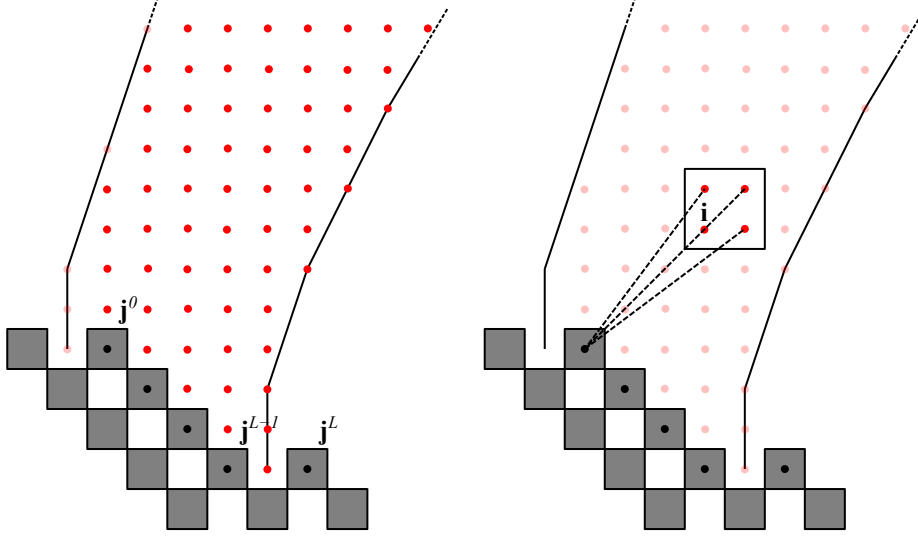


Figure 16: In red an example of $A(\ell)$ for ℓ as in (iii) of Remark 8. On the left, lighter dots are outside $A(\ell)$. On the right, the projection of the centers of a 2×2 -square on a common point of ℓ .

see Fig. 16. For simplicity we can assume, up to translations, that $\ell = \{\mathbf{j}^l\}_{l=0}^L = \{(l, -l)\}_{l=0}^{L-1} \cup \{(L+1, -L+1)\}$. From the symmetry assumption (H1) there holds

$$\pi_E^\varphi(\mathbf{i}) \ni \begin{cases} \mathbf{j}^0 & i_1 - i_2 \leq 1 \\ \mathbf{j}^l & 2l - 1 \leq i_1 - i_2 \leq 2l + 1 \text{ with } 0 < l < L. \end{cases}$$

This can be seen by characterizing the projection of points $\mathbf{i} \in A(\ell)$ of coordinates $\mathbf{i} = (h, h)$ and $(h+1, h)$ with $h \in \mathbb{N}$, since the other cases reduce to this situation from the translation invariance of the distance. Thus, assume by contradiction that there exist h and $0 < l < L$ such that $\varphi(\mathbf{i} - \mathbf{j}^l) = \varphi(h-l, h+l) < \varphi(h, h) = \varphi(\mathbf{i} - \mathbf{j}^0)$. We reduce to $l \leq h$ from the fact that φ is monotonic. Then, by (H1) and convexity we get

$$\varphi(h, h) \leq \frac{1}{2}\varphi(h+l, h-l) + \frac{1}{2}\varphi(h-l, h+l) = \varphi(h-l, h+l),$$

leading to a contradiction. As for the case $\mathbf{i} = (h+1, h)$, assuming that $\varphi(\mathbf{i} - \mathbf{j}^l) < \varphi(\mathbf{i} - \mathbf{j}^0)$ again by (H1) and convexity we get

$$\varphi(h+1, h) \leq \frac{h+1}{2h+1}\varphi(h+1-l, h+l) + \frac{h}{2h+1}\varphi(h+l, h+1-l) = \varphi(h+1-l, h+l)$$

and we obtain a contradiction. Hence, for every $\mathbf{i} \in A(\ell)$ such that $Z(Q(\mathbf{i})) \subset A(\ell)$ there holds

$$\left(\bigcap_{\mathbf{j} \in Z(Q(\mathbf{i}))} \pi_E^\varphi(\mathbf{j}) \right) \cap (\ell \setminus \{\mathbf{j}^L\}) \neq \emptyset; \quad (5.20)$$

again, as for (5.18), (5.20) means that the lattice points inside $Q(\mathbf{i})$ project onto a common point of ℓ , see Fig. 16. An analog of (5.20) holds in the case (iv) of Remark 8.

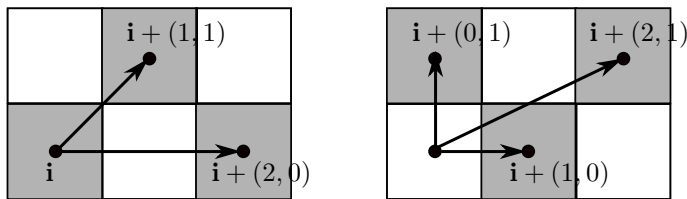


Figure 17: The triples of points involved in (5.21).

Remark 32. In order to compare the energies of checkerboard configurations with different parities inside certain rectangular tiles, it will be useful to establish some inequalities involving the dissipation term.

Consider E as in the statement of Proposition 30 and $\ell \in \mathcal{E}(E)$ such that $\ell \subset \{\mathbf{x} \in \mathbb{R}^2 : x_2 > 0\}$ and $s(\ell) \in [0, 1]$. For the sake of simplicity we can assume (up to a translation) that $\mathbf{j}^L = (0, 0)$ where $\ell = \{\mathbf{j}^l\}_{l=0}^L$. If $s(\ell) \in [0, \frac{1}{3}]$, for every $\mathbf{i} \in A(\ell)$ with $i_1 \in 2\mathbb{Z}$ such that (5.18) holds, from (5.8) and the properties of φ one can infer (see Fig. 17) the inequality

$$\begin{aligned} d^\varphi(\mathbf{i}, E) + d^\varphi(\mathbf{i} + (1, 1), E) + d^\varphi(\mathbf{i} + (2, 0), E) \\ \leq d^\varphi(\mathbf{i} + (0, 1), E) + d^\varphi(\mathbf{i} + (1, 0), E) + d^\varphi(\mathbf{i} + (2, 1), E). \end{aligned} \quad (5.21)$$

The same inequality holds if $s(\ell) \in (\frac{1}{3}, 1]$, for every $\mathbf{i} \in A(\ell)$ with $\mathbf{i} \in \mathbb{Z}_e^2$ such that (5.20) holds.

Indeed, (5.18) and (5.20) ensure the existence of some $\mathbf{j}' \in \ell$ such that $d^\varphi(\mathbf{j}, E) = \varphi(\mathbf{j} - \mathbf{j}')$ for every $\mathbf{j} \in Z(Q(\mathbf{i}))$. Hence (5.8) reads

$$d^\varphi(\mathbf{i}, E) + d^\varphi(\mathbf{i} + (1, 1), E) \leq d^\varphi(\mathbf{i} + (0, 1), E) + d^\varphi(\mathbf{i} + (1, 0), E). \quad (5.22)$$

Now, from the fact that $i_2 \geq j'_2$ (see Remark 31) and the monotonicity of the norm φ , we have $\varphi(\mathbf{i} + (2, 0) - \mathbf{j}') \leq \varphi(\mathbf{i} + (2, 1) - \mathbf{j}')$, whence we get

$$d^\varphi(\mathbf{i} + (2, 0), E) \leq d^\varphi(\mathbf{i} + (2, 1), E). \quad (5.23)$$

Inequality (5.21) then follows by adding term by term (5.22) and (5.23).

Remark 33. As a last preparatory remark to the proof of Proposition 30, we analyze and motivate assumption (5.13) on the sets that intervene in minimization problem (5.15). Assumption (5.13) ensures that for every discrete edge there are infinitely many 2×2 -squares whose centers project onto it. This property is crucial to define a well-posed covering argument (see Section 5.5). Specifically, let E be as in the statement of Proposition 30 and $\ell \in \mathcal{E}(E)$ be such that $\ell \subset \{\mathbf{x} \in \mathbb{R}^2 : x_2 > 0\}$ and

$$s(\ell) \in [0, 1]. \quad (5.24)$$

We claim that, for every such ℓ the following property holds:

$$\text{for every } h \in \mathbb{N} \text{ there exists } \mathbf{i} \in A(\ell) \cap (\mathbb{Z} \times \{h\}) \cap \mathbb{Z}_e^2 : Z(Q(\mathbf{i})) \subset A(\ell), \quad (5.25)$$

where we have set $\ell = \{\mathbf{j}^l\}_{l=0}^L$ and $\mathbf{j}^L = (0, 0)$ for simplicity. This claim is proved inductively (on parameter labeling clockwise consecutive discrete edges) by showing that for any triple of consecutive edges of E , say ℓ^-, ℓ, ℓ^+ with ℓ^- satisfying (5.25), we can find a point $\mathbf{i} \in (\mathbb{Z} \times \{h\}) \cap \mathbb{Z}_e^2$ for which, thanks to (5.13) and the translation invariance of the distance, there holds $d^\varphi(\mathbf{j}, \ell) \leq d^\varphi(\mathbf{j}, \ell^- \cup \ell^+)$ for every $\mathbf{j} \in Z(Q(\mathbf{i}))$ and every $h \geq 0$.

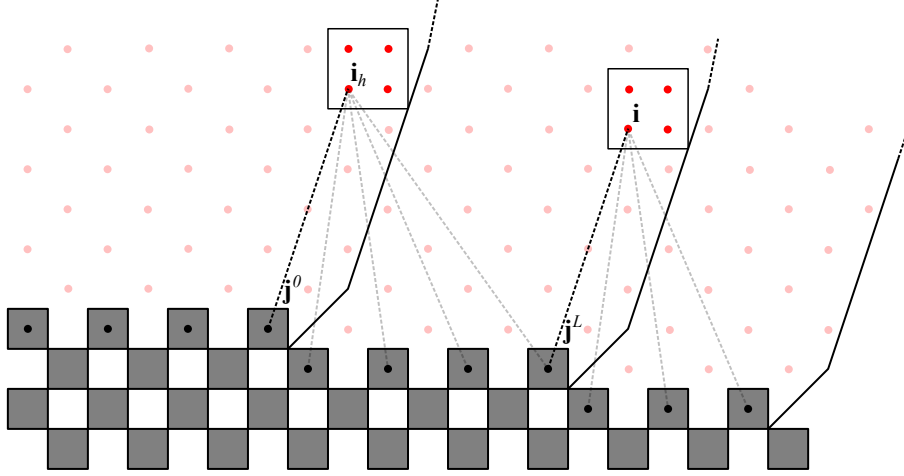


Figure 18: An example of the situation described in Remark 33 in the case $s(\ell) \leq \frac{1}{3}$. The lighter dots represent the points of \mathbb{Z}_e^2 inside $A(\ell^-)$, $A(\ell)$ and $A(\ell^+)$.

Let $\ell_0 = \{\mathbf{j}_0^l\}_{l=0}^{L_0}$ be the first (clockwise-ordered) edge such that $s(\ell) \geq 0$ and set

$$\ell'_0 := \begin{cases} \ell_0 & \text{if } \nu(\ell_0) = (0, 1) \\ \{\mathbf{j}_0^0\} & \text{otherwise.} \end{cases}$$

It is straightforward that (5.25) is satisfied for $\ell = \ell'_0$ (reasoning as in Remark 31) where we have set

$$A(\mathbf{j}_0^0) = \{\mathbf{i} \in \mathbb{Z}^2 : \pi_E^{\varphi}(\mathbf{i}) \ni \mathbf{j}_0^0\}. \quad (5.26)$$

Consider $\ell, \ell^-, \ell^+ \in \mathcal{E}(E)$ satisfying (5.24), with ℓ^- preceding ℓ , ℓ preceding ℓ^+ . Write $\ell^- = \{\mathbf{j}^{-,l}\}_{l=0}^{L^-}$ and $\ell^+ = \{\mathbf{j}^{+,l}\}_{l=0}^{L^+}$. We point out that if ℓ^- coincide with $\ell_0 = \{\mathbf{j}_0^0\}$ then $\ell = \ell_0$.

Assume that ℓ^- satisfies (5.25). Consider first the case $s(\ell) \leq \frac{1}{3}$ (see Fig. 18). For any fixed $h \in \mathbb{N}$, we set $\mathbf{i}_h = \operatorname{argmax} \{i_1 : \mathbf{i} \in \mathbb{Z}_e^2, Z(Q(\mathbf{i})) \subset A(\ell^-), i_2 = h + 1\}$, which is well defined since we have assumed that ℓ^- satisfies (5.25). By Remark 31 and by definition of $A(\ell^-)$ (5.17), there holds

$$d^\varphi(\mathbf{j}, E) = \varphi(\mathbf{j} - \mathbf{j}_0) < d^\varphi(\mathbf{j}, \ell) \quad \text{for every } \mathbf{j} \in Z(Q(\mathbf{i}_h)). \quad (5.27)$$

Set $\mathbf{i} := \mathbf{i}_h + (2L - 1, -1)$ and note that $\mathbf{i} \in \mathbb{Z}_e^2$ and $i_2 = h$. Note also that the definition of \mathbf{i}_h yields $Z(Q(\mathbf{i})) \cap A(\ell^-) = \emptyset$. Then, by (5.27) and the translation invariance of the distance, since $\mathbf{j}_0 + (2L - 1, -1) = \mathbf{j}_L$ we get

$$d^\varphi(\mathbf{j}, \ell) = \varphi(\mathbf{j} - \mathbf{j}_L) < d^\varphi(\mathbf{j}, \ell + (2L - 1, -1)), \quad \text{for every } \mathbf{j} \in Z(Q(\mathbf{i})).$$

Now, (5.13) yields $d^\varphi(\mathbf{j}, \ell + (2L - 1, -1)) \leq d^\varphi(\mathbf{j}, \ell^+)$. Indeed, if $s(\ell^+) \leq \frac{1}{3}$ then $L^+ \leq L$ by (5.13), thus $\ell^+ \subset \ell + (2L - 1, -1)$. If instead $s(\ell^+) > \frac{1}{3}$ then by the monotonicity of φ we get $d^\varphi(\mathbf{j}, \ell^+) \geq \varphi(\mathbf{j} - \mathbf{j}^L)$.

Now consider the case $s(\ell) > \frac{1}{3}$ (Fig. 19). For any fixed $h \in \mathbb{N}$, we set

$$\mathbf{i}_h = \operatorname{argmax} \{i_1 : \mathbf{i} \in \mathbb{Z}_e^2, Z(Q(\mathbf{i})) \subset A(\ell^-), i_2 = h + L - 1\},$$

which is well defined as above. By Remark 31 and by definition of $A(\ell^-)$ (5.19) there holds

$$d^\varphi(\mathbf{j}, E) = \varphi(\mathbf{j} - \mathbf{j}^0) \leq \varphi(\mathbf{j} - \mathbf{j}_0) = d^\varphi(\mathbf{j}, \ell) \quad \text{for every } \mathbf{j} \in Z(Q(\mathbf{i}_h)), \quad (5.28)$$

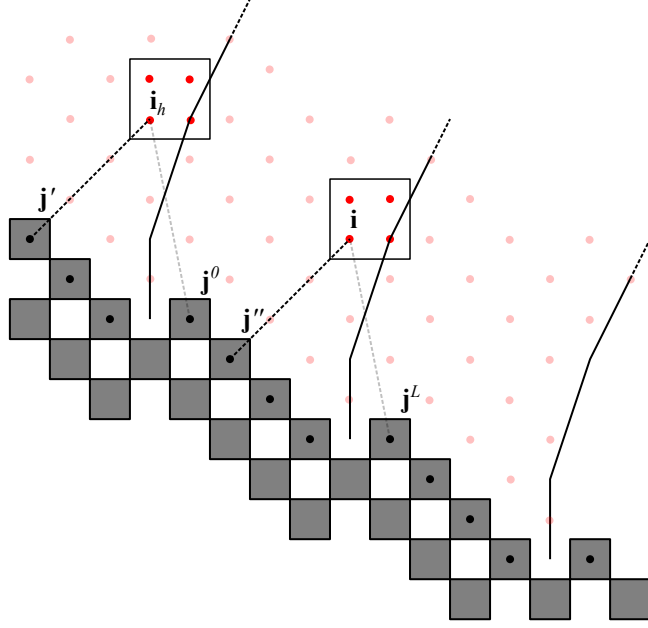


Figure 19: An example of the situation described in Remark 33 in the case $s(\ell) < \frac{1}{3}$. The lighter dots represent those points of \mathbb{Z}_e^2 lying inside $A(\ell^-)$, $A(\ell)$ and $A(\ell^+)$.

for some $\mathbf{j}' \in \{j^{-,l}\}_{l=0}^{L^- - 1}$. Again, set $\mathbf{i} := \mathbf{i}_h + (L - 1, -L + 1)$ and note that $\mathbf{i} \in \mathbb{Z}_e^2$ and $i_2 = h$. Reasoning as above we have $Z(Q(\mathbf{i})) \cap A(\ell^-) = \emptyset$. By (5.28), the translation invariance of the distance and since $\mathbf{j}'' := \mathbf{j}' + (L^- + 1, -L^- + 1) \in \{\mathbf{j}_l\}_{l=0}^{L^- - 1} \subset \ell$ we get

$$d^\varphi(\mathbf{j}, \ell) = \varphi(\mathbf{j} - \mathbf{j}'') \leq \varphi(\mathbf{j} - \mathbf{j}^L), \quad \text{for every } \mathbf{j} \in Z(Q(\mathbf{i})).$$

From (5.13) we have $s(\ell) > \frac{1}{3}$ and $L^+ \geq L$, thus $\varphi(\mathbf{j} - \mathbf{j}^L) = d^\varphi(\mathbf{j}, \ell^+)$, arguing as in Remark 31.

5.5 Proof of Proposition 30

We are now ready to prove the main result on the structure of the minimizer of $\mathcal{F}_\alpha^\varphi(\cdot, E)$. For the covering argument that we will introduce, the 2×2 -squares are not sufficient. Therefore, we define a new class of tiles for the covering.

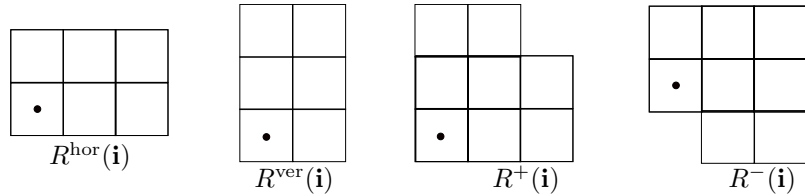


Figure 20: The different tiles of the covering.

Definition 34. For every $\mathbf{i} \in \mathbb{Z}^2$ we set

$$\begin{aligned} R^{\text{hor}}(\mathbf{i}) &:= Q(\mathbf{i}) \cup q(\mathbf{i} + (2, 0)) \cup q(\mathbf{i} + (2, 1)), & R^+(\mathbf{i}) &:= R^{\text{ver}}(\mathbf{i}) \cup R^{\text{hor}}(\mathbf{i}), \\ R^{\text{ver}}(\mathbf{i}) &:= Q(\mathbf{i}) \cup q(\mathbf{i} + (0, 2)) \cup q(\mathbf{i} + (1, 2)), & R^-(\mathbf{i}) &:= R^{\text{ver}}(\mathbf{i} + (1, -1)) \cup R^{\text{hor}}(\mathbf{i}), \end{aligned}$$

where $Q(\mathbf{i})$ is defined as in (5.6) (see Fig. 20).

For every discrete edge $\ell \in \mathcal{E}(E)$, we will define a covering of the region outside E projecting onto ℓ . We warn the reader that the choice of the tiles will depend both on the slope $s(\ell)$ and the neighboring edges. Heuristically, where the discrete projection π_E^φ behaves as in the case of the distance from a point, we will still use the tiles $Q(\mathbf{i})$, as in the proof of Proposition 27. In order to match the coverings of the regions projecting onto adjacent edges, we will need tiles $R^{\text{hor}}(\mathbf{i})$ and $R^{\text{ver}}(\mathbf{i})$ (see Steps 2 and 3 of the proof), in which the even checkerboard is the minimizer by virtue of Remark 32. Moreover, we will take into account that the effective boundary $\partial^{\text{eff}} E$ may present some irregularities due to the discrete nature of the problem (see Steps 4 and 5). In that case, where needed, we will use the “siding tiles” $R^+(\mathbf{i})$ and $R^-(\mathbf{i})$ which are compatible with the rest of the covering and still favor the even configurations in the local minimum problems therein.

Proof of Proposition 30. According to the discussion in Remark 8, we reduce the description of the covering corresponding to the discrete edges of E contained in $\{\mathbf{x} \in \mathbb{R}^2 : x_2 \geq 0\}$ complying with

$$0 \leq s(\ell) \leq 1, \quad (5.29)$$

as the covering for the remaining edges can be obtained symmetrically. We divide the proof into several steps.

Step 1: ordering of the discrete edges. We label in clockwise order the set of discrete edges of E ; namely, $\{\ell_m\}_{m=1}^{m_1} \subset \mathcal{E}(E)$. For our convenience, writing $\ell_1 = \{\mathbf{j}^l\}_{l=0}^L$, with a slight abuse of notation, in the case that $s(\ell_1) = 0$ we write (without relabelling) $\ell_1 = \{\mathbf{j}_1^l\}_{l=\lfloor \frac{L}{2} \rfloor}^L$. If $s(\ell_1) > 0$ we set $\ell_0 := \{\mathbf{j}_1^0\}$. Now we set

$$m_0 := \max \left\{ 0 \leq m \leq M : s(\ell_m) \leq \frac{1}{3} \right\}.$$

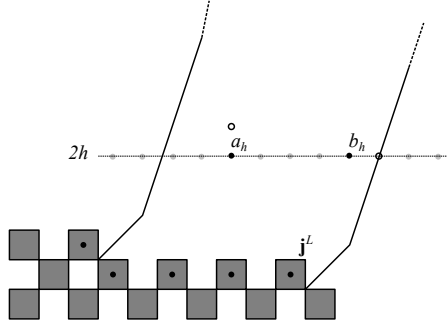


Figure 21: The point $(a_h, 2h + 1) \in A(\ell)$ (black circle on the left). The point $(b_h + 1, 2h) \in A(\ell_{m+1})$ (black circle on the right). The gray points represent $\mathbb{Z} \times \{2h\}$.

Step 2: covering of the region outside E projecting onto ℓ_m with $0 < m < m_0$. We set $\ell_m := \{\mathbf{j}^l\}_{l=0}^L$ assuming, without loss of generality, that $\mathbf{j}^L = (0, 0)$. We also define

$$\begin{aligned} a_h &:= \min\{h' \in 2\mathbb{Z} : (h', 2h + 1) \in A(\ell_m)\}, \\ b_h &:= \max\{h' \in 2\mathbb{Z} : (h' + 1, 2h) \in A(\ell_m)\}, \end{aligned} \quad (5.30)$$

for every $h \in \mathbb{N}$, where $A(\ell)$ is defined in (5.17) (see Fig. 21). In the case $m = 1$ and $s(\ell_1) = 0$, the set $A(\ell_1)$ is still as in (5.17) with $\{\mathbf{j}^l\}_{l=\lfloor \frac{L}{2} \rfloor}^L$ in place of $\{\mathbf{j}^l\}_{l=1}^L$. Note that, by Remark 33,

assumption (5.13) yields that a_h and b_h are well-defined for every $h \in \mathbb{N}$. We then introduce the set

$$\mathcal{J}(\ell_m) := \bigcup_{h \geq 0} \{(h', 2h) : h' \in 2\mathbb{Z}, a_h \leq h' \leq b_h\}. \quad (5.31)$$

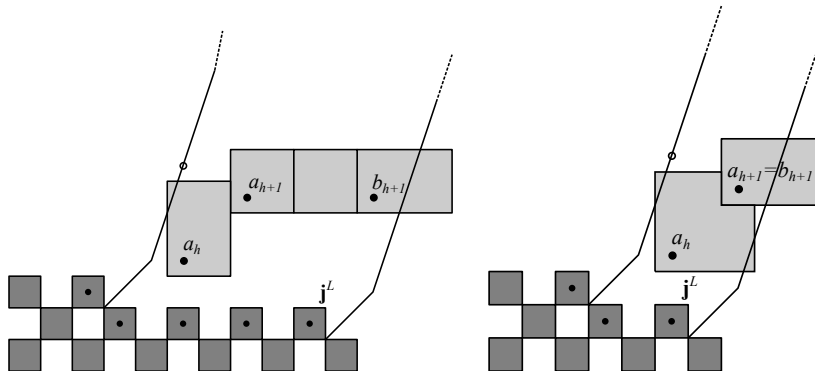


Figure 22: Examples of coverings defined in (5.32). The black circle represents the point $(a_{h-1}, 2h+3)$.

Correspondingly, for every $h \in \mathbb{N}$ we define the following covering (see Fig. 22):

$$C(\mathbf{i}) := \begin{cases} R^{\text{ver}}(\mathbf{i}) & \mathbf{i} = (a_h, 2h) \text{ and } (a_h, 2h+3) \notin A(\ell_m) \\ Q(\mathbf{i}) & \mathbf{i} = (a_h, 2h) \text{ and } (a_h, 2h+3) \in A(\ell_m) \\ Q(\mathbf{i}) & i_1 \in 2\mathbb{Z}, a_h < i_1 < b_h \\ R^{\text{hor}}(\mathbf{i}) & \mathbf{i} = (b_h, 2h) \end{cases}, \quad \text{if } a_h < b_h, \quad (5.32)$$

$$C(\mathbf{i}) := \begin{cases} R^+(\mathbf{i}), & \mathbf{i} = (a_h, 2h) \text{ and } (a_h, 2h+3) \notin A(\ell_m) \\ R^{\text{hor}}(\mathbf{i}), & \mathbf{i} = (a_h, 2h) \text{ and } (a_h, 2h+3) \in A(\ell_m) \end{cases}, \quad \text{if } a_h = b_h,$$

(see Fig. 23 for an example of $\{C(\mathbf{i}) : \mathbf{i} \in \mathcal{J}(\ell_m)\}$).

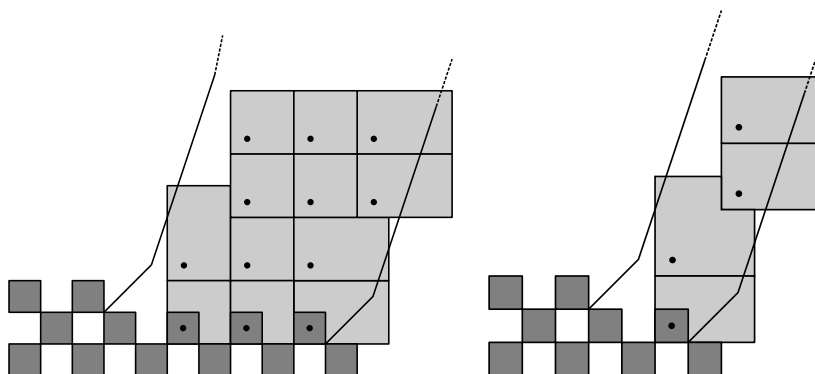


Figure 23: Examples of whole coverings defined in formula (5.32). The black dots represent the points of $\mathcal{J}(\ell_m)$.

Step 3: covering of the region outside E projecting onto ℓ_m with $m_0 \leq m \leq m_1 - 1$. As before, we label clockwise the set of points $\{\mathbf{j}^r\}_{r \geq 0} = \bigcup_{m=m_0+1}^{m_1} \ell_m \setminus \{\ell_0\}$. For every $m_0 + 1 \leq$

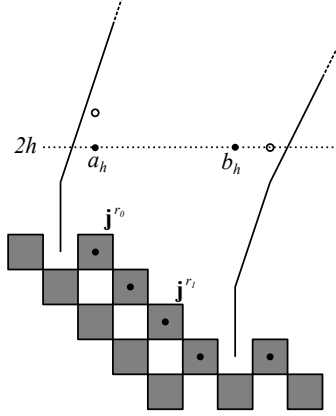


Figure 24: The point $(a_h, 2h + 1) \in A(\ell_m)$ (black circle on the left). The point $(b_h + 1, 2h) \in A(\ell_m)$ (black circle on the right).

$m \leq m_1 - 1$, writing $\ell_m = \{\mathbf{j}^l\}_{l=0}^L$ we define

$$r_0 := \min\{r \in 2\mathbb{Z} : \mathbf{j}^r \in \ell_m\} \text{ and } r_1 := \max\{r \in 2\mathbb{Z} : \mathbf{j}^r \in \ell_m \setminus \{\mathbf{j}^L\}\}. \quad (5.33)$$

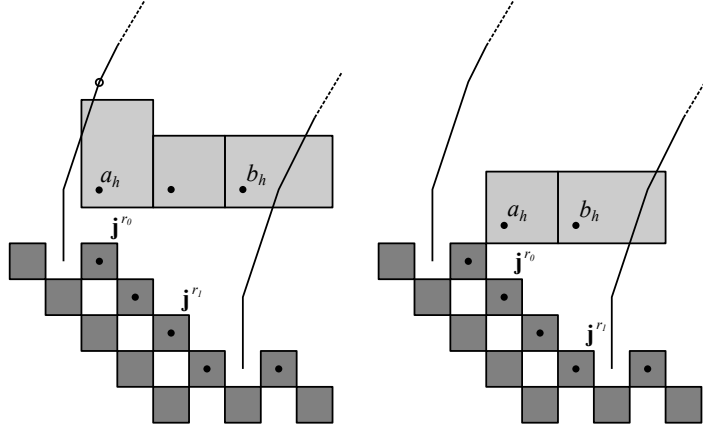


Figure 25: Examples of coverings of the two possible parities defined in formula (5.32). The black circle represents the point $(a_h, 2h + 3)$.

Fix first ℓ_m with $m_0 + 1 < m \leq m_1 - 1$ and assume, without loss of generality, that $\mathbf{j}^{r_1} = (0, 0)$. Now, for every $h \in \mathbb{N}$ we determine the integers a_h and b_h as in (5.30) (see Fig. 24), which are well defined by Remark 33, where $A(\ell)$ is as in (5.19). Correspondingly, we define the sets $\mathcal{J}(\ell_m)$ as in (5.31) and $C(\mathbf{i})$ for every $\mathbf{i} \in \mathcal{J}(\ell_m)$ as in (5.32), respectively (see Figg. 25 and 26).

The covering outside the discrete edges ℓ_{m_0} and ℓ_{m_0+1} must be treated separately. Let r_0, r_1 be as in (5.33) with $m = m_0 + 1$. Again, we assume that $\mathbf{j}^{r_1} = (0, 0)$, define a_h, b_h as in (5.30) for every $h \in \mathbb{N}$ with $A(\ell_{m_0}) \cup A(\ell_{m_0+1})$ in place of $A(\ell_m)$ and the set $\mathcal{J}(\ell_{m_0} \cup \ell_{m_0+1})$ as in (5.31). The sets $C(\mathbf{i})$ are defined, for every $\mathbf{i} \in \mathcal{J}(\ell_{m_0} \cup \ell_{m_0+1})$, as in (5.32) with $A(\ell_{m_0}) \cup A(\ell_{m_0+1})$ in place of $A(\ell_m)$ (see Fig. 27). Note that, in this case $a_h \neq b_h$ for every $h \in \mathbb{N}$.

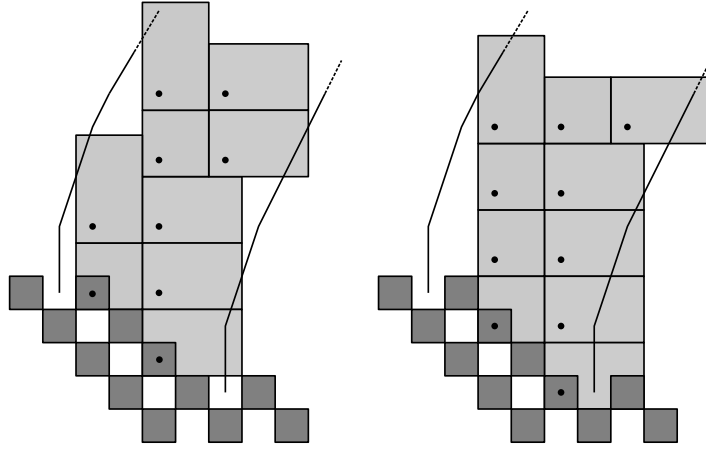


Figure 26: Examples of whole coverings defined in formula (5.32) of two different parities. The black dots represent the points of $\mathcal{J}(\ell_m)$.

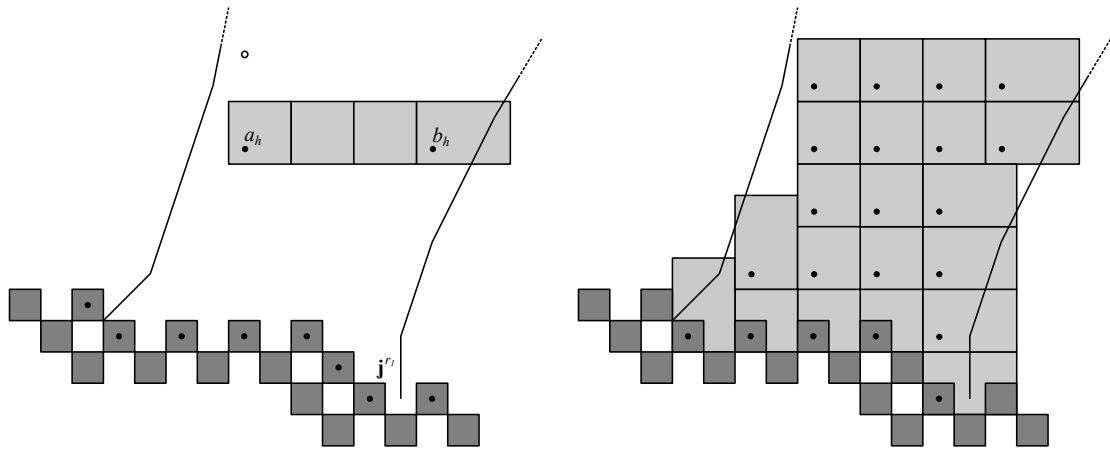


Figure 27: On the left, an example of a_h and b_h , and the black circle represents the point $(a_h, 2h + 3)$. On the right the corresponding covering, where the black dots represent the points of $\mathcal{J}(\ell_{m_0-1} \cup \ell_{m_0})$.

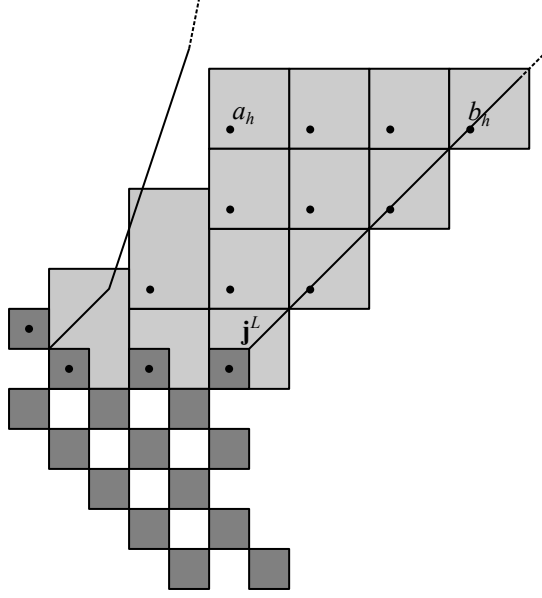


Figure 28: Example of covering outside ℓ_{m_1} in the case (i).

Step 4: covering of the region outside E projecting onto ℓ_{m_1} . We set $\ell_{m_1} = \{\mathbf{j}^l\}_{l=0}^L$ with $\mathbf{j}^L = (0, 0)$. There are different possible cases depending on $\nu(\ell_{m_1})$:

(i) let $m_0 = m_1$; *i.e.*, $s(\ell_m) \leq \frac{1}{3}$ for every m . We set, for every $h \in \mathbb{N}$, a_h as in (5.30), $b_h = 2h$ and $\mathcal{J}(\ell_{m_1})$ as in (5.31). Then, $C(\mathbf{i})$ is defined as in (5.32) for every $\mathbf{i} \in \mathcal{J}(\ell_{m_1}) \setminus \{(b_h, 2h)\}_{h \in \mathbb{N}}$ and $C((b_h, 2h)) = Q((b_h, 2h))$ for every $h \in \mathbb{N}$ (Fig. 28);

(ii) let $\frac{1}{3} < s(\ell_{m_1}) < 1$ and let r_1 be defined as in (5.33) with $m = m_1$. Then a_h and b_h are as in (5.30) for every $h \in \mathbb{N}$ with $A(\ell_{m_1})$ or $A(\ell_{m_1}) \cup A(\ell_{m_1-1})$ in place of $A(\ell_m)$ whether $m_1 - 1 > m_0$ or $m_1 - 1 = m_0$, respectively. We define $\mathcal{J}(\ell_{m_1})$ as in (5.31). If $\mathbf{j}^{r_1} = \mathbf{j}^{L-2}$, $C(\mathbf{i})$ is defined as in (5.32). Whereas, if $\mathbf{j}^{r_1} = \mathbf{j}^{L-1}$, $C(\mathbf{i})$ is defined as in (5.32) for every $\mathbf{i} \in \mathcal{J}(\ell_{m_1}) \setminus \{\mathbf{j}^{r_1}, \mathbf{j}^{r_1} + (0, 2)\}$ and

$$C(\mathbf{j}^{r_1}) = \emptyset, \quad C(\mathbf{j}^{r_1} + (0, 2)) = R^-(\mathbf{j}^{r_1} + (0, 2)).$$

Then, setting $A(\mathbf{j}^L) = \{\mathbf{i} \in \mathbb{Z}^2 : i_1, i_2 > 0, \pi_E^\varphi(\mathbf{i}) = \mathbf{j}^L\}$, we introduce the integers

$$a'_h = \begin{cases} \min\{h' \in 2\mathbb{Z} : (h', 2h+1) \in A(\mathbf{j}^L)\} & \text{if } \mathbf{j}^{r_1} = \mathbf{j}^{L-2} \\ \min\{h' \in 2\mathbb{Z} + 1 : (h', 2h+2) \in A(\mathbf{j}^L)\} & \text{if } \mathbf{j}^{r_1} = \mathbf{j}^{L-1} \end{cases}$$

$$b'_h = \begin{cases} 2h & \text{if } \mathbf{j}^{r_1} = \mathbf{j}^{L-2} \\ 2h+1 & \text{if } \mathbf{j}^{r_1} = \mathbf{j}^{L-1}. \end{cases}$$

Now, we define $\mathcal{J}(\ell'_{m_1})$ as in (5.31) with a'_h, b'_h in place of a_h and b_h , and the tile $C(\mathbf{i})$ as in (5.32) for every $\mathbf{i} \in \mathcal{J}(\mathbf{j}^L) \setminus \{(b'_h, b'_h)\}_{h \in \mathbb{N}}$, and $C((b'_h, b'_h)) = Q((b'_h, b'_h))$ (see Fig. 29);

(iii) consider now the case $s(\ell_{m_1}) = 1$. Let r_0 be defined as in (5.33) with $m = m_1$. Without relabeling, we set $\ell_{m_1} := \{\mathbf{j}^l\}_{l=0}^{\lfloor \frac{L}{2} \rfloor}$ and assume $\mathbf{j}^{\lfloor \frac{L}{2} \rfloor} = (0, 0)$. Here the covering depends on the parity of L . If L is even, a_h is defined as in (5.30) with $m = m_1$ and $b_h = 2h$ for every $h \in \mathbb{N}$. $\mathcal{J}(\ell_{m_1})$ is defined as in (5.31). Then $C(\mathbf{i})$ is defined as in (5.32) for every $\mathbf{i} \in \mathcal{J}(\ell_{m_1}) \setminus \{(b_h, 2h)\}_{h \in \mathbb{N}}$ and $C((b_h, 2h)) = Q((b_h, 2h))$ (Figure 30). If L is odd, analogously to what done in case (ii), for

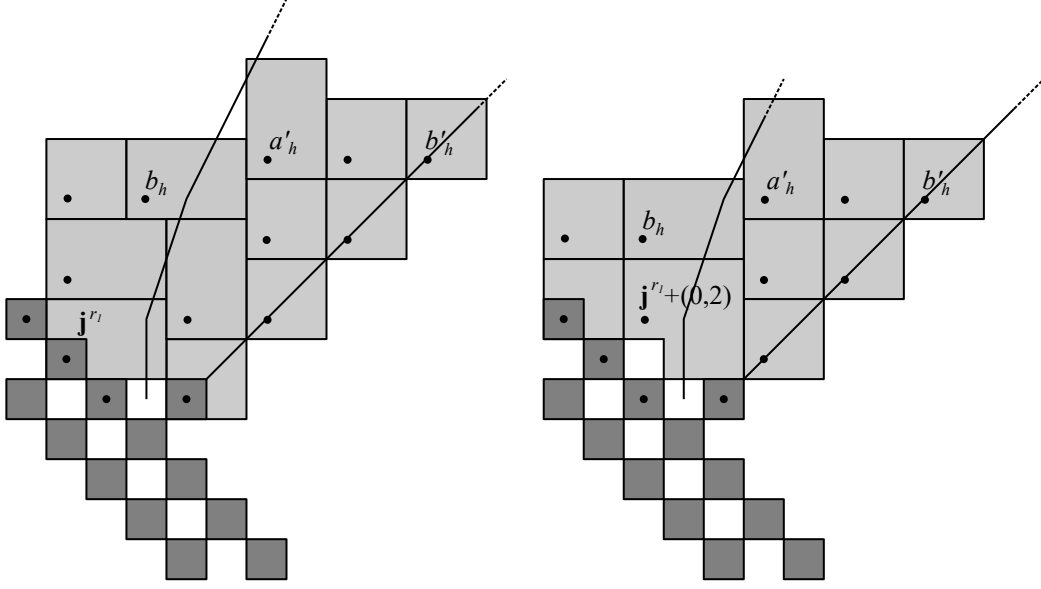


Figure 29: The covering in the cases $\mathbf{j}^{r_1} = \mathbf{j}^{L-1}$ (on the left) and $\mathbf{j}^{r_1} = \mathbf{j}^L$ (on the right).

every $h \in \mathbb{N}$ we define

$$a_h = \begin{cases} \min\{h' \in 2\mathbb{Z} : (h', 2h+1) \in A(\ell_{m_1})\} & \text{if } \mathbf{j}^{r_0} \neq \mathbf{j}^L \\ \min\{h' \in 2\mathbb{Z} + 1 : (h', 2h+2) \in A(\mathbf{j}^L)\} & \text{if } \mathbf{j}^{r_0} = \mathbf{j}^L \end{cases}$$

$$b'_h = \begin{cases} 2h & \text{if } \mathbf{j}^{r_0} \neq \mathbf{j}^L \\ 2h+1 & \text{if } \mathbf{j}^{r_1} = \mathbf{j}^L. \end{cases}$$

Then $\mathcal{J}(\ell_{m_1})$ is defined as in (5.31) and $C(\mathbf{i})$ is defined as in (5.32) for every $\mathbf{i} \in \mathcal{J}(\ell_{m_1}) \setminus \{(b_h, 2h)\}_{h \in \mathbb{N}}$ and

$$C_h((b_h, b_h)) = \begin{cases} R^-((b_h, b_h)) & \text{if } h = 0 \\ R((b_h, b_h)) & \text{if } h > 0, \end{cases}$$

see Fig. 31.

Step 5: covering of the region outside E projecting onto ℓ_0 . We define the set

$$\mathcal{S}_0 = \begin{cases} E(\{\mathbf{i} \in \mathbb{Z}^2 : i_1 = j_1^{\lceil \frac{\ell}{2} \rceil} - 1, i_2 \geq 1\}) & \text{if } s(\ell_1) = 0, \\ \emptyset & \text{if } 0 < s(\ell_1) < \frac{1}{3}, \\ E(\{\mathbf{i} \in \mathbb{Z}^2 : i_1 = j_1^0, i_2 \geq 0\}) & \text{if } \frac{1}{3} < s(\ell_1) \leq 1. \end{cases} \quad (5.34)$$

(see Fig. 32).

If ℓ is such that $0 < s(\ell) < \frac{1}{3}$, we define $\mathcal{J}(\ell_0) = \{(0, 2h)\}_{h \in \mathbb{N}}$ and for every $h \in \mathbb{N}$

$$b_h = \max\{h' \in 2\mathbb{Z} \mid (h'+1, 2h) \in A(\mathbf{j}^0)\},$$

where $A(\ell_0)$ is as in (5.26). Then, for every $\mathbf{i} \in \mathcal{J}(\ell_0)$ we choose the tile

$$C(\mathbf{i}) = \bigcup \{q((k, 2h)) \cup q((k, 2h+1)) : k \in \mathbb{Z}, -b_h - 2 \leq k \leq b_h + 2, i_2 = 2h\}, \quad (5.35)$$

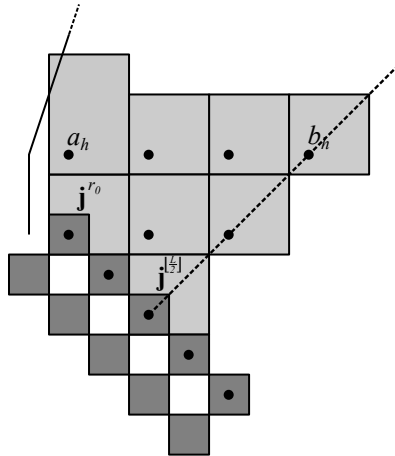


Figure 30: The covering considered in (iii) in the case L even.

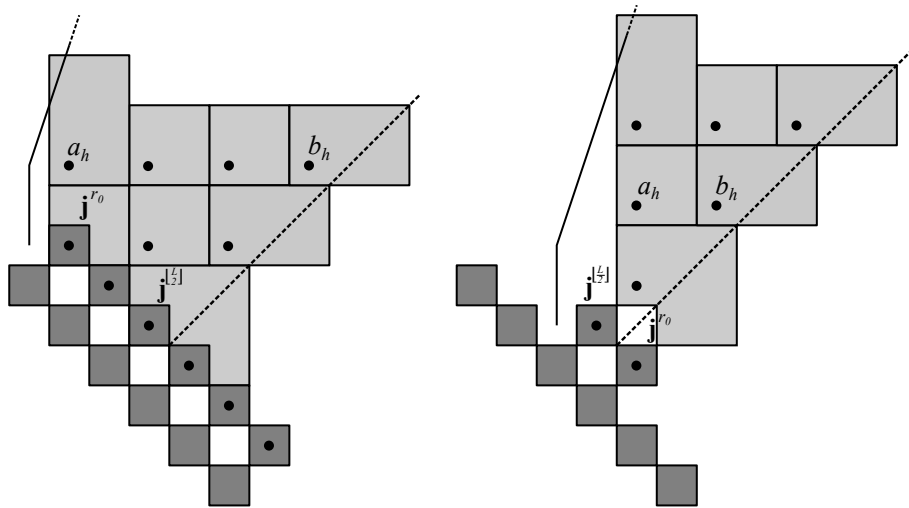


Figure 31: The coverings defined in (iii), in the case L odd, for $j^{r_0} \neq j^L$ (on the left) and $j^{r_0} = j^L$ (on the right).

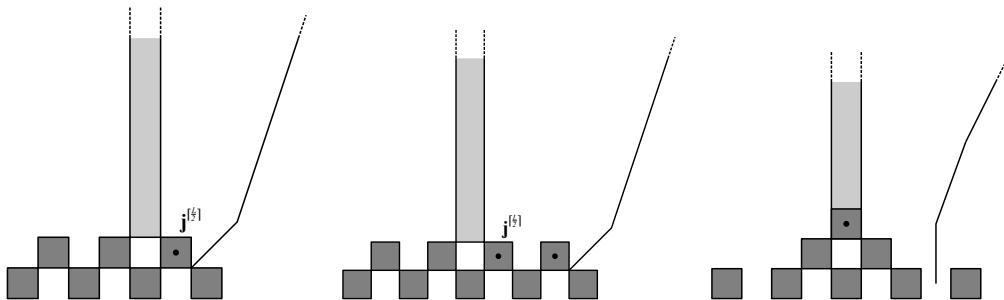


Figure 32: The covering S_0 in the cases listed in (5.34).

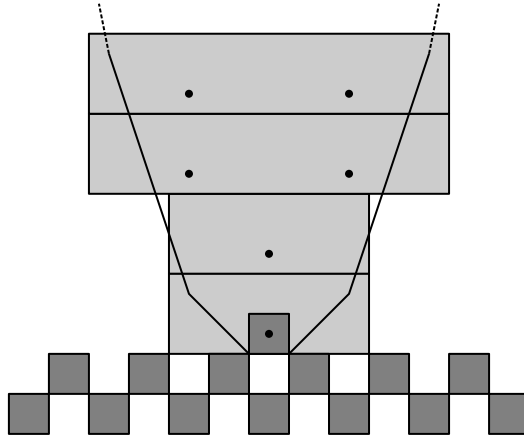


Figure 33: Example of $C(\mathbf{i})$, $\mathbf{i} \in \mathcal{J}(\ell_0)$. The black dots represent the lattice points $(\pm b_h, 2h)$.

see Fig. 33.

Step 6: compatibility between different coverings. Here, we note that the family of sets $\{C(\mathbf{i}) : \mathbf{i} \in \mathcal{J}(\ell_m), 0 \leq m \leq m_1, \mathbf{i} \in \mathcal{J}(\ell'_{m_1})\}$ is a covering of $E(\{\mathbf{i} \in \mathbb{Z}^2 : \inf_{\mathbf{j} \in Z(E)} \|\mathbf{i} - \mathbf{j}\|_1, i_2 \geq i_1\})$, which is the region of plane “outside” the edges as in Step 1. We point out that, if case (ii) of Step 4 does not hold, then $\mathcal{J}(\ell'_{m_1}) = A(\ell'_{m_1}) = \emptyset$. Indeed, for every pair $\ell, \ell' \in \mathcal{E}(E)$ with ℓ' preceding ℓ , the sets

$$\bigcup_{\mathbf{i} \in \mathcal{J}(\ell')} C(\mathbf{i}) \quad \text{and} \quad \bigcup_{\mathbf{i} \in \mathcal{J}(\ell)} C(\mathbf{i})$$

are non-overlapping and their union does not leave uncovered regions.

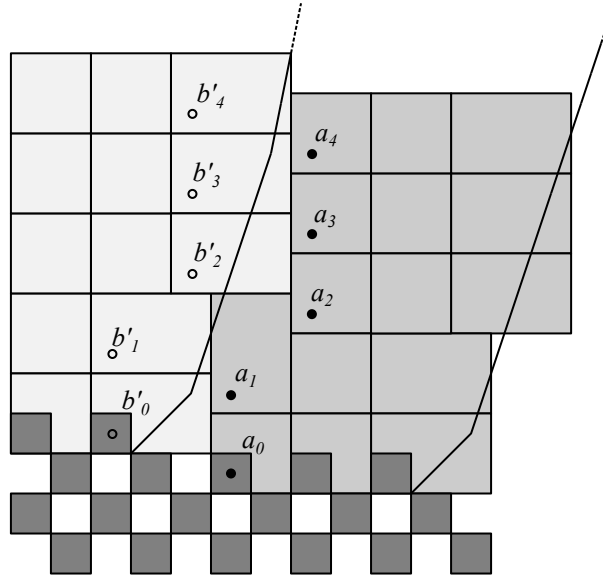


Figure 34: Matching of the coverings outside a pair of adjacent discrete edges.

We denote by a_h, b_h and a'_h, b'_h the values defined in (5.30) corresponding to ℓ and ℓ' , respec-

tively. We assume, for simplicity, that $\mathbf{j}^L = (0, 0)$. Hence, every $\mathbf{i} \in \mathcal{J}(\ell)$ and $\mathbf{i}' \in \mathcal{J}(\ell')$ are such that $i_2 = 2h$ and $i'_2 = 2h + 1 + 2h_0$, where $h_0 = 0$ if $0 \leq s(\ell) \leq \frac{1}{3}$ and $2h_0 = r_1 - r_0$ otherwise, where r_0 and r_1 are defined in Step 3. Therefore, in this coordinate system, the definition of b'_{h-h_0} reads

$$b'_{h-h_0} = \max\{h' \in 2\mathbb{Z} + 1 : (h' + 1, 2h + 1) \in A(\ell')\}.$$

Now, it is sufficient to note that, if $Q((a_h, 2h)) = R^{\text{ver}}((a_h, 2h))$ then $a_{h+1} = a_h + 2$, while if $Q((a_h, 2h)) = Q((a_h, 2h))$ then $a_{h+1} = a_h$, as it immediately follows from (5.32) (see Fig. 34).

The covering of the regions projecting onto discrete edges $\ell \in \mathcal{E}(E)$ not fulfilling (5.29) can be obtained symmetrically; we use the notation $\mathcal{J}(\ell)$ and $C(\mathbf{i})$ to denote the sets obtained symmetrically as in (5.31) and (5.32) respectively. With \mathcal{C}_0 we denote the union of the set \mathcal{S}_0 defined in (5.34) and its symmetric analogs.

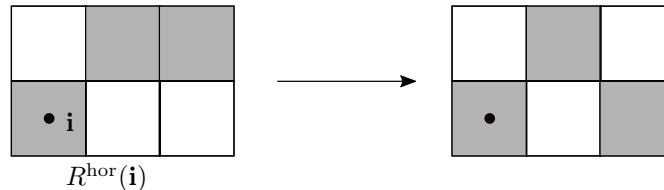


Figure 35: The checkerboard configurations are energetically favorable inside each $R^{\text{hor}}(\mathbf{i})$.

Step 7: local minimum problems on $C(\mathbf{i})$. As a next step, we prove that the configuration with minimal energy inside each tile $C(\mathbf{i})$ is the even checkerboard, for any $\mathbf{i} \in \mathcal{J}(\ell)$, $\ell \in \mathcal{E}(E)$; *i.e.*,

$$\mathcal{F}_\alpha^\varphi(E(\mathbb{Z}_e^2) \cap C(\mathbf{i}), E) \leq \mathcal{F}_\alpha^\varphi(F \cap C(\mathbf{i}), E) \quad (5.36)$$

for every $F \in \mathcal{D}$, and the same for \mathcal{C}_0 ; *i.e.*,

$$\mathcal{F}_\alpha^\varphi(E(\mathbb{Z}_e^2) \cap \mathcal{C}_0, E) \leq \mathcal{F}_\alpha^\varphi(F \cap \mathcal{C}_0, E). \quad (5.37)$$

Indeed, if $C(\mathbf{i}) = Q(\mathbf{i})$ from Remark 31 either (5.18) or (5.20) holds. Hence, by arguing as in the proof of Proposition 27, from (5.8) we get (5.36).

If $C_h(\mathbf{i}) = R^{\text{hor}}(\mathbf{i})$, we can restrict the minimization in (5.36) to the checkerboard configurations. Indeed, if $\mathbf{j} \in Z(R^{\text{hor}}(\mathbf{i}))$ has a nearest neighbor \mathbf{j}' then by suitably shifting one of them towards an “empty” location the corresponding variation of the energy is at most $-2 + \alpha < 0$ (see Fig. 35); the case $\alpha > 2$ is trivial. Moreover, by the definition of b_h we have that either (5.18) or (5.20) is satisfied, thence from Remark 32, (5.21) holds yielding (5.36). The cases of $C(\mathbf{i}) = R^{\text{ver}}(\mathbf{i})$, $C(\mathbf{i}) = R^+(\mathbf{i})$ and $C(\mathbf{i}) = R^-(\mathbf{i})$ can be treated analogously.

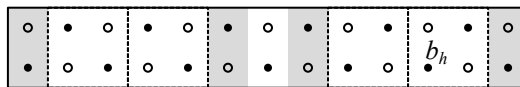


Figure 36: The lattice points involved in (5.38). The black dots are points of \mathbb{Z}_e^2 , circles are points of \mathbb{Z}_o^2 . The energy contribution of the even checkerboard in the white regions is negative.

Now consider the case $C(\mathbf{i})$ as in (5.35) with $\mathbf{i} \in \mathcal{J}(\ell_0)$. Reasoning as above, we can reduce minimum problem (5.36) to a comparison between the energies of the two checkerboards. Then, for every $h \in \mathbb{N}$, $k \in 2\mathbb{Z}$ with $0 < |k| \leq b_h$, the even checkerboard has minimum energy in

$Q((k, 2h))$, as above. Hence (5.36) is proved if

$$\begin{aligned} \varphi(0, 2h) + 2\varphi(1, 2h+1) + 2d^\varphi((b_h+2, 2h), E) \\ \leq \varphi(0, 2h+1) + 2\varphi(1, 2h) + 2d^\varphi((b_h+2, 2h+1), E); \end{aligned}$$

that is,

$$\varphi(1, 2h+1) + d^\varphi((b_h+2, 2h), E) \leq \frac{1}{2} + \varphi(1, 2h) + d^\varphi((b_h+2, 2h+1), E), \quad (5.38)$$

see Fig. 36. If $(b_h+2, 2h+1) \notin A(\ell_0)$ the inequality above is trivial, since $d^\varphi((b_h+2, 2h), E) \leq \varphi(1, 2h)$ and $d^\varphi((b_h+2, 2h), E) \leq \varphi(1, 2h+1)$. If, instead, $(b_h+2, 2h+1) \in A(\ell_0)$ (5.38) reduces to

$$\varphi(1, 2h+1) + \varphi(b_h+2, 2h) \leq \frac{1}{2} + \varphi(1, 2h) + \varphi(b_h+2, 2h+1),$$

which holds from (5.8) and (H3).

Reasoning as in point (c) of the proof of Proposition 27 there holds

$$\mathcal{F}_\alpha^\varphi(E(\mathbb{Z}_e^2) \cap \mathcal{C}_0, E) \leq \mathcal{F}_\alpha^\varphi(F \cap \mathcal{C}_0, E).$$

As a final remark, we note that for every $\mathbf{i} \in E(\mathbb{Z}_e^2)$ such that $d^\varphi(\mathbf{i}, E) > \frac{4}{\alpha}$ the variation of removing $q(\mathbf{i})$ is negative, hence

$$\operatorname{argmin}_{E' \supset E} \mathcal{F}_\alpha^\varphi(E', E) \subset E \left(\left\{ \mathbf{i} \in \mathbb{Z}^2 : d^\varphi(\mathbf{i}, E) < \frac{4}{\alpha} \right\} \right).$$

Step 8: conclusion. Set

$$\mathcal{J} := \left(\bigcup_{\ell \in \mathcal{E}(E)} \mathcal{J}(\ell) \right) \cap \left\{ \mathbf{i} \in \mathbb{Z}^2 : d^\varphi(\mathbf{i}, E) < \frac{4}{\alpha} \right\}.$$

An analogous argument as that in the proof of Proposition 27 (see (5.12)) shows that

$$\mathcal{F}_\alpha^\varphi(E', E) \geq \sum_{\mathbf{i} \in \mathcal{J}} \mathcal{F}_\alpha^\varphi(E' \cap C(\mathbf{i}), E) + \mathcal{F}_\alpha^\varphi(E' \cap \mathcal{C}_0, E)$$

for every $E' \supset E$, $E' \in \mathcal{D}$. By virtue of Step 7 we get

$$\min_{E' \supset E} \mathcal{F}_\alpha^\varphi(E', E) \geq \sum_{\mathbf{i} \in \mathcal{J}} \mathcal{F}_\alpha^\varphi(E(\mathbb{Z}_e^2) \cap C(\mathbf{i}), E) + \mathcal{F}_\alpha^\varphi(E(\mathbb{Z}_e^2) \cap \mathcal{C}_0, E) = \mathcal{F}_\alpha^\varphi(E(\mathcal{J} \cup Z(E)), E)$$

which implies that the ground state of the energy is achieved by the even checkerboard configuration. Lastly, the monotonicity constraint yields the uniqueness of the solution. \square

We will apply Proposition 30 iteratively to each $E = E_\alpha^k$, $k \geq 1$ in order to characterize the solutions of the recursive scheme (5.2) (see Theorem 38). Indeed, as shown with Proposition 27, the first step E_α^1 coincides with $E(B_\frac{\varphi}{\alpha} \cap \mathbb{Z}_e^2)$ which satisfies the symmetry conditions (5.14) and, thanks to the following Lemma, the non-degeneracy condition (2.3).

Lemma 35. *If φ satisfies (H1) and (H2), then for every $r > 2$ the set $E = B_r^\varphi \cap \mathbb{Z}_e^2$ satisfies (2.3).*

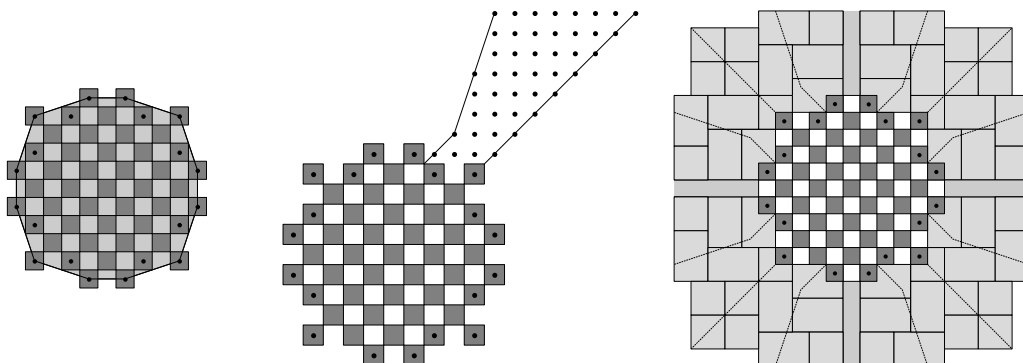


Figure 37: From the left, the set E_α^1 and the polygon $\text{conv}(Z(E_\alpha^1))$, the lattice sets $A(\ell)$, $\ell \in \mathcal{E}(E)$ and, lastly, the corresponding covering.

Proof. By the symmetric assumption (H1) we can restrict our analysis to points $\mathbf{i} \in \partial^{\text{eff}} E$ with $i_2 \geq i_1 \geq 0$. We subdivide the proof into two cases. If $i_1 = 0$, then $i_2 > 0$ from (H2) and the condition $r > 2$. Since $(0, 0) \in Z(E)$ we have that $(0, i_2 - 2) \in Z(E)$. By (H1) the point $(\pm i_2, 0) \in Z(E)$ then, by the \mathbb{Z}_e^2 -convexity of E we get that $(\pm 1, i_2 - 1) \in Z(E)$. Since for every \mathbf{i}' with $i'_2 > i_2$, $\mathbf{i}' \notin Z(E)$ thus \mathbf{i} is non-degenerate. If, instead, $i_1 > 0$, for every $\mathbf{j} \in Z(E)$ such that $\|\mathbf{j} - \mathbf{i}\|_1 \leq 2$, by the symmetry with respect to the coordinate axes of φ we get that $(-j_1, j_2)$, $(j_1, -j_2) \in Z(E)$. The \mathbb{Z}_e^2 -convexity and the fact that $(0, 0) \in Z(E)$ yield that $(j_1 - 2, j_2)$, $(j_1, j_2 - 2)$, $(j_1 + 1, j_2 - 2) \in Z(E)$. This implies that \mathbf{i} is non-degenerate. \square

We conclude this section with some examples clarifying the role of compatibility assumption (5.13) and non-degeneracy condition (H2).

Example 36. Consider φ the Euclidean norm and set $\alpha = 0.7$. Then the resulting E_α^1 complies with (5.13) and the lattice sets $A(\ell)$ fulfill (5.25), as it can be noted in Fig. 37.

If we choose instead $\varphi = \|\cdot\|_3$ and $\alpha = 0.71$, the compatibility condition (5.13) is violated for E_α^1 as shown in Fig. 38. This also provides an example in which (5.25) is not satisfied, hence the indices a_h and b_h introduced in Step 2 of Proposition 30 are not well defined.

Example 37 (one-dimensional motion). We consider an absolute norm which does not satisfy the normalization assumption $\varphi(1, 0) = \varphi(0, 1) = 1$; that is,

$$\varphi(\mathbf{x}) = |x_1| + 2|x_2|, \quad \text{for every } \mathbf{x} \in \mathbb{R}^2,$$

and take $\frac{4}{3} < \alpha < 2$. Then Proposition 27 applies in this case and gives

$$E_\alpha^1 = q((-2, 0)) \cup q((0, 0)) \cup q((2, 0)).$$

Even though Proposition 30 cannot be applied on such set, it is straightforward to see in a direct way that the solution of 5.2 $\{E_\alpha^k\}$ is given by

$$E_\alpha^k = \bigcup_{h=0}^k (q((-2h, 0)) \cup q((2h, 0))), \quad k \geq 0,$$

see Fig. 39. The resulting minimizing movement will be the family of horizontal line segments

$$E(t) = \lim_{\varepsilon \rightarrow 0} E_{\varepsilon, \tau}(t) = \lim_{\varepsilon \rightarrow 0} \varepsilon E_\alpha^{\lfloor \frac{t}{\varepsilon} \rfloor} = [-2\alpha t, 2\alpha t] \times \{0\}, \quad t \geq 0.$$

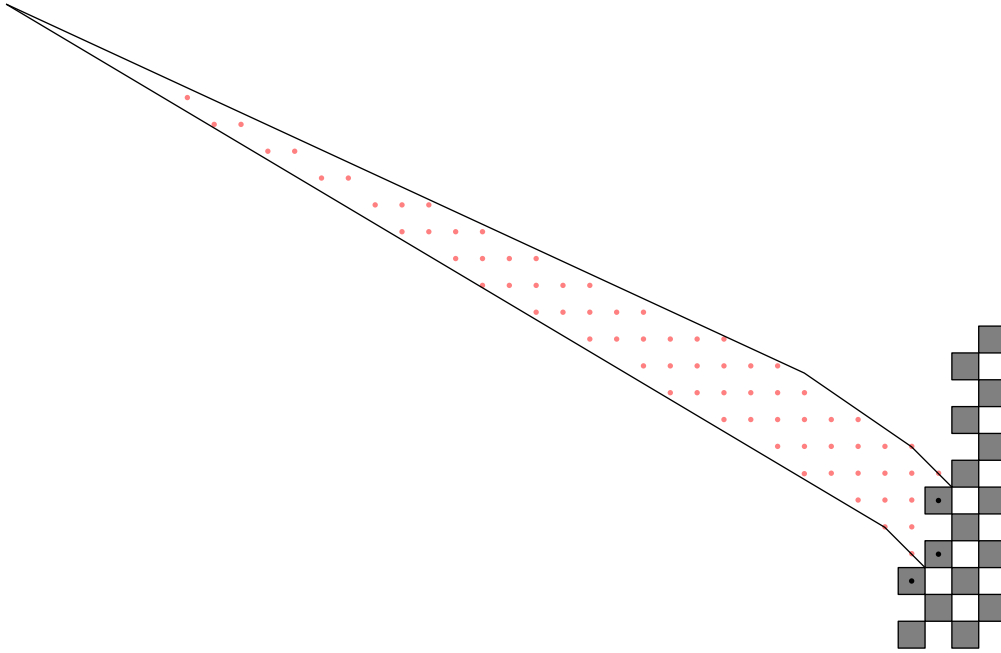


Figure 38: The discrete edge ℓ represented with black dots does not satisfy the compatibility condition (5.13). The red dots denote the points of $A(\ell)$ which does not comply with (5.25).

5.6 Nucleation and growth of a set

By virtue of Proposition 30, we can characterize the time-discrete flow $\{E_\alpha^k\}_{k \geq 0}$ solution of (5.2). This evolution admits an alternative interpretation, based on a geometric iterative process that we will call *nucleation of the initial set*. Indeed, the set of centers of the k -th step of the discrete evolution $Z(E_\alpha^k)$ can be obtained from that of the previous step $Z(E_\alpha^{k-1})$ by adding (in the Minkowski sense) the nucleus $\mathcal{N}_\alpha^\varphi$ (see Definition 28); *i.e.*, a lattice set that characterizes the motion.

Theorem 38. *Let φ be a symmetric absolute normalized norm satisfying (H3), and let $\alpha > 0$ be such that $\alpha \notin \Lambda^\varphi$. If $E(\mathcal{N}_\alpha^\varphi)$ satisfies assumption (5.13) then there exists a unique discrete solution $\{E_\alpha^k\}$ of (5.2) which is given, for any $k \geq 1$, by*

$$Z(E_\alpha^k) = \underbrace{\mathcal{N}_\alpha^\varphi + \cdots + \mathcal{N}_\alpha^\varphi}_{k\text{-times}}. \quad (5.39)$$

In particular, $E_\alpha^k \in \mathcal{A}_{\text{conv}}^e$ for every $k \geq 1$.

Proof. We first note that, for a lattice set \mathcal{J} such that $E(\mathcal{J})$ belongs to $\mathcal{A}_{\text{conv}}^e$ and satisfies (5.13)

$$E(\underbrace{\mathcal{J} + \mathcal{J} + \cdots + \mathcal{J}}_{m\text{-times}}) \in \mathcal{A}_{\text{conv}}^e \text{ still satisfies (5.13), for every } m \in \mathbb{N}. \quad (5.40)$$

It will suffice to show (5.40) for $m = 2$, as the claim for $m \geq 3$ will follow by an induction argument on the number m of the summands. Setting $\mathcal{Q} := \text{conv}(\mathcal{J})$, property (2.8) with $\Lambda = \mathbb{Z}_e^2$ and $m = 2$ reads as $(\mathcal{Q} \cap \mathbb{Z}_e^2) + (\mathcal{Q} \cap \mathbb{Z}_e^2) = 2\mathcal{Q} \cap \mathbb{Z}_e^2$, yielding that $E(\mathcal{J} + \mathcal{J}) \in \mathcal{A}_{\text{conv}}^e$. Moreover, a property equivalent to (5.13) is that all the discrete vertices of $E(\mathcal{J})$ belongs to $\partial\mathcal{Q}$. This implies

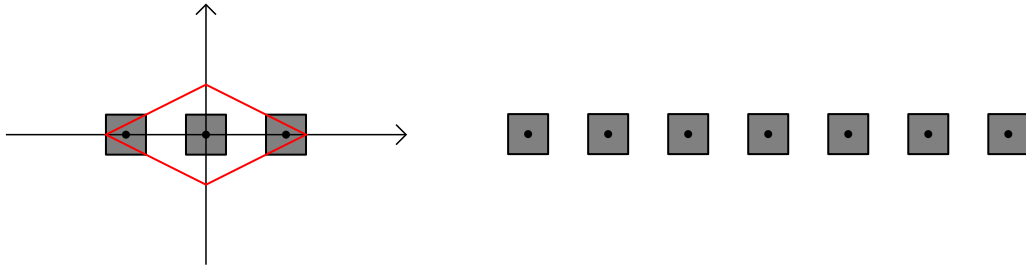


Figure 39: On the left the set E_α^1 and the boundary of $B_{\frac{4}{\alpha}}^\varphi$ in red. On the right the discrete solution E_α^k after two steps.

that the set of outward unit normal vectors of \mathcal{Q} coincide with the set of (discrete) outward unit normal vectors of $E(\mathcal{J})$. In particular, every edge l of \mathcal{Q} identifies a finite chain of discrete edges of $E(\mathcal{J})$ having the same unit normal vector $\nu(l)$. This fact depends only on $\nu(l)$ and not on the length of l . Proposition 10 with $A = B = \mathcal{Q}$ implies that the set of outward unit normal vectors of $2\mathcal{Q}$ coincide with that of \mathcal{Q} . Hence, the edge $l + l$ of $2\mathcal{Q}$ corresponds to a chain of a finite number of discrete edges of $E(\mathcal{J} + \mathcal{J})$ having the same unit normal vector $\nu(l)$. The \mathbb{Z}_ε^2 -convexity of $E(\mathcal{J} + \mathcal{J})$ implies (5.13).

Going back to the proof of (5.39), we argue by induction on the step k . By Proposition 27 and Lemma 35 $Z(E_\alpha^1) = \mathcal{N}_\alpha^\varphi$ complies with all the assumptions on E of Proposition 30. Now, let $k \geq 2$ and assume that

$$Z(E_\alpha^{k-1}) = \underbrace{\mathcal{N}_\alpha^\varphi + \dots + \mathcal{N}_\alpha^\varphi}_{(k-1)\text{-times}}.$$

For what remarked in (5.40), all the hypotheses of Proposition 30 are satisfied. Then, taking into account (5.16) with $E = E_\alpha^{k-1}$, we have that

$$Z(E_\alpha^k) = Z(E_\alpha^{k-1}) + \mathcal{N}_\alpha^\varphi. \quad (5.41)$$

Indeed, setting $\mathcal{J}_k := Z(E_\alpha^{k-1}) + \mathcal{N}_\alpha^\varphi$, we have

$$\max\{d^\varphi(\mathbf{i}, \mathbf{j}) : \mathbf{i} \in \mathcal{J}_k, \mathbf{j} \in Z(E_\alpha^{k-1})\} \leq \max_{\mathbf{i} \in \mathcal{N}_\alpha^\varphi} \varphi(\mathbf{i}) < \frac{4}{\alpha},$$

and this shows that $\mathcal{J}_k \subseteq Z(E_\alpha^k)$. On the other hand, if $\mathbf{i} \in Z(E_\alpha^k)$, there exist $\mathbf{i}' \in Z(E_\alpha^{k-1})$ and $\mathbf{i}'' \in \mathcal{N}_\alpha^\varphi$ such that $\mathbf{i} = \mathbf{i}' + \mathbf{i}''$. This comes by noting that by (5.16) there exists $\mathbf{i}' \in Z(E_\alpha^{k-1})$ such that $\varphi(\mathbf{i} - \mathbf{i}') = d^\varphi(\mathbf{i}, E_\alpha^{k-1}) < \frac{4}{\alpha}$, thus $\mathbf{i}'' = \mathbf{i} - \mathbf{i}' \in \mathcal{N}_\alpha^\varphi$. This yields (5.39). Moreover, again by (5.40) we get that the Minkowski sum in (5.41) preserves assumption (5.13), so E_α^k still satisfies (5.13) and the thesis is proved. \square

6 The limit motion

In this section we characterize the minimizing movements of scheme (3.4) as $\tau, \varepsilon \rightarrow 0$ in the critical regime $\varepsilon = \alpha\tau$ for any positive value of the parameter α outside the singular set Λ^φ , under the assumption that $E(\mathcal{N}_\alpha^\varphi)$ complies with (5.13).

As already explained at the beginning of Section 5, we also prove the existence of a value for α depending only on the chosen norm φ , above which every minimizing movement is trivial. For every α below the pinning threshold, instead, the limit motion is a family of expanding sets,

nucleating from the origin with constant velocity, as the limit set $E(t)$ turns out to be a dilation of the (renormalized) polygon

$$P_\alpha^\varphi := \begin{cases} \left(\max_{i \in \mathcal{N}_\alpha^\varphi} i_1 \right)^{-1} \text{conv}(\mathcal{N}_\alpha^\varphi) & \text{if } \mathcal{N}_\alpha^\varphi \neq \{(0,0)\} \\ \{(0,0)\} & \text{if } \mathcal{N}_\alpha^\varphi = \{(0,0)\} \end{cases} \quad (6.1)$$

Note that $\max_{i \in \mathcal{N}_\alpha^\varphi} i_1 \in \{2\lfloor \frac{2}{\alpha} \rfloor, \lfloor \frac{4}{\alpha} \rfloor\}$, from the definition of $\mathcal{N}_\alpha^\varphi$ and the fact that $\varphi(i_1, 0) = i_1$, $i_1 \in \mathbb{N}$.

Theorem 39. *Let φ be a symmetric absolute normalized norm satisfying (H3), let $\alpha > 0$ be given such that $\alpha \notin \Lambda^\varphi$ and let $\mathcal{F}_{\varepsilon, \tau}^\varphi$ be defined by (3.3). Let $\mathcal{N}_\alpha^\varphi$ be as in Definition 28. If the set $E(\mathcal{N}_\alpha^\varphi)$ satisfies assumption (5.13), then there exists a unique minimizing movement $E : [0, +\infty) \rightarrow \mathcal{X}$ for the scheme (3.4) at regime $\varepsilon = \alpha\tau$ defined by*

$$E(t) = v_\alpha^\varphi t P_\alpha^\varphi \quad \text{for every } t \geq 0, \quad (6.2)$$

where P_α^φ is defined in (6.1) and $v_\alpha^\varphi = \alpha \max_{i \in \mathcal{N}_\alpha^\varphi} i_1$. Moreover, there exists a unique discrete solution $E_{\varepsilon, \tau}(t)$ of scheme (3.4) at regime $\varepsilon = \alpha\tau$ and there holds

$$\chi_{E_{\varepsilon, \tau}(t)} \xrightarrow{*} \frac{1}{2} \chi_{E(t)}, \quad \text{for every } t \geq 0 \quad \text{as } \varepsilon \rightarrow 0. \quad (6.3)$$

Proof. By a scaling argument, for every discrete solution $E_{\varepsilon, \tau}^k$ of (3.4) in the regime $\varepsilon = \alpha\tau$ we have $E_{\varepsilon, \tau}^k = \varepsilon E_\alpha^k$ for every $k \geq 0$, where E_α^k denotes a discrete solution of (5.2). Then, by Theorem 38 there exists a unique minimizing movement of scheme (3.4) at regime $\varepsilon = \alpha\tau$. Since, by Proposition 12 and (6.1),

$$\underbrace{\mathcal{N}_\alpha^\varphi + \dots + \mathcal{N}_\alpha^\varphi}_{k\text{-times}} = \left(k \frac{v_\alpha^\varphi}{\alpha} P_\alpha^\varphi \right) \cap \mathbb{Z}_e^2,$$

we get that $\text{conv}(Z_\varepsilon(E_{\varepsilon, \tau}(t))) = \varepsilon \frac{v_\alpha^\varphi}{\alpha} \lfloor \frac{\alpha t}{\varepsilon} \rfloor P_\alpha^\varphi$. Moreover, noting that $d_{\mathcal{H}}(F, \text{conv}(Z_\varepsilon(F))) < \varepsilon$ for any $F \in \mathcal{A}_\varepsilon$, we get

$$d_{\mathcal{H}}\left(E_{\varepsilon, \tau}(t), v_\alpha^\varphi t P_\alpha^\varphi\right) < \varepsilon + v_\alpha^\varphi \left(t - \frac{\varepsilon}{\alpha} \lfloor \frac{\alpha t}{\varepsilon} \rfloor \right)$$

which tends to zero as $\varepsilon \rightarrow 0$, for any $t \geq 0$, whence (6.2) follows. Eventually, from the fact that $|E_{\varepsilon, \tau}(t) \cap A| \rightarrow \frac{1}{2}|A|$ as $\varepsilon \rightarrow 0$ for any open set $A \subset E(t)$, we get (6.3). \square

Definition 40 (pinning threshold). We define the *pinning threshold* of the motion obtained by solving scheme (3.4) as

$$\alpha_\varphi := \inf\{\alpha > 0 : E^\alpha(t) \equiv \{(0,0)\} \text{ for every } E^\alpha \text{ minimizing movement of (3.4)}\}. \quad (6.4)$$

It turns out that α_φ is related to the singular set Λ^φ defined in (5.4) as follows.

Proposition 41. *The pinning threshold is given by $\alpha_\varphi = \frac{4}{\varphi(1,1)} = \max \Lambda^\varphi$.*

Proof. We note that $B_{\frac{4}{\alpha}}^\varphi \cap \mathbb{Z}_e^2 = \{(0,0)\}$ if and only if $\alpha > \frac{4}{\varphi(1,1)}$, thus Proposition 27 yields the result. \square

Remark 42. The results of Theorems 38 and 39 can be extended to solutions of a minimizing-movements scheme with a more general initial datum E^0 . Indeed, let $E_{\text{disc}}^0 \in \mathcal{A}_{\text{conv}}^e$ be a set satisfying (2.3), (5.13) and (5.14). We can apply Proposition 30 with $E' = E_{\text{disc}}^0$ obtaining the first step of the discrete solution corresponding to scheme (5.2) with $E_\alpha^0 = E_{\text{disc}}^0$. Then, if $E(\mathcal{N}_\alpha^\varphi)$ satisfies assumption (5.13), from the same arguments of the proof of Theorem 38 there exists a unique discrete solution of the scheme

$$\begin{cases} E_\alpha^0 = E_{\text{disc}}^0 \\ E_\alpha^{k+1} \in \operatorname{argmax}_{E' \in \mathcal{D}, E' \supset E} \mathcal{F}_\alpha^\varphi(E', E_\alpha^k) \quad k \geq 1, \end{cases}$$

which is given, for any $k \geq 1$, by $Z(E_\alpha^k) = Z(E_{\text{disc}}^0) + \underbrace{\mathcal{N}_\alpha^\varphi + \dots + \mathcal{N}_\alpha^\varphi}_{k\text{-times}}$.

We therefore obtain a limit result analogous to that of Theorem 39, provided the initial datum E^0 can be approximated by a sequence of admissible sets $E_{\varepsilon_j}^0 \in \mathcal{A}_{\varepsilon_j}$ whose rescaled sets $\frac{1}{\varepsilon_j} E_{\varepsilon_j}^0 \in \mathcal{A}_{\text{conv}}^e$ satisfy (2.3), (5.13) and (5.14). This implies, in particular, that E^0 must be a convex symmetric set with respect to coordinated axes and bisectors $x_1 = \pm x_2$. Then there exists (up to subsequences) a minimizing movement $E : [0, +\infty) \rightarrow \mathcal{X}$ for the scheme

$$\begin{cases} E_{\varepsilon, \tau}^0 = E_\varepsilon^0 \\ E_{\varepsilon, \tau}^{k+1} \in \operatorname{argmin}_{E' \in \mathcal{D}_\varepsilon, E' \supset E_{\varepsilon, \tau}^k} \mathcal{F}_{\varepsilon, \tau}^\varphi(E', E) \quad k \geq 1 \end{cases} \quad (6.5)$$

at regime $\varepsilon = \alpha\tau$ defined by

$$E(t) = E^0 + v_\alpha^\varphi t P_\alpha^\varphi \quad \text{for every } t \geq 0. \quad (6.6)$$

Moreover, there exists a unique discrete flat flow $E_{\varepsilon_j, \tau_j}(t)$ of the scheme (6.5) along the sequence $\varepsilon_j = \alpha\tau_j$ and there holds $\chi_{E_{\varepsilon_j, \tau_j}(t)} \xrightarrow{*} \frac{1}{2} \chi_{E(t)}$ for every $t \geq 0$ as $j \rightarrow +\infty$.

6.1 Examples of explicit evolutions

We continue our analysis by providing several examples of minimizing movements that can be completely characterized, which exhibit interesting phenomena that may appear due to the discrete nature of our problem.

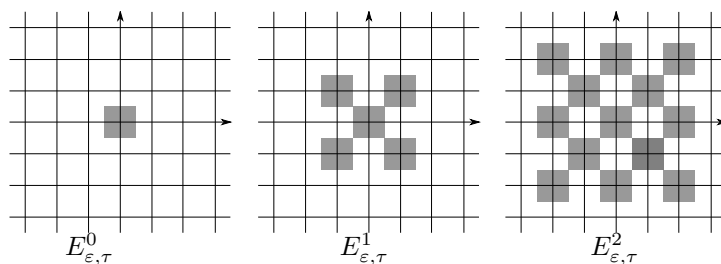


Figure 40: Some steps of the discrete evolution.

Example 43 (the ℓ^∞ -norm). The solutions of the unconstrained scheme (3.5) have already been analyzed in any dimension in the case $\varphi = \|\cdot\|_\infty$ in [12], where it has been proved that every step of the discrete evolution is an even ε -checkerboard (see Fig. 40). Thus, solutions of (3.4) and

(3.5) coincide. The singular set (5.4) corresponds to $\Lambda^\varphi = \{\frac{4}{n}\}_{n \in \mathbb{N}}$ and the pinning threshold is $\alpha_\varphi = 4$. Here, since $\mathcal{N}_\alpha^\varphi = \left[-\frac{4}{\alpha}, \frac{4}{\alpha}\right]^2 \cap \mathbb{Z}_e^2$ for every $\alpha \notin \Lambda^\varphi$, $E(\mathcal{N}_\alpha^\varphi)$ always fulfills (5.13). Therefore, from Theorem 39, for every $\alpha \notin \Lambda^\varphi$ the minimizing movement is

$$E(t) = \left[-\alpha \left\lfloor \frac{4}{\alpha} \right\rfloor t, \alpha \left\lfloor \frac{4}{\alpha} \right\rfloor t \right]^2, \quad \text{for every } t \geq 0.$$

We note that, for this choice of the norm φ , the polygon $P_\alpha^\varphi = [-1, 1]^2$ does not depend on α .

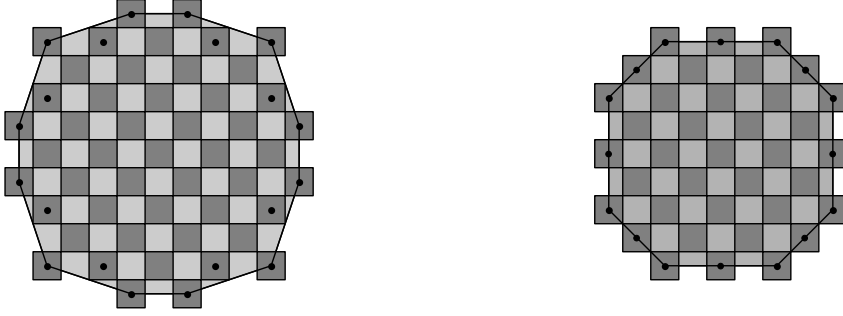


Figure 41: For different choices of α the polygon P_α^φ may have different shapes.

Example 44 (α -depending shape of P_α^φ). Contrarily to the previous example, in the case of the Euclidean norm the polygon P_α^φ may change with α (see, for instance, Fig. 41 corresponding to $\alpha = 0.85$ on the left and $\alpha = 0.7$ on the right). Therefore, the limit motions corresponding to the two different values of α are not homothetic. This phenomenon may happen for those norms φ whose balls are not polygons or are polygons having a unit normal vectors different from $(0, \pm 1)$, $(\pm 1, 0)$ or $(\pm \frac{1}{\sqrt{2}}, \pm \frac{1}{\sqrt{2}})$.

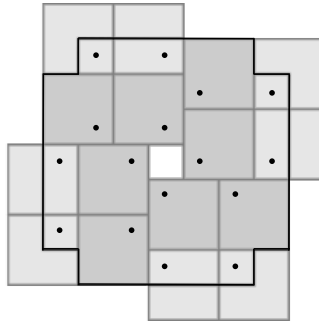


Figure 42: The picture clarifies the 2×2 -square covering $\mathcal{S}_o(E)$ for a set E , whose boundary is marked by a bold black line. The darker 2×2 -squares are respectively in $\mathcal{S}_o^c(E)$, the lighter ones in $\mathcal{S}_o^b(E)$. The areas in white are those left uncovered.

Example 45 (the ℓ^1 -norm). We consider now $\varphi = \|\cdot\|_1$. Also in this case, as for the ∞ -norm, the structure of φ facilitates the analysis of the unconstrained scheme (3.5). We then study the rescaled problem

$$\begin{cases} E^0 = q \\ E_\alpha^{k+1} \in \operatorname{argmin}_{E' \in \mathcal{D}} \mathcal{F}_\alpha^\varphi(E', E) \quad k \geq 1, \end{cases} \quad (6.7)$$

where we separately examine the cases in which the minimizer of the first step contains q or not. For this, in addition to $\mathcal{S}_e(E)$ of Definition 26 we introduce the family

$$\mathcal{S}_o(E) := \{Q(\mathbf{j}) : Q(\mathbf{j}) \cap E \neq \emptyset \text{ and } j_1 \text{ even}, j_2 \text{ odd}\} \quad (6.8)$$

which is a covering of $E \setminus q$ (see Fig. 42) and, accordingly, we consider the partition $\mathcal{S}_o(E) = \mathcal{S}_o^b(E) \cup \mathcal{S}_o^c(E)$.

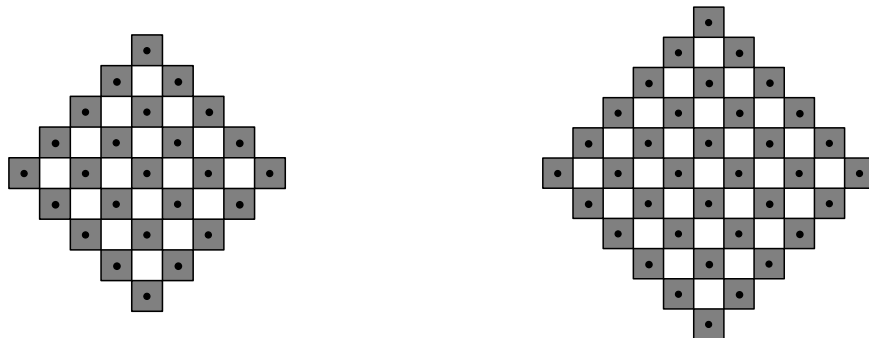


Figure 43: An example of E_α^e (on the left) and E_α^o (on the right).

Now, in the case of scheme (6.7) with the monotonicity constraint, Proposition 27 and (5.4) ensure that, if $\alpha \notin \{\frac{2}{n} : n \in \mathbb{N}\}$ then $\operatorname{argmin}_{E \supset q} \mathcal{F}_\alpha^\varphi(E, q) = E(\mathbb{Z}_e^2 \cap B_{\frac{1}{\alpha}}^\varphi) =: E_\alpha^e$. In the unconstrained case, an analogous argument as in the proof of Proposition 27, with \mathcal{S}_o in place of \mathcal{S}_e , shows that if $\alpha \notin \{\frac{4}{2n-1} : n \in \mathbb{N}\}$ then $\operatorname{argmin}_{E \not\supset q} \mathcal{F}_\alpha^\varphi(E, q) = E(\mathbb{Z}_o^2 \cap B_{\frac{1}{\alpha}}^\varphi) =: E_\alpha^o$. This proves that E_α^1 is either an even or an odd checkerboard. We remark that B_r^φ is a regular rhombus (of radius r) and so are the convex hulls of $Z(E_\alpha^e)$ and $Z(E_\alpha^o)$. The checkerboard sets E_α^e and E_α^o are pictured in Fig. 43.

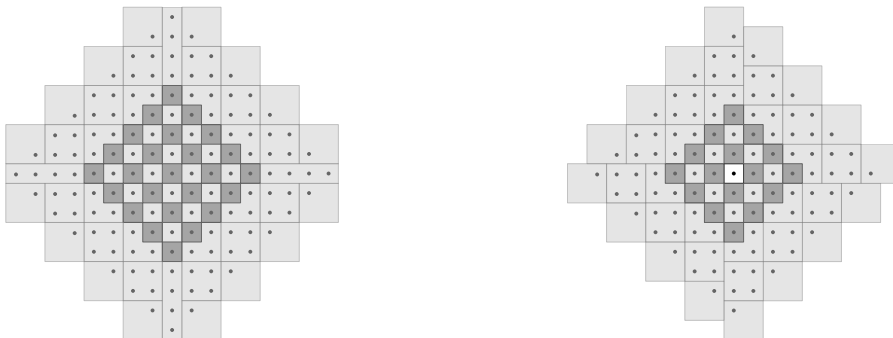


Figure 44: On the left the covering $\mathcal{S}_e(E(J^e))$ and the set E_α^e . On the right the covering $\mathcal{S}_o(E(J^o))$ and the set E_α^o . The darker dots represent J^e and J^o respectively.

The relevant point of this example is that, for this choice of the norm, the shape of the minimizers is very simple and the 2×2 -square covering argument of Section 5.1 directly applies to the k^{th} -step E_α^k , $k \geq 1$, without any further adjustment. Moreover, it provides a covering of \mathbb{R}^2 (in the even case) or $\mathbb{R}^2 \setminus q$ (in the odd case) and not only of $\mathbb{R}^2 \setminus E(\operatorname{conv}(Z(E_\alpha^{k-1})))$, see Figure 44. Thus, the corresponding localization argument allows to study the unconstrained

problem. Indeed, if $E_\alpha^1 = E_\alpha^e$ then for every $Q(\mathbf{j}) \in \mathcal{S}_e(E(\mathcal{J}^e))$ we get

$$\mathcal{F}_\alpha^\varphi(Q(\mathbf{j}) \cap E(\mathbb{Z}_e^2), E_\alpha^1) = \min_{E \in \mathcal{D}} \mathcal{F}_\alpha^\varphi(Q(\mathbf{j}) \cap E, E_\alpha^1), \quad \mathcal{F}_\alpha^\varphi(\mathcal{C}_0 \cap E(\mathbb{Z}_e^2), E_\alpha^1) \leq \min_{E \in \mathcal{D}} \mathcal{F}_\alpha^\varphi(\mathcal{C}_0 \cap E, E_\alpha^1)$$

whereas if $E_\alpha^1 = E_\alpha^o$ then for every $Q(\mathbf{j}) \in \mathcal{S}_o(E(\mathcal{J}^o))$ we get

$$\mathcal{F}_\alpha^\varphi(Q(\mathbf{j}) \cap E(\mathbb{Z}_o^2), E_\alpha^1) \leq \min_{E \in \mathcal{D}} \mathcal{F}_\alpha^\varphi(Q(\mathbf{j}) \cap E, E_\alpha^1),$$

where

$$\mathcal{J}^e = \left\{ \mathbf{i} \in \mathbb{Z}_e^2 : d^\varphi(\mathbf{i}, E_\alpha^1) < \frac{4}{\alpha} \right\}, \quad \mathcal{J}^o = \left\{ \mathbf{i} \in \mathbb{Z}_o^2 : d^\varphi(\mathbf{i}, E_\alpha^1) < \frac{4}{\alpha} \right\}$$

which gives that $Z(E_\alpha^2) \in \{\mathcal{J}^e, \mathcal{J}^o\}$. This yields, after an inductive argument, that E_α^k is either an even or an odd checkerboard. The parity of E_α^k will be determined by a comparison between the two possible (checkerboard) configurations. Nevertheless, a change of parity is eventually not energetically favorable. Indeed, assume E_α^k to be *e.g.* an even checkerboard and set $\mathcal{J} = \{\mathbf{i} \in \mathbb{Z}_o^2 : d^\varphi(\mathbf{i}, E_\alpha^k) < \frac{4}{\alpha}\}$, we then get

$$\begin{aligned} \mathcal{F}_\alpha^\varphi(E(\mathcal{J}), E_\alpha^k) - \mathcal{F}_\alpha^\varphi(E_\alpha^k, E_\alpha^k) &\geq -4\#Z(E(\mathcal{J})) + 2\alpha\#Z(E_\alpha^k) + 4\#Z(E_\alpha^k) + c \\ &\geq -8\left(\frac{4(k+1)}{\alpha}\right)^2 + 2\alpha\left(\frac{4(k+1)}{\alpha}\right)^2 - 8\left(\frac{4k}{\alpha}\right)^2 + c \\ &= -c'k + c''k^2 + c, \end{aligned}$$

for some positive constants c, c', c'' . Since for k large enough the contribution above is positive, for every fixed $\alpha \notin \{\frac{4}{n}\}_{n \in \mathbb{N}}$ there exists an index $k_\alpha \in \mathbb{N}$ such that

$$Z(E_\alpha^k) = Z(E_\alpha^{k_\alpha}) + \underbrace{\mathcal{N}_\alpha^\varphi + \dots + \mathcal{N}_\alpha^\varphi}_{(k-k_\alpha)\text{-times}}, \quad \text{for every } k \geq k_\alpha.$$

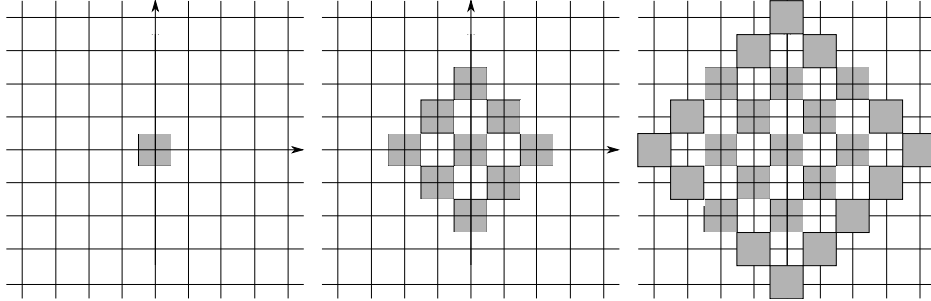


Figure 45: Some steps of the even evolution.

We can characterize the limit motion as follows. For every $\alpha > 0$ such that $\alpha \notin \{\frac{4}{n}\}_{n \in \mathbb{N}}$ there exists a unique minimizing movement of unconstrained scheme (3.5) $E : [0, +\infty) \rightarrow \mathcal{X}$ and it satisfies

$$E(t) = 2\alpha \left\lfloor \frac{2}{\alpha} \right\rfloor t\mathcal{R}, \quad \text{for every } t \geq 0, \quad (6.9)$$

where \mathcal{R} is the regular rhombus of radius 1. Note that, by Theorem 39, this coincides with the minimizing movement of the constrained scheme (3.4).

At least for the first step, the comparison between the energies of the two possible minimizers; *i.e.*, E_α^e and E_α^o , can be performed by a straightforward computation. This induces a partition

into subintervals of the set $(0, +\infty) \setminus \{\frac{4}{n} : n \in \mathbb{N}\}$, wherein one configuration is energetically more favourable than the other one. Setting $R := \lfloor \frac{4}{\alpha} \rfloor$, we get

$$\mathcal{F}_\alpha^\varphi(E_\alpha^e, q) = -4 \left(2 \left\lfloor \frac{R}{2} \right\rfloor + 1 \right)^2 + 4\alpha \sum_{j=1}^{\lfloor \frac{R}{2} \rfloor} (2j)^2, \quad (6.10)$$

$$\mathcal{F}_\alpha^\varphi(E_\alpha^o, q) = -4 \left(2 \left\lfloor \frac{R+1}{2} \right\rfloor \right)^2 + 4\alpha \sum_{j=1}^{\lfloor \frac{R+1}{2} \rfloor} (2j-1)^2 + \alpha. \quad (6.11)$$

After comparing the values in (6.10) and (6.11) we get that when R is even

$$\mathcal{F}_\alpha^\varphi(E_\alpha^e, q) < \mathcal{F}_\alpha^\varphi(E_\alpha^o, q) \quad \text{if and only if} \quad \alpha < \frac{4(2R+1)}{2R(R+1)-1},$$

while when R is odd

$$\mathcal{F}_\alpha^\varphi(E_\alpha^e, q) < \mathcal{F}_\alpha^\varphi(E_\alpha^o, q) \quad \text{if and only if} \quad \alpha > \frac{4(2R+1)}{2R(R+1)+1}.$$

Thus, for the following values of α

$$\alpha_C(R) := \begin{cases} \frac{4(2R+1)}{2R(R+1)+1} & \text{if } R \text{ is odd,} \\ \frac{4(2R+1)}{2R(R+1)-1} & \text{if } R \text{ is even,} \end{cases}$$

the energies of the two checkerboards coincide and we also obtain that

$$E_\alpha^1 = \begin{cases} E_\alpha^e & \text{if } \alpha \in \bigcup_{h \geq 1} (\alpha_C(2h+1), \alpha_C(2h)) \cup (\alpha_C(1), +\infty), \\ E_\alpha^o & \text{if } \alpha \in \bigcup_{h \geq 0} (\alpha_C(2h+2), \alpha_C(2h+1)). \end{cases} \quad (6.12)$$

In particular, (6.12) provides an example of a discrete solution having an oscillating behavior; that is, a change of parity from a step to another, at least from $E_\alpha^0 = q$ to $E_\alpha^1 = E_\alpha^o$.

In this case, the pinning threshold of unconstrained problem (3.5) is $\alpha_p = 2$, as can be seen in formula (6.9). This is the same as that of the constrained problem (3.4), given by Proposition 41. In the constrained problem, for every $\alpha > 2$, since $\mathcal{N}_\alpha^\varphi = \{(0, 0)\}$, $E_\alpha^k = q$ for every $k \geq 1$. Whereas, in the unconstrained problem, by (6.12) we get that if $2 < \alpha < \frac{12}{5}$ the discrete motion is not trivial; that is, $E_\alpha^k = \bigcup_{\|\mathbf{i}\|_1=1} q(\mathbf{i})$ for every $k \geq 1$, even though the limit motion is pinned.

Example 46 (a strongly anisotropic norm). We now give, along the lines of Example 37, another example where the discrete minimizers are (degenerate) checkerboard sets and the limit set is one-dimensional; *i.e.*, a linearly growing segment. For this, we construct *ad hoc* a strongly anisotropic *non-absolute* norm φ such that $\varphi(1, 1) < \varphi(1, 0) = \varphi(0, 1)$. Namely, we consider the symmetric positive definite matrix $\mathbf{A} = (a_{ij})$ such that $a_{11} = a_{22} > 1$, $a_{12} < 0$ and

$$\frac{1}{8} < a_{11} + a_{12} < \frac{1}{2}, \quad 2 < a_{11} - a_{12}. \quad (6.13)$$

Correspondingly, we define the elliptic norm

$$\varphi(\mathbf{x}) := \sqrt{\mathbf{x}^t \mathbf{A} \mathbf{x}} = \sqrt{a_{11}(x_1^2 + x_2^2) + 2a_{12}x_1x_2}, \quad (6.14)$$

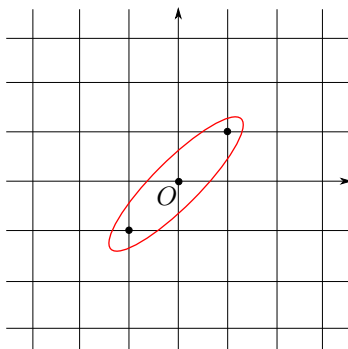


Figure 46: The unit ball of φ for $a_{11} = 2$ and $a_{12} = -\frac{5}{3}$.

whose unit ball is pictured in Fig. 46.

Assumption (6.13) ensures that $\varphi(1, 1) = \sqrt{2(a_{11} + a_{12})} < \sqrt{a_{11}} = \varphi(1, 0) = \varphi(0, 1)$. In addition, we assume that

$$\frac{4}{\sqrt{a_{11}}} < \alpha \leq \frac{2\sqrt{2}}{\sqrt{a_{11} + a_{12}}}. \quad (6.15)$$

In this case, if we let $E_\alpha^0 = q$, the set of centers of the first step is

$$\mathcal{N}_\alpha^\varphi = Z(E_\alpha^1) = \left\{ \mathbf{i} \in \mathbb{Z}^2 : \varphi(\mathbf{i}) \leq \frac{4}{\alpha} \right\} = \{(-1, -1), (0, 0), (1, 1)\}, \quad (6.16)$$

whence, arguing by induction on the step k , we infer that

$$Z(E_\alpha^k) = \{(j, j) : |j| = 0, 1, \dots, k\}, \quad k \geq 1. \quad (6.17)$$

A similar computation as for the proof of Theorem 38 shows that an analogous characterization

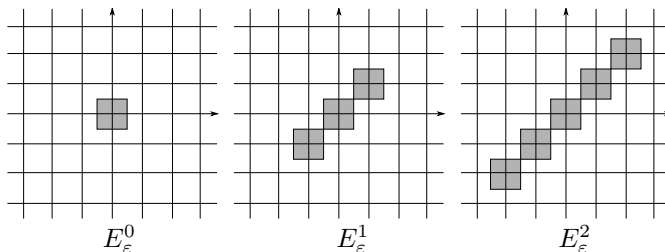


Figure 47: Some steps of the evolution.

for $Z(E_\alpha^k)$ by means of the Minkowski sum as in (5.39) holds. The polygon P_α^φ here reduces to the line segment \mathcal{L} of length $2\sqrt{2}$ centered at 0 with slope 1. In Fig. 47 some steps of the discrete evolution are represented. Note that the proof of (6.16)-(6.17) does not require any covering argument in the fashion of Section 5.3 or any monotonicity assumption (5.13). The following characterization of the limit evolution immediately follows from the proof of Theorem 39.

Proposition 47. *Let α be such that (6.15) holds. Then there exists a unique minimizing movement of (3.4) $E^\alpha(t) = \alpha\mathcal{L}t$ where \mathcal{L} is the line segment above.*

6.2 Further results and conjectures

In this section we focus on the non-trivial issue of addressing our problem without the monotonicity constraint. If on the one hand in the case of the ℓ^∞ -norm (Example 43), the monotonicity constraint did not play any role, on the other hand in Example 45 we proved that the first step of the unconstrained scheme (6.7) for the ℓ^1 -norm can be either an even or an odd checkerboard set. The idea of the proof was to follow the argument of Proposition 27, replacing, when using the 2×2 -square coverings, the family $\mathcal{S}_e(E)$ with $\mathcal{S}_o(E)$ defined in (6.8) in the case $E \not\supseteq q$. This approach works for every absolute norm φ . Therefore, when removing the monotonicity constraint in the minimization scheme, we find the following generalization of Proposition 27.

Proposition 48. *Let φ be an absolute norm, let $\alpha > 0$ be such that $\alpha \notin \Lambda^\varphi$ and let $\mathcal{F}_\alpha^\varphi$ be as in (5.1). Then the first minimization problem of scheme (6.7) admits the only solutions*

$$E_\alpha^1 = \operatorname{argmin}_{E \in \mathcal{D}} \mathcal{F}_\alpha^\varphi(E, q) = \begin{cases} E(\mathbb{Z}_e^2 \cap B_{\frac{\alpha}{4}}^\varphi) \in \mathcal{A}^e, & \text{if } q \subset E_\alpha^1, \\ E(\mathbb{Z}_o^2 \cap B_{\frac{\alpha}{4}}^\varphi) \in \mathcal{A}^o, & \text{if } q \not\subset E_\alpha^1. \end{cases}$$

At this point, we are forced to depart from Example 45 for the determination of the sets E_α^k , $k \geq 2$, as the delicate construction of a covering needed in the proof of Proposition 30 strongly relies on the monotonicity constraint on the discrete evolution and thence is no longer enough to infer an analogous result for the subsequent steps of the evolution. The investigation of this issue has therefore to be deferred to further contributions. Anyway, motivated by the previous ‘‘positive’’ examples, we do believe that under suitable assumptions on the norm φ and the geometry of the competitors in the minimization problem one can still infer a (checkerboard) structure result as in Proposition 30 and a characterization by means of Minkowski sums, analogous to that of Theorem 38. Within this scenario, oscillations of the minimizers between checkerboards of different parity, in principle, cannot be excluded. However, energetic considerations suggest that these may occur only for a finite number of steps, depending on α : heuristically, a change of parity at step k involves a variation of the perimeter term of order k which cannot match, for k large, the corresponding increasing of the bulk term of order k^2 . In order to see this we may assume, without loss of generality, that $Z(E_\alpha^{k+1}) = (k+1)\mathcal{N}_\alpha^\varphi \subset \mathbb{Z}_o^2$ and $Z(E_\alpha^k) = k\mathcal{N}_\alpha^\varphi \subset \mathbb{Z}_e^2$ for some $k \geq 1$, as an interchanging of the parity of the sets would provide an analogous estimate. Then, by virtue of (2.7)–(2.9), the variation of the energy $\mathcal{F}_\alpha^\varphi$ from an even checkerboard E_α^k to the odd one E_α^{k+1} is bounded from below by

$$\begin{aligned} & -4(\#Z(E_\alpha^{k+1}) - \#Z(E_\alpha^k)) + \alpha \min\{\varphi(1, 0), \varphi(0, 1)\} (\#Z(E_\alpha^k) + \#Z(E_\alpha^{k+1})) \\ & = -4\#((k+1)\mathcal{N}_\alpha^\varphi \cap \mathbb{Z}_o^2) + 4\#(k\mathcal{N}_\alpha^\varphi \cap \mathbb{Z}_e^2) + \alpha(\#(k\mathcal{N}_\alpha^\varphi \cap \mathbb{Z}_e^2) + \#((k+1)\mathcal{N}_\alpha^\varphi \cap \mathbb{Z}_o^2)) \\ & \geq -4\#((k+1)\mathcal{N}_\alpha^\varphi \cap \mathbb{Z}_o^2) + 4\#(k\mathcal{N}_\alpha^\varphi \cap \mathbb{Z}_e^2) + \alpha\#(k\mathcal{N}_\alpha^\varphi \cap \mathbb{Z}^2) \\ & = \alpha|\operatorname{conv}(\mathcal{N}_\alpha^\varphi)|k^2 + C'_\alpha k + C''_\alpha. \end{aligned} \tag{6.18}$$

Thus, there exists $k_\alpha := k(\alpha)$ such that the right-hand side in (6.18) is positive for $k \geq k_\alpha$. As a consequence, the change of parity is not energetically favorable (definitely in k), and we expect either $E_\alpha^k \in \mathcal{A}_{\operatorname{conv}}^e$ or $E_\alpha^k \in \mathcal{A}_{\operatorname{conv}}^o$ for every $k \geq k_\alpha$ to hold as a result of iterated Minkowski sums with the even nucleus $\mathcal{N}_\alpha^\varphi$ of (3.5). In conclusion, since a finite number of oscillations is neglected in the limit, an analogous characterization of the limit evolution as in Theorem 39 holds.

We summarize our conjecture as follows.

Conjecture. *Under suitable assumptions on φ and for suitable values of α , the discrete solutions $\{E^k\}$ of scheme (3.5) satisfy*

$$\text{either } Z(E_\alpha^k) = \left\{ \mathbf{i} \in \mathbb{Z}_e^2 : d^\varphi(\mathbf{i}, E_\alpha^{k-1}) < \frac{4}{\alpha} \right\} \quad \text{or} \quad Z(E_\alpha^k) = \left\{ \mathbf{i} \in \mathbb{Z}_o^2 : d^\varphi(\mathbf{i}, E_\alpha^{k-1}) < \frac{4}{\alpha} \right\}.$$

Moreover, there exists an index $k_\alpha \in \mathbb{N}$ such that

$$Z(E_\alpha^k) = Z(E_\alpha^{k_\alpha}) + \underbrace{\mathcal{N}_\alpha^\varphi + \cdots + \mathcal{N}_\alpha^\varphi}_{(k-k_\alpha)\text{-times}}, \quad \text{for every } k \geq k_\alpha.$$

As for the limit evolution, there exists a unique minimizing movement $E : [0, +\infty) \rightarrow \mathcal{X}$ for scheme (3.5) defined by $E(t) = v_\alpha^\varphi t P_\alpha^\varphi$ for every $t \geq 0$, where P_α^φ and v_α^φ are as in the statement of Theorem 39.

Acknowledgements

A. Braides acknowledges the MIUR Excellence Department Project awarded to the Department of Mathematics, University of Rome Tor Vergata, CUP E83C18000100006. G. Scilla has been supported by the Italian Ministry of Education, University and Research through the Project “Variational methods for stationary and evolution problems with singularities and interfaces” (PRIN 2017).

References

- [1] R. Alicandro, A. Braides and M. Cicalese, Phase and anti-phase boundaries in binary discrete systems: a variational viewpoint. *Netw. Heterog. Media* **1** (2006), 85–107.
- [2] L. Ambrosio, N. Fusco and D. Pallara, *Functions of Bounded Variations and Free Discontinuity Problems*. Oxford University Press, Oxford, 2000.
- [3] F. Almgren and J. E. Taylor, Flat flow is motion by crystalline curvature for curves with crystalline energies. *J. Diff. Geom.* **42** 1 (1995), 1–22.
- [4] F. Almgren, J. E. Taylor and L. Wang, Curvature driven flows: a variational approach. *SIAM J. Control Optim.* **50** (1993), 387–438.
- [5] H. Barki, F. Denis and F. Dupont, Contributing vertices-based Minkowski sum computation of convex polyhedra. *Comput. Aided Des.* **41**(7) (2009), 525–538.
- [6] A. Braides. *Γ -convergence for Beginners*. Oxford University Press, Oxford, 2002.
- [7] A. Braides, *Local Minimization, Variational Evolution and Γ -convergence*. Lecture Notes in Mathematics **2094**. Springer Verlag, Berlin, 2013.
- [8] A. Braides, M. Cicalese. Interfaces, modulated phases and textures in lattice systems. *Arch. Ration. Mech. Anal.* **223** (2017), 977–1017.
- [9] A. Braides, M. Cicalese and N. K. Yip, Crystalline Motion of Interfaces between Patterns. *J. Stat. Phys.* **165**(2) (2016), 274–319.
- [10] A. Braides, M.S. Gelli and M. Novaga, Motion and pinning of discrete interfaces. *Arch. Ration. Mech. Anal.* **195** (2010), 469–498.
- [11] A. Braides and G. Scilla, Motion of discrete interfaces in periodic media. *Interfaces Free Bound.* **15** (2013), 451–476.
- [12] A. Braides and G. Scilla, Nucleation and backward motion of discrete interfaces. *C. R. Math. Acad. Sci. Paris* **351** (2013), 803–806.

- [13] A. Braides and M. Solci, Motion of discrete interfaces through mushy layers. *J. Nonlinear Sci.* **26** (2016), 1031–1053.
- [14] A. Braides and M. Solci. *Geometric Flows on Planar Lattices*, Birkhäuser, to appear.
- [15] D. Ciccarese, *Influence of temporal and spatial heterogeneity on microbial spatial self-organization*. Ph.D. thesis, (2020) <https://doi.org/10.3929/ethz-b-000401169>
- [16] S. Daneri and E. Runa, Exact Periodic Stripes for Minimizers of a Local/Nonlocal Interaction Functional in General Dimension. *Arch. Rational Mech. Anal.* **231** (2019), 519–589.
- [17] J. J. De Yoreo and P. G. Vekilov, Principles of Crystal Nucleation and Growth. *Reviews in Mineralogy and Geochemistry* **54** (1) (2003), 57–93.
- [18] R. J. Gardner, P. Gronchi and C. Zong, Sums, projections and sections of lattice sets, and the discrete covariogram. *Discrete Comput. Geom.*, **34** (2005), 391–409.
- [19] A. Giuliani, J. L. Lebowitz and E. H. Lieb, Checkerboards, stripes, and corner energies in spin models with competing interactions. *Phys. Rev. B* **84** (2011), 064205.
- [20] V. Kalikmanov, *Nucleation Theory*, Lecture Notes in Physics LNP, Lecture Notes in Physics, Springer Netherlands, 860 (2013).
- [21] M. Lindner and S. Roch, On the integer points in a lattice polytope: n -fold Minkowski sum and boundary. *Beitr. Algebra Geom.* **52** (2011), 395–404.
- [22] M. Marinacci and L. Montrucchio, On concavity and supermodularity, *J. Math. Anal. Appl.* **344** (2008), 642–654.
- [23] M. Mimura, H. Sakaguchi and M. Matsushita, Reaction-diffusion modelling of bacterial colony patterns, *Physica A: Statistical Mechanics and its Applications* **282** (1-2) (2000), 283–303.
- [24] K. Murota. *Discrete convex analysis*. SIAM Monographs on Discrete Mathematics and Applications. Society for Industrial and Applied Mathematics (SIAM), Philadelphia, PA (2003).
- [25] G. A. Pick, *Geometrisches zur Zahlenlehre*, Lotos, Naturwissenschaftliche Zeitschrift **19** (1899), 311–319.
- [26] M. Ruf, Motion of discrete interfaces in low-contrast random environments. *ESAIM: COCV* **24** (3) (2018), 1275–1301.
- [27] G. Scilla, Motion of discrete interfaces in low-contrast periodic media. *Netw. Heterog. Media* **9** (2014), 169–189.
- [28] G. Scilla, Motion of discrete interfaces on the triangular lattice. *Milan J. Math.* **88** (2020), 315–346.

A. Braides, DIPARTIMENTO DI MATEMATICA, UNIVERSITÀ DI ROMA “TOR VERGATA”, VIA DELLA RICERCA SCIENTIFICA 1, 00133 ROMA, ITALY
E-mail address, A. Braides: braides@mat.uniroma2.it

G. Scilla, DIPARTIMENTO DI MATEMATICA ED APPLICAZIONI “R. CACCIOPPOLI” , UNIVERSITÀ DI NAPOLI FEDERICO II, VIA CINTIA MONTE SANT’ANGELO, 80126 NAPOLI, ITALY
E-mail address, G. Scilla: giovanni.scilla@unina.it

A. Tribuzio, DIPARTIMENTO DI MATEMATICA, UNIVERSITÀ DI ROMA “TOR VERGATA”, VIA DELLA RICERCA SCIENTIFICA 1, 00133 ROMA, ITALY
E-mail address, A. Tribuzio: tribuzio@mat.uniroma2.it